KINETIC MECHANISM AND MODULATION OF GLUTAMATE TRANSPORTERS

by

Anastassios Tzingounis

A DISSERTATION

Presented to the Neuroscience Graduate Program

And the Oregon Health & Science University

School of Medicine

in partial fulfillment of

the requirements for the degree of

Doctor of Philosophy

October 2002

School of Medicine
Oregon Health and Science University

CERTIFICATE OF APPROVAL

This is to certify that the Ph.D. thesis of

Anastassios Tzingounis

has been approved

[redacted]
Michael P. Kavanaugh, Ph.D., Mentor

[redacted]
Craig E. Jahr, Ph.D., Member

[redacted]
David Kabat, Ph.D., Member

[redacted]
H. Peter Larsson, Ph.D., Member

TABLE OF CONTENTS

TABLE OF CONTENTS iii

DEDICATION vii

ACKNOWLEDGEMENTS viii

ABSTRACT ix

INTRODUCTION 1

Figure 1. EAAT topology. 4

CHAPTERS:

1. A KINETIC MODEL FOR GLUTAMATE UPTAKE. 35

ABSTRACT 36

INTRODUCTION 37

MATERIALS AND METHODS 38

RESULTS 40

Figure 1. Cysteine is transported by EAAT3 as a neutral zwitterion. 42

Figure 2. Electrostatic effects of extracellular proton and substrate concentrations. 45

Figure 3. Electrostatic effects of $[Na^+]_o$, but not $[K^+]_o$, are similar to $[H^+]_o$. 47

Figure 4. Glutamate and protons reciprocally influence both the steady

state kinetic parameters K_m and I_{max}. 50

Figure 5. Glutamate and Na^+ reciprocally influence both the steady state kinetic parameters K_m and I_{max}. 53

Figure 6. Transporters have one selective sodium-binding site. 56

Figure 7. Two sodium ions bind before glutamate. 59

Figure 8. Intracellular ions affect the EAAT3 macroscopic kinetics. 62

Table I. Kinetic parameters with Na^+ the major intracellular cation. 66

Figure 9. Replacement of intracellular potassium by sodium slows the recovery of the peak anion current from steady-state. 68

Figure 10. The recovery rate of the anion current from steady-state depends on the membrane potential. 71

Figure 11. Alternating access computer model. 74

Figure 12. Simulations of the steady-state glutamate induced currents. 77

Figure 13. Simulation of the EAAT3 outside-out patch kinetics. 79

Figure 14. Kinetic data and model simulations for EAAT1, EAAT2, and EAAT4. 82

DISCUSSION 81

2. ARACHIDONIC ACID ACTIVATES A PROTON CURRENT IN THE RAT GLUTAMATE TRANSPORTER EAAT4. 89

ABSTRACT 90

INTRODUCTION 91

EXPERIMENTAL PROCEDURES 92

RESULTS 93

Figure 1. Arachidonic acid enhances the magnitude of glutamate-induced currents recorded in voltage-clamped oocytes expressing rat EAAT4. 94

Figure 2. Arachidonate dose-dependently increases the transport current without increasing glutamate flux. 97

Figure 3. Arachidonate did not enhance the NO_3^--selective transporter anion conductance. 100

Figure 4. Arachidonate enhances a proton-selective current. 103

DISCUSSION 102

3. THE NEURONAL GLUTAMATE TRANSPORTER EAAT3 FUNCTIONS AS A PENTAMER OF INDEPENDENT SUBUNITS. 106

ABSTRACT 107

INTRODUCTION 108

MATERIALS AND METHODS 110

RESULTS 112

Figure 1. Cross-linking of bovine serum albumin and neuronal specific glutamate transporter, EAAT3. 113

Figure 2. Substitution of Arg^{443} to Cys changes the amino acid selectivity of EAAT3 116

Figure 3. R443C co-express with wild type EAAT3. 119

Figure 4. EAAT3 is functionally a monomer. 122

DISCUSSION 124

DISCUSSION AND CONCLUDING REMARKS 128

REFERENCES 136

APPENDIX I 170

Figure 1. Extracellular pH affects EAAT3's anion conductance kinetics. 170

Figure 2. Protons determine the occupancy of the Na^+-bound states. 172

DEDICATION

In memory of

my grandmother Florence Krithari

and

grandfather Anastassios Tzingounis, M.D.

ACKNOWLEDGEMENTS

I am indebted to several people without their help, support, and patience this dissertation would not have been completed. First, I would like to thank my advisor Michael P. Kavanaugh for his support and guidance. I also thank, the members of my committee, Craig E. Jahr, David Kabat, and H. Peter Larsson, for helpful discussions. I am particularly grateful to Craig Jahr for all his help and encouragement along the years.

I am grateful to several previous members of the Kavanaugh Lab. Scott Eliasof, Alex Stein, and Shirin Arastu for helpful discussions. However, I am thankful and immensely grateful to Navid Madani and Hans Koch for their friendship and for making the lab a fun place to be. This experience would not have been the same without them.

I cannot imagine reaching this point without the support of Jacques Wadiche, Thanos Tzounopoulos, Sonal Das, and Ngan Vo. I thank Jacque for his help, discussions, patience, friendship and acting as a big brother. I thank Thanos for being himself. His honesty and friendship mean the world to me. This past five years would not have been the same without my fellow classmates Sonal and Ngan. I never knew how it feels to have sisters, but now I do. I am so grateful to have them as friends.

Finally, I want to thank my parents and my younger brother Giorgo. I will also like to thank the latest member of the family Alexander. I do not have enough words to thank my mother and father for their sacrifices, support, and love. None of this would have taken place if it were not for them. Lastly, I am profoundly grateful to have Giorgo as my brother.

ABSTRACT

Glutamate transporters comprise a family of secondary transporters that are responsible for maintaining low extracellular glutamate levels in the central nervous system (CNS). The kinetics and modulation of several recombinant glutamate transporters were investigated in an effort to understand their behavior under different conditions. The first chapter describes the development of a kinetic model for glutamate transporters. During this process we determined the transporter's extracellular substrate binding order (Na^+-Na^+-H^+/Glu- -Na^+) by measuring the dependence of the steady-state and pre-steady-state transporter currents on glutamate, H^+, Na^+, K^+ and membrane potential. Kinetic simulations suggested that a voltage independent transition allows access of the $Na^+/H^+/Glu^-$ complex to the intracellular compartment, while the K^+-coupled reorientation of the transporter is the rate-limiting voltage dependent step in the cycle. In addition, we show that the cycling rate of the anion conductance in outside-out patches is determined by the nature of the intracellular cation and membrane potential. The model allowed us to estimate that the probability of glutamate transport following binding to the transporter at –70 mV is about 50% for the glial transporters EAAT1 and EAAT2 and the neuronal transporter EAAT3. This capture efficiency suggests that these transporters might remove synaptic glutamate through rapid binding and unbinding leading to buffered diffusion. In contrast, the capture efficiency of the Purkinje cell specific transporter EAAT4 is greater than 90 %. The second chapter describes the effect of arachidonic acid, a known second messenger, to EAAT4. We demonstrate that glutamate

application in the presence of arachidonic acid to oocytes expressing EAAT4 gates a proton selective thermodynamically uncoupled current. This proton conductance is present in conjunction to the previously described uncoupled anion flux resident in glutamate transporters. Lastly, in the third chapter, we used whole cell recordings to oocytes expressing wild type transporters along with transporters that have diminished L-glutamate activity in order to determine EAAT3's subunit stochiometry. In conjunction to biochemical studies we propose that the neuronal transporter EAAT3 forms homopentamers in which each subunit acts as an independent transporter.

INTRODUCTION

In the brain, excitatory amino acid transporters (EAATs) regulate glutamate levels by preventing excessive receptor activation and thereby allowing for normal excitatory synaptic transmission. However, the role of EAATs in physiological as well as pathophysiological brain function is not completely understood (for recent reviews see Bergles et al., 1999; Danbolt, 2001). Following its liberation from the presynaptic boutons, glutamate diffuses rapidly to the synaptic space and activates postsynaptic receptors. The amplitude and time course of the glutamate waveform dictates the extent of glutamate receptor activation (Bergles et al., 1999; Clements, 1996; Kullmann et al., 1999). The time course of the synaptically released glutamate is partly dependent upon transporter density and location as well as transporter binding, unbinding, and translocation rate constants (Clements, 1996; Barbour, 2001; Dehnes et al., 1998; Diamond and Jahr, 1997; Glavinovic, 1999; Holmes, 1995; Lehre and Danbolt, 1998; Min et al., 1998; Rusakov and Kullmann, 1998; Tong and Jahr, 1994). Therefore, to evaluate the role of EAATs in the central nervous system a detailed analysis of their complex kinetics and the mechanism of their regulation is required.

In the last decade, the molecular identification of glutamate transporters has led to an extensive study on their properties. Therefore, in this introduction, attention has been paid on presenting what is currently known about the transporters molecular identity, topology, pharmacology, quaternary structure, functional and structural properties, and finally the transporters modulation by interacting proteins and intracellular cascades.

A. Molecular Structure and Topology

The existence of multiple glutamate transporter subtypes was proposed prior to the cloning of various isoforms. This proposal stemmed from the observation that the dihydrokainate (DHK) and L-α-aminoadipate (L-aa) blockade of glutamate uptake differs between brain regions (Robinson et al., 1991). In 1992, this prediction became a reality with the identification of three glutamate transporters. GLAST (Storck et al., 1992) and GLT-1 (Pines et al., 1992) were isolated from rat brain libraries while EAAC1 (Kanai and Hediger, 1992) was identified from a rabbit intestine. Subsequently, low stringency screening of human brain cDNA libraries led to the identification of their human homologs (GLAST/EAAT1, GLT-1/EAAT2, EAAC1/EAAT3) (Arriza et al., 1994; Kanai et al., 1994; Kawakami et al., 1994; Manfras et al., 1994). Besides the three original transporters, Amara and colleagues isolated two more human EAATs, EAAT4 (Fairman et al., 1995) and EAAT5 (Arriza et al., 1997) through homology based screening of a human cortex and retina cDNA libraries. In addition, two homologous neutral amino acid transporters ASCT-1 (Arriza et al., 1993) and ASCT-2 (Utsunomiya-Tate et al., 1996) were identified. Unlike EAAT1-3, which are localized throughout the CNS (see for review Danbolt, 2001) EAAT4 is specifically found on Purkinje cells of cerebellum (Fairman et al., 1995; Lin et al., 1998) while EAAT5 is localized only to the retina (Arriza et al., 1997; Eliasof et al., 1998). For clarity, in this dissertation, the EAAT nomenclature has been adopted for the glutamate transporters, unless is otherwise stated.

Early on, it became apparent that the different glutamate transporter subtypes share similar hydropathy plots (Kanai et al., 1993; Lolkema and Slotboom, 1998; Slotboom et al., 1996). However, it is only now that a consensus seems to have been

reached regarding the topology of the glutamate transporters (Kanner et al., 2001; although see Seal et al., 1998). There are six membrane-spanning domains in the N-terminal half of the transporters with the N terminus of the protein located intacellularly. Similarly, the C-terminus part of the protein is found on the intracellular side (Figure 1). A P-loop like structure is localized between TM6 and TM7 containing a conserved serine stretch (Slotboom et al., 1999). Another P-loop with an opposite polarity from the first is located between TM7 and TM8. Between this re-entrant sequence and TM8 an extremely exposed hydrophobic sequence seems to lie in close association with the membrane. TM8, on the other hand, is an aliphatic α-helix (Slotboom et al., 2001) which lies along a narrow aqueous pore through the protein that is distinct from the large water filled pore formed by the first re-entrant loop – between helixes 6 and 7 (see also Leighton et al., 2002). A recent study by Brocke et al. (2001) demonstrated that residues found on the different loops could interact. Application of either $Cu_{(II)}(1,10\text{-phenanthroline})_3$ or micromolar concentrations of Cadmium inhibit transport (K_i = 500 nM) when applied to rat EAAT2 transporters engineered with the double mutation A364C/S440C - A364C (GLT-1 numbering) is located in the first loop while S440C is in the second loop (Figure 1). This suggests that the two cysteines residues are in such close approximation to each other that they could form a high affinity-binding site for cadmium.

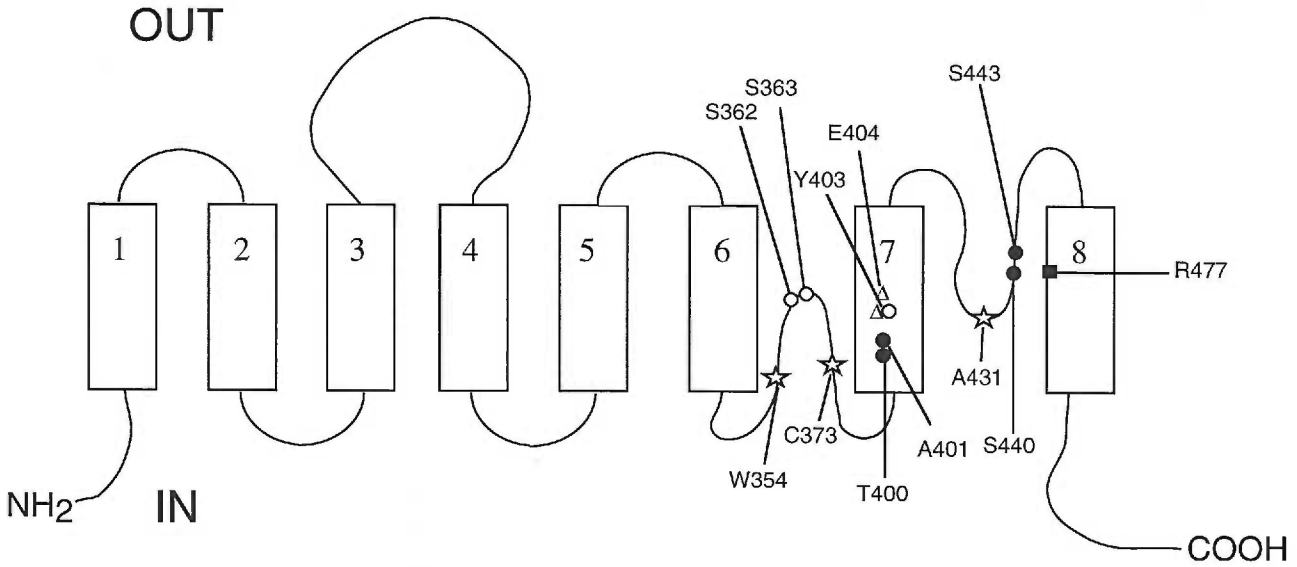

■ interaction of γ-carboxyl group of L-glutamate, L-aspartate; K^+ site interaction
● Na^+ site interaction
Δ K^+ site interaction
☆ accessbility from the intracellular side of the membrane
○ accessbility from both sides of the membrane

Figure 1. EAAT topology. Numbering of amino acids is based on GLT-1 sequence.

B. Pharmacology and Substrate Specificity

Glutamate transporters have been originally classified under the system XAG^- (Palacin et al., 1998) based on their ability to transport L-glutamate, L-aspartate, and D-aspartate with high affinity (K_m < 100 μM). However, it is now apparent that their substrate specificity is much more complex than it was originally reported. The study of glutamate transport has been enhanced by the availability of glutamate analogues that act as inhibitors. However, most of the competitive inhibitors of glutamate uptake are themselves substrates for the transporters (for review see Bridges et al., 1999).

EAATs can discriminate between L and D-glutamate enantiomers (Kanner and Schuldiner, 1987). Interestingly, not all transporters seem to select for analogues of L-glutamate. Vandenberg et al. (1997) demonstrated that (2S, 4R)-4-methylglutamate and 4-methylene-glutamate are substrates for EAAT1 (K_m = 54 μM and 391 μM, respectively), but competitive inhibitors for EAAT2 (K_i = 3.4 μM and 39 μM, respectively). Also, threo-3-methylglutamate (T3MG) blocked glutamate transport by EAAT2 (K_i = 18 μM), but had no effect on EAAT1. A recent study showed that T3MG is not a transportable inhibitor of EAAT4 but, surprisingly, produced substrate-like currents in oocytes expressing EAAT4 (Eliasof et al., 2001). Furthermore, (2S, 4R)-4-methylglutamate and L-threo-4-hydroxyglutamate were shown to be substrates for both EAAT1 (K_m = 61 μM) and EAAT2 (K_m = 48 μM).

Unlike glutamate derivatives, EAATs recognize aspartate analogues. Analogues of aspartate that contain a small group at the γ-carbon, such as α-threo-hydroxy-aspartate (THA), are usually substrates while compounds that have bulky groups, like threo-β-

benzyloxyaspartate (TBOA), are competitive antagonists (Shigeri et al., 2001; Shimamoto et al., 1998). THA has been shown to be a substrate for EAAT1-4 (Arriza et al., 1994; Fairman et al., 1995), but a competitive inhibitor at EAAT5 (Arriza et al., 1997). Furthermore, modification of the distal carboxyl group to hydroxyl, sulfate, or thiol leads to the generation of substrates with different apparent affinities. Thus, L-serine-O-sulfate, L-cysteate, L-cysteinesulfinate, and L-cysteine are transported (Bouvier et al., 1991; Klockner et al., 1994; Zerangue and Kavanaugh, 1996a,b; but see Arriza et al., 1994).

Another group of analogues that have proven useful in identifying the properties of the glutamate binding sites are the derivatives of L-trans-2,4-pyrrolidine dicarboxylate (PDC). These are cyclic compounds that contain a conformationally locked glutamate structure either in an extended or folded conformation. In these compounds the α-amino group of glutamate is embedded in a cyclic structure (Bridges et al., 1991). Analyses of these compounds led Esslinger et al. (1998) to propose that only the extended conformations are transportable substrates. Furthermore, two subsequent studies concluded that steric volume excess might determine which analogue is a substrate (Campiani et al., 2001; Koch et al., 1999). It was shown that 2,3-PDC and 3,4-MPDC, two inhibitors representing the folded glutamate conformation possess excess steric volume along the carbon backbone while the substrates 2,4-PDC and 2,4-MPDC allow a uniform volume distribution on the carbon backbone.

Although great progress has been made in identifying substrates and inhibitors for glutamate transporters we still lack sufficient tools to differentiate among the various subtypes. Kainate and its derivative DHK are the only selective blockers, since they bind

only to EAAT2 with high affinity (K_i = 18 μM; Arriza et al., 1994; Wadiche et al., 1995a). TBOA a widely used non-transportable substrate binds with high affinity to all subtypes (Shigeri et al., 2001; Shimamoto et al., 1998). What has become clear is that compounds that bind to EAAT1 also interact with EAAT3 (Arriza et al., 1994), while EAAT2 and EAAT5 seem to have a unique pharmacological profile. EAAT4, on the contrary, exhibits the most non-selective pharmacological profile (Koch and Kavanaugh, unpublished observations). Finally, two groups recently described the isolation of two toxins (Tx3-4; PhTx4) from the spider *Phoneutria nigriventer* that inhibit synaptosonal glutamate uptake (Mafra et al., 1999; Reis et al., 1999, 2000). These data suggest that the toxins attenuate EAAT2 uptake, the major transporter in the synaptosomal preparation (Koch et al., 1999). Further work, however, is needed before we can conclude the specificity of these toxins.

C. Quaternary structure and Interacting proteins

It has yet to be resolved whether glutamate transporters function as monomers or oligomers. Immunoprecipitation and chemical cross-linking studies suggested that the transporters are composed of multiple subunits. Membrane preparations from homogenized rat brains exposed to cross-linking reagents followed by SDS gel electrophoresis suggested that EAAT1 and EAAT2 do not interact with each other but may associate as homomultimers. In particular, EAAT1 and EAAT2 form trimers and dimers, while EAAT3 and EAAT4 can form either trimers or dimers, respectively (Dehnes et al., 1998; Haugeto et al., 1996). These data, then, suggest that EAATs exist in clusters of identical subunits. Recently, by applying freeze-fracture electron microscopy

to oocytes expressing EAAT3, Eskandari et al. (2000) identified particles that were pentagonal in shape. These particles exhibited five-fold symmetry and were the appropriate size for a homopentamer of EAAT3 proteins. On this basis it was suggested that EAATs might need the pentameric structure to support the anion channel (see Anion conductance section), but that they function as monomers for glutamate transport. Although this is an intriguing hypothesis there are as of yet no data to support the notion that oligomerization is necessary for the formation of the anion conductance. Evidence that multimer formation is required for transporter function is also lacking. A series of radiation inactivation experiments have suggested that the functional transporter unit is approximately either 3.9 or 2.5 times the monomer size (Beliveau et al., 1990; Haugeto et al., 1996). However, it is also possible that the irradiation experiments indicate the presence of interacting proteins associated with EAATs.

In agreement with this hypothesis, Marie et al., (1999) proposed that the Muller-cell transporter EAAT1 associates with an interacting protein. Disruption of interactions of the C- and N-termini of EAAT1 with other proteins was achieved by perfusing Muller cells with peptides identical to the eight amino acids at the C- or N-termini of the transporter. Dialysis with the C-terminus peptide had no effect on the maximum current, but increased the affinity of the transporter for glutamate, while the N-terminus had no effects. As a result, it was postulated that the peptide is interfering with the binding of a transporter-interacting protein that has yet to be identified.

Recently, several novel transporter-interacting proteins were identified. Jackson et al. (2001) characterized two proteins, GTRAP41 and GTRAP48, that specifically interact with the intracellular C-terminal domain of EAAT4. Co-expression of EAAT4 with either

GTRAP41 or GTRAP48 produces a two to four-fold increase in glutamate uptake by stabilizing EAAT4 in the membrane cell surface. Also, Lin et al. (2001) described the identification of an EAAT3-associated protein, GTRAP3-18, which had been previously identified as a retinoic-acid-responsive gene. GTRAP3-18 localizes to the cell membrane and cytoplasm, and specifically interacts with the C-terminal intracellular domain of EAAT3 as well as $G\alpha_{13}$. Increasing the expression of GTRAP3-18 in HEK293 cells reduces glutamate transport by lowering substrate affinity (glutamate K_m from 9 μM to 40 μM), thus, GTRAP3-18 is an endogenous inhibitor of EAAT3. Lin et al. (2001) also found a similar decrease in the glutamate affinity when they truncated the C-terminus of EAAT3. This suggests that the GTRAP3-18 might mediate its effect by inhibiting an interaction of the C-terminus with the transporter. More recently, Marie et al. (2002) have identified a cytoplasmic LIM protein, Ajuba, which interacts with the amino terminus of EAAT2. However, coexpression of Ajuba with EAAT2 did not affect the K_m or V_{max} for glutamate transport. Another interacting protein candidate, although not yet demonstrated to directly associate with the EAATs, is syntaxin 1A. Beckman et al. (1999) showed that glutamate uptake in neuronal hippocampal cultures is increased ~160 % in the presence of botulinum toxin C1, a selective inhibitor of syntaxin 1A. In their study they demonstrated that the GABA transporter GAT1 and syntaxin 1A interact and proposed that neuronal glutamate transporters may also form a complex with syntaxin 1A. In summary, these initial observations indicate that protein-protein interactions are likely to play important roles in modulating transporter activity.

D. Functional Analysis

1. Stochiometry

In the last decade, there has been much controversy regarding the number of ions that are coupled to glutamate transport. Although there was some agreement that multiple Na^+ ions, a pH-changing ion, and one K^+ are coupled to glutamate uptake, the exact stochiometry was uncertain. Several reports suggested that 3 Na^+ ions accompany glutamate uptake (Barbour et al., 1988, Kanner and Sharon, 1978; Klockner et al., 1993) while others claimed only 2 Na^+ ions are involved (Bouvier et al., 1992; Erecinska et al., 1983; Kanai et al., 1995; Kanner and Bendahan, 1982; Stallcup et al., 1979). Another unresolved issue was the nature of the pH-changing ion (see Proton binding) that was coupled to glutamate transporters (Bouvier et al., 1992; Erecinska et al., 1983; Kanai et al., 1995; Nelson et al., 1983). Bouvier et al. (1992) suggested that an OH^- is countertransported, while Zerangue and Kavanaugh (1996a) suggested that a H^+ is the transported ion. The latter hypothesis is based on the observation that L-cysteine is transported by the EAATs as zwitterion and in the absence of any intracellular acidification (Zerangue and Kavanaugh, 1996b). The number of ions coupled to glutamate uptake was finally resolved by Zerangue and Kavanaugh (1996b) when they measured the reversal potential of glutamate transporters under different extracellular ionic concentrations of Na^+, H^+, and K^+. They fit their data to a zero-flux equation relating membrane potential to the transmembrane ion gradients, $V_m = (RT/F)\bullet(n_{Na} + n_H - n_{Glu} - n_K)^{-1}\bullet\ln(Na_o/Na_i)^{nNa}\bullet(H_o/H_i)^{nH}\bullet(K_i/K_o)^{nK}\bullet(Glu_o/Glu_i)^{nGlu}$. They concluded that glutamate transport is coupled to 3 Na^+, 1 H^+, and 1 K^+. Similar results where obtained by Levy et al. (1998) for EAAT2.

2. Anion conductance

Studies of glutamate transporters on dissociated salamander photoreceptors (Eliasof et al., 1993) led to the postulation that glutamate transporters might be associated with a chloride channel (see also Tachibana and Kaneko, 1988). It is now established that all the EAATs, to varying degrees, allow the flux of anions in channel-like fashion (Arriza et al., 1997; Fairman et al., 1995; Wadiche et al., 1995b). The relative magnitude of anion conductance follows the sequence: EAAT5 ~ EAAT4 > EAAT1 > EAAT3 > EAAT2. In particular, 95-100% of the steady-state current induced by glutamate in EAAT5 (Arriza et al., 1997) and EAAT4 (Fairman et al., 1995) is mediated by anions while for EAAT1-3 this number varies from 27-50% (Wadiche et al., 1995b). The anion current is thermodynamically uncoupled from amino acid uptake (Wadiche et al., 1995b), and as a result, amino acid flux is independent of the chloride gradient. Also, the anion conductance is inversely related to the rate of amino acid flux (Wadiche and Kavanaugh, 1998) and its activation by substrate and Na^+ has a similar concentration dependency to the activation of amino acid transport (Billups et al., 1996; Fairman et al., 1995; Larsson et al., 1996; Mennerick et al., 1999; Wadiche et al., 1995b). Recently, efforts were made to study the biophysical properties of the anion channel. It was found that chaotropic anions are more permeant than chloride, with SCN^- being 62-fold more permeant (Wadiche and Kavanaugh, 1998). In addition, Larsson et al. (1996) determined that the single channel conductance is 0.7 pS in the presence of chloride ions for the glutamate transporter(s) expressed in cone photoreceptors, while Wadiche and Kavanaugh (1998) estimated a conductance of 0.7 fS for EAAT1.

However, anions may not be completely inert regarding transport kinetics. Two studies (Auger and Attwell, 2000; Billups et al., 1996) suggested that the translocation rate of glutamate in both the forward and reverse mode decreased in the presence of permeant anions. The conclusion in the Billups et al. (1996) study was based on the observation that extracellular application of ClO_4^- in Muller cells decreases the K^+ stimulated reverse current, while Auger and Attwell (2000) reported that synaptically activated transporter currents decay more slowly when either NO_3^- or ClO_4^- is included in the recording pipette compared to conditions where gluconate or Cl^- is the major anion. In addition, it was found that the glutamate K_m is higher in oocytes expressing EAAT2 when dialyzed overnight with gluconate to deplete $[Cl^-]_i$ (Vandenberg et al., 1998). Lastly, the salamander transporter sEAAT2B has a dependency on extracellular chloride. In the absence of $[chloride]_o$ glutamate uptake is decreased by 70 % (Eliasof et al., 1998). This suggests that, at least in some of the transporters, there might be interactions between chloride and coupled ions or substrates.

3. Water transport

It has been recently demonstrated that Na^+ coupled transporters are capable of shuttling water against its concentration gradient (Loo et al., 1999; Meinild et al., 1998, 2000; Zeuthen et al., 1997). MacAulay et al. (2001, 2002) demonstrated that EAAT1 also transports water. This group estimated that 436 water molecules are transported per unit charge. Also, glutamate application to oocytes expressing EAAT1 increased the oocytes water permeability. The physiological role of water transport through the transporters is not apparent, but it may contribute to the cell's osmotic regulation.

4. Activation of glutamate transporters by monovalent cations.

i. Sodium binding

Early studies in synaptosomes had established that glutamate transport requires the presence of extracellular Na^+ (Kanner and Bendahan, 1982; Kanner and Sharon, 1978). However, a quantitative relationship was not established until the use of electrophysiological techniques, which took advantage of the electrogenicity of glutamate uptake (Brew and Attwell, 1987). It was shown that 3 Na^+ ions are required for glutamate transport (Levy et al., 1998; Zerangue and Kavanaugh, 1996b) with a Na^+ K_m that ranges between 16 mM to 72 mM depending on the EAAT isoform and experimental conditions (Barbour et al., 1988; Barbour et al., 1991; Borre and Kanner, 2001; Eliasof et al., 1998; Fairman et al., 1998; Kanai et al., 1995; Klockner et al., 1993, 1994; Pines et al., 1995; Zerangue and Kavanaugh, 1996b; Watzke et al., 2001).

There is considerable evidence demonstrating that the apparent Na^+ affinity is dependent on extracellular glutamate (Kanai et al., 1995). At lower glutamate concentrations (10-30 μM) the K_m is higher while at increased glutamate values the K_m decreases. The Hill coefficient for Na^+ is also dependent on glutamate concentration, being ~1.2 at high [glutamate] and ~2-3 at low glutamate concentrations (Kanai et al., 1995). As a result, Kanai et al. (1995) suggested that one Na^+ might bind after glutamate. However, this proposal had not received much attention in the literature and it has been assumed that all Na^+ ions bind before glutamate (see for review Billups et al., 1998; Danbolt et al., 2001). Recently, Watzke et al. (2001) also proposed that at least one Na^+ ion must bind after glutamate. These authors found that the Na^+ I_{max} and K_m depends on

glutamate and that there is a reciprocal dependency of the glutamate I_{max} and K_m on $[Na^+]_o$. Also, uncaging glutamate (flash photolysis) to human embryonic kidney 293 (HEK293) cells expressing rat EAAT3 led to a rapid inward coupled charge movement that was dependent on extracellular Na^+ concentration. In particular, Watzke et al. (2001) demonstrated that the amplitude and not the decay kinetics of this rapid charge movement depended on extracellular $[Na^+]$. To account for these observations, Watzke et al. (2001) proposed that at least one Na^+ ion must bind after glutamate. They also suggested that this binding is rate-limited by a Na^+ and voltage independent conformational change and that the last Na^+ ion(s) transverses 55 – 61 % of the electrical field. The dependency of glutamate and Na^+ I_{max} and K_m on the extracellular Na^+ and glutamate concentration has also been reported for EAAT1 (Klockner et al., 1993; 1994). Lastly, another feature of transport correctly predicted by this model is that the apparent affinity for extracellular Na^+ is dependent on the identity of the substrate (Vandenberg et al., 1998).

A different view of Na^+ binding, has been put forth by Auger and Attwell (2000), who have argued against the possibility that Na^+ ions can bind after glutamate. Similar to Watzke et al. (2001), they examined Na^+ dependent transient currents in response to rapid glutamate applications. They reasoned that if Na^+ binds after glutamate, there should be an outward current following the rapid removal of glutamate. However, this argument assumes that the vast majority of the transporters are on an extracellular glutamate bound state and that glutamate and Na^+ would unbind to the outside instead of translocating inside following the rapid removal of glutamate. In short, one would not necessarily expect to observe such a current.

An issue that has not received much attention is whether the apparent affinity of extracellular Na^+ is voltage dependent. The presence of EAAT-specific Na^+ pre-steady state transient currents elicited by voltage jumps in cells expressing EAATs has led to the conclusion that Na^+ binding or a conformational change driven by Na^+ is voltage dependent (Wadiche et al., 1995a; Wadiche and Kavanaugh, 1998; Watzke et al., 2001; but see Mennerick et al., 1999). As a result, one expects that the Na^+ apparent affinity is voltage dependent, becoming lower with depolarization. However, in EAAT1 the Na^+ K_m is voltage independent (22 mM, -120 mV; 20 mM, -20 mV; Klockner et al., 1993; see also Barbour et al., 1991). In accordance with this result, Mennerick et al. (1999) showed that TBOA, a competitive antagonist for EAATs, blocked the same amount of Na^+ dependent capacitance charge at –70 mV and +70 mV. How can one explain these observations? Mennerick et al. (1999) suggested that TBOA may bind prior to Na^+ ions, or that Na^+ binding is not voltage dependent. However, it is also possible in EAAT1 glutamate (or TBOA) binding is voltage dependent. Then, at positive potentials although Na^+ binding decreases, the substrate binding increases and counteracts the Na^+ effect, thereby leading to similar apparent affinities at the two potentials.

Finally, until recently it was thought that only extracellular Na^+ could support amino acid transport through the EAATs even though Li^+ could replace at least one Na^+ in EAAT2 (Grunewald and Kanner, 1995). Borre et al. (2001) reported that EAAT3 could transport either glutamate or aspartate in the presence of extracellular Li^+. These authors demonstrated that 130 mM Li^+ can support up to 40 % of the aspartate uptake and ~15-20 % of the glutamate uptake seen with 130 mM Na^+ in oocytes expressing EAAT3. Stein and Kavanaugh (unpublished observations) also investigated the effects of Li^+ in

EAATs and found that Li^+ drives glutamate transport in EAAT1, EAAT3, and EAAT4 but not EAAT2 or EAAT5. Therefore, caution should be used when Li^+ is replaced for Na^+ to eliminate glutamate transport by the EAATs.

ii. Potassium binding

As mentioned earlier, glutamate transport requires the intracellular presence of K^+ (Barbour et al., 1988; Kanner and Sharon, 1978). Other monovalent cations such as Cs^+ (Barbour et al., 1988, 1991; Danbolt et al., 1990; Kataoka et al., 1997), Rb^+ (Barbour et al., 1991), or NH_4^+ (Mort et al., 2001; Zhang et al., 1998) can substitute for K^+. In Muller cells the following sequence for activating transport was observed $K^+ > Rb^+ > > Cs^+ >>>> Na^+$. The intracellular K^+ apparent affinity has been calculated to range between 16-35 mM (Amato et al., 1994; Barbour et al., 1988, 1991), although potassium K_m values are usually underestimated since all the measurements have taken place in the presence of intracellular 5-15 mM Na^+ (intracellular Na^+ K_m = 3 mM; Szatkowski et al., 1990), which will drive the transporters away from K^+-bound states. Similar apparent affinities have been reported for the extracellular K^+ binding site (Zerangue and Kavanaugh, 1996b). Interestingly, Amato et al. (1994) demonstrated that the intracellular K^+ apparent affinity is dependent on the identity of the substrate. For example, the D-aspartate steady-state current was five fold lower than the glutamate current and the potassium K_m was five fold lower for D-aspartate than glutamate. Thus, the slowing of the substrate bound steps is correlated with a higher intracellular K^+ affinity, consistent with a ping-pong model for glutamate transport (Amato et al., 1994; Kanner and Marva, 1982).

iii. Proton binding

An issue of controversy in the last decade is the identity of the pH-changing ion transported by EAATs. Recent work has focused on two possibilities: that a proton is cotransported with glutamate, or that a hydroxyl anion is countertransported. Bouvier et al. (1992) suggested that an OH^- is countertransported based on the observation that glutamate induced currents are larger in the presence of intracellular chaotropic ions (i.e SCN^-), suggesting an intracellular anion binding site. However, the subsequent finding that there is an uncoupled anion current through the EAATs (see Anion conductance) confounded this conclusion. Zerangue and Kavanaugh (1996a) proposed that a proton is cotransported along with glutamate and Na^+ in a step distinct from K^+ countertransport. This proposal stemmed from experiments with L-cysteine, a neutral amino acid that can serve as a glutamate transporter substrate. Unlike glutamate and its analogues, transport of L-cysteine does not induce intracellular acidification as measured by fluorescent dyes indicating that L-cysteine is recognized by the transporter as a neutral zwitterion (Zerangue and Kavanaugh, 1996a). Consistent with the conclusion that a H^+ is transported water containing deuterium isotope (D_2O) slows the EAAT3 presteady state anion current kinetics (Watzke et al., 2000).

Although the coupling of a proton to glutamate transport is widely accepted (Auger and Attwell, 2000; Levy et al., 1998; Watzke et al., 2000; Zerangue and Kavanaugh, 1996a,b), its binding order with respect to glutamate is unresolved. Some groups (Otis and Jahr, 1998; Otis and Kavanaugh, 1998) have suggested that the proton may bind after glutamate, while another proposed that the proton binds before glutamate (Watzke et al., 2000; see also Seal et al., 2001). The evidence for proton binding before glutamate is

based on the observation that the glutamate I_{max} is independent of extracellular pH (Watzke et al., 2000). However, this finding is inconsistent with previous work in both native and recombinant transporters (Auger and Attwell, 2000; Billups and Attwell, 1996; Fairman et al., 1998; Zerangue and Kavanaugh, 1996a) where an increase in the extracellular pH decreases the glutamate induced current. The reason for this discrepancy is unknown. In addition, Watzke et al. (2000) showed that the glutamate K_m, but not the maximal current (I_{max}) in both the forward and reverse transport modes of EAAT3 is dependent on the proton concentration on the cis-side of the membrane (Watzke et al., 2000).

A different binding order for protons and glutamate was proposed recently (Auger and Attwell, 2000). Studying the Purkinje neuron transporter, these authors showed that changing extracellular pH from 7.5 to 8.5 did not affect the rise kinetics of either a synaptically-activated transporter current or a transporter current activated by glutamate jumps in excised outside-out nucleated patches (see also Watzke et al., 2000). However, this pH change is sufficient to decrease the steady-state D-aspartate induced transport current in Purkinje cells. As a result, they proposed that a H^+ is countertransported with K^+ since computer simulations with the H^+ binding either before or after glutamate could not reproduce their experimental findings. This model, however, has several shortcomings as it fails to describe key experimental evidence. For instance, L-cysteine is transported without an intracellular pH change (Zerangue and Kavanaugh, 1996a), and at higher pH_o, the glutamate affinity is lower (Watzke et al., 2000; see also Chapter 1). In fact, the "proton countertransport" model predicts the opposite: as extracellular pH increases glutamate affinity also increases. However, a careful analysis of the effect of

protons on the transport kinetics is necessary before we conclude which model is consistent with all the data.

5. Voltage dependence of glutamate transport currents

Brew and Attwell (1987) using whole cell recordings in isolated Muller cells were the first to directly study the voltage dependence of the glutamate transport current (I-V). Since then several investigators have measured glutamate induced currents at different membrane potentials in various preparations (Barbour et al., 1991; Kanai et al., 1994,1995; Wadiche et al., 1995a,b). Irrespective of the EAAT subtype, at saturating glutamate concentrations (>100 μM) the I-V increases monotonically as the membrane potential becomes more hyperpolarized. Reducing extracellular Na^+ leads to a scaling down and a leftward shift of the I-V (Brew and Attwell, 1987). The leftward shift might be a result of the voltage sensitivity of the external Na^+ binding to the glutamate transporter. Therefore, at low Na^+ concentrations hyperpolarized potentials (<-40 mV; Brew and Atwell, 1987) will attenuate Na^+ binding and consequently the glutamate induced transport current. Consequently, the I-V shifts towards more negative membrane potentials (Brew and Attwell, 1987). Consistent with this, the glutamate induced I-V decreases and shifts to the left when Li^+, which has a 10 fold lower affinity than Na^+ (Wadiche et al., 1995a), replaces extracellular Na^+ (Stein and Kavanaugh, unpublished observations).

In contrast to EAAT3's non-saturating I-V at hyperpolarized potentials, at low glutamate concentrations the I-V saturates becoming almost voltage independent (Kanai et al. 1994). To explain this, Kanai et al. (1994) proposed that at low glutamate

concentrations, the voltage independent glutamate binding becomes rate limiting, although other explanations cannot be excluded (see Chapter 1).

Furthermore, it has been proposed that the I-V does not saturate at high glutamate concentrations because glutamate translocation from outside to inside is the rate-limiting electrogenic step in the cycle (Kanai et al., 1995). However, this view is now in question due to recent studies that suggest the early steps of the cycle might be rapid (Auger and Attwell, 2000; Grewer et al., 2000; Otis and Jahr, 1998; Otis and Kavanaugh, 2000; Watzke et al., 2001). Therefore, it is possible that at negative potentials a step with voltage sensitive transition rates subsequent to glutamate translocation limits the cycle. Candidates for this step are intracellular Na^+ release, intracellular glutamate unbinding, K^+ binding to the empty transporter, or K^+ driven re-orientation of the transporter outside. In summary, although significant progress has been made in our understanding the effect membrane potential has on glutamate transport kinetics we still do not know which steps in the cycle mediate the translocation of charge.

E. Kinetic Analysis

1. Substrate affinity and Binding rates.

An inspection of the literature shows that the glutamate K_m for activating the transport current ranges between 15-20 μM for EAAT1-EAAT3 (see for review Bridges et al., 1999). On the contrary, EAAT4 has approximately a ten-fold higher affinity for glutamate (Fairman et al., 1995) while EAAT5 has the lowest affinity compared to the other transporters (62 μM; Arriza et al., 1997). However, the affinities for radiolabeled glutamate uptake are significantly lower than their current counterparts (48, 97, 62 μM

for EAATs 1-3, respectively; Arriza et al., 1994). This discrepancy is quite apparent in rat EAAT1 (GLAST). Klockner et al. (1993) measured that the K_m for the glutamate induced current in oocytes expressing rat EAAT1 is 11 μM, while the K_m for uptake in oocytes was 77 μM (Storck et al., 1992). Similar results were obtained for EAAT3 (current K_m = ~20 μM; uptake K_m = ~160 μM; Koch and Kavanaugh, unpublished observations). No explanation has been offered for the discrepancy between the two experimental values.

In conjunction with the steady-state affinities, glutamate concentration jumps to outside-out patches from either brain slices or cells expressing recombinant transporters have allowed us to measure the glutamate dependence of the presteady-state anion current. This presumably reflects early parts of the cycle and thus approximates the glutamate K_d (k_{off}/k_{on}) value. In all cases studied to date the pre-steady state peak anion current has a lower affinity compared to the steady state current. For rat EAAT3 (Grewer et al., 2000), the glial (Bergles et al., 1997; Bergles and Jahr, 1997), and Purkinje cell transporters (Otis and Jahr, 1998), there is a four to ten fold difference between the peak and steady-state apparent affinity values, while for EAAT1 the difference is only 1.6 (Wadiche and Kavanaugh, 1998). This difference is explained by the following relationship. In any cyclical transport model under zero-trans conditions (substrate on only one side; as in the above measurements) the apparent affinity is approximated by $K_m = K_d \cdot r/(f+r)$, where K_d is the intrinsic dissociation constant and f is the translocation rate to the interior and r is the re-orientation rate from inside to outside (Lauger, 1991). Therefore, the magnitude of the difference between the intrinsic and apparent affinity is also dependent on the nature of the rate-limiting step. However, this equation assumes

100 % transport and capture efficiency. As a result, the above relationship is merely a simplification.

It has been proposed that the initial role of glutamate transporters in clearing glutamate after its release in the synaptic cleft is through rapid binding, and then, a subsequent transport step (Diamond and Jahr, 1997; Tong and Jahr, 1994; but see Auger and Attwell, 2000; Mennerick et al., 1999). Inherent to this hypothesis is that glutamate binding to the transporters should be rapid. Using rapid application of different concentrations of glutamate to either outside-out patches or whole cells one can measure the rate of onset of the anion current at different glutamate concentrations. Based on these measurements, the binding rates for recombinant EAAT1 (Mennerick et al., 1999; Wadiche and Kavanaugh, 1998), the Purkinje neuron transporter (Otis and Jahr, 1998), and EAAT3 (Grewer et al., 2000) yielded estimates of $6.8 \cdot 10^6$ $M^{-1}s^{-1}$, $1.8 \cdot 10^7$ $M^{-1}s^{-1}$, and $2 \cdot 10^7$ $M^{-1}s^{-1}$, respectively. Therefore, EAATs bind glutamate rapidly with rates similar to glutamate binding in ionotropic receptors (Hausser and Roth, 1997; Jonas et al., 1993).

2. Modeling

Since glutamate transporters may play a key role in fast synaptic transmission several investigators have attempted to elucidate transport kinetics and develop models to explain their behavior. Currently, four different models have been developed that simulate various aspects of glutamate transport kinetics.

Before I describe the different kinetic models, I will first summarize the most important kinetic observations to date regarding glutamate transport that these models

attempt to interpret. Schwartz and Tachibana (1990) suggested that the early parts of the glutamate cycle might be fast. They showed that glutamate uncaging (flash photolysis) to retinal Muller cell leads to the rapid activation of a transporter-associated current. At the time, they did not distinguish whether the current reflected the anion conductance or the coupled current. However, only recently has it been considered that the Na^+ bound steps of the cycle might be rapid. This suggestion is based on the observation that in the absence of permeant anions glutamate jumps to outside-out patches or cells expressing glutamate transporters leads to the generation of a fast Na^+ dependent coupled current (Auger and Attwell, 2000; Bergles and Jahr, 1997; Grewer et al., 2000; Otis and Kavanaugh, 1998; Bergles et al., submitted). Furthermore, in all EAATs studied to date a glutamate concentration jump leads to a submillisecond activation of an anion conductance that relaxes to steady-state. However, the speed of the decay to steady state varies among the transporter subtypes with EAAT4 having the slowest decay (Tzingounis et al, Soc Neur Abs 2000) followed by EAAT1 (Mennerick et al., 1999; Wadiche and Kavanaugh, 1998) then, EAAT3 (Grewer et al., 2000), and finally EAAT2 being the fastest (Otis and Kavanaugh, 2000; Bergles et al., submitted). Several studies also compared the kinetics of the coupled current to the anion current and found that in some cases the coupled current kinetics are faster than the kinetics of the anion current (Auger and Attwell, 2000; Bergles and Jahr, 1997; Grewer et al., 2000; Otis and Kavanaugh, 2000; Wadiche and Jahr, 2001; Watzke et al., 2001). Despite these qualitative similarities, models developed to describe transport kinetics differ from each other. However, one important similarity among the models is that the major conducting state is gated by the extracellular glutamate bound state (Auger and Attwell, 2000; Grewer et al.,

2000; Otis and Jahr, 1998; Otis and Kavanaugh, 2000; Wadiche and Kavanaugh, 1998; Watzke et al., 2001).

Wadiche and Kavanaugh (1998) developed a model to describe the basic properties of the macroscopic kinetics of the anion current induced by rapid application of either L-glutamate or D-aspartate to outside-out patches excised from oocytes expressing EAAT1. Their four state model tentatively placed the rate-limiting step of the cycle as translocation of the substrate bound transporter from outside to inside. Their model is consistent with their experimental finding that in EAAT1 the decay to steady-state is slow and dependent on the substrate (see also Bergles and Jahr, 1998; Watzke and Grewer, 2002). The slow substrate translocation step near the anion conducting state can account for the observation that substrates with a slow turnover rate more effectively activate the anion current. Their model also suggested that it is twice as likely that a glutamate molecule will unbind outside instead of being transported.

Otis and Jahr (1998) developed a model to describe the anion kinetics of the transporter expressed in Purkinje cells. Their model contains the minimum number of states predicted for a transporter that binds 3 Na^+ ions, 1 glutamate, 1 H^+, and 1 K^+ ion. They suggested that the rate-limiting step in the transport cycle might be glutamate unbinding to the inside. In addition, they proposed that the Na^+ binding sites are equal and independent of each other and that the proton might bind after glutamate. However, they did not exclude other possibilities for the proton binding order. An important suggestion by their model is that following translocation, one Na^+ unbinds first before glutamate.

Auger and Attwell (2000) modified this model by suggesting that the proton is exchanged with K^+ in a step separate from Na^+ and glutamate translocation. They also suggested that the conformation associated with translocation of the glutamate bound transporter from outside to inside is the major charge-moving step in the forward cycle accounting for the fast coupled currents observed in the absence of anions.

A fourth model suggested by Watzke et al. (2001), based on their studies of rat EAAT3, proposes that a Na^+ ion binds after glutamate. This Na^+ binding occurs within the electrical field and generates a rapid charge movement rate-limited by a Na^+ and voltage independent conformational change. Subsequent to Na^+ binding, a somewhat slower electrogenic glutamate translocation takes place. They also suggested that the rise of the anion current is correlated with the rapid decay of the Na^+ transient.

Foremost, these models illustrate that there is little consensus on how to either qualitatively or quantitatively account for the kinetics of glutamate transport. In principle more than one of the presented models could be correct because they describe different transporters. However, it is more likely that what differs among the subtypes are rates for entering and leaving each state.

3. Cycling rate

One parameter in question is the rate at which transporters cycle (turnover rate). Initially, biochemical studies suggested that transporters cycle at 1 s^{-1} (Danbolt et al., 1990). However, Wadiche et al (1995a) using electrophysiological techniques were able to estimate more accurately the turnover rate for EAAT2 expressed in Xenopus oocytes and more recently for EAAT1 (Wadiche and Kavanaugh, 1998). They estimated that

transporters cycle slowly, 14.6 s^{-1} – 16 s^{-1} (-80 mV) and that this rate is voltage dependent, becoming slower at depolarized potentials. They also showed that the turnover rate is dependent on the identity of the substrate. One caveat to their measurements is that oocytes contain ~10-15 mM glutamate and Na^+ (Zerangue and Kavanaugh, 1996a,b) which could possibly slow down the cycling rate (Otis and Kavanaugh, 1998). Recently, Bergles and Jahr (1998) estimated that the transporters cycle at much faster rate, 40–50 s^{-1} (see also Otis and Kavanaugh, 2000), by measuring the recovery rate of appearance and reappearance of the anion current in outside-out patches taken from hippocampal astrocytes (expressing EAAT1 and EAAT2). In addition, in patches removed from Purkinje neurons, the recovery time constant of the anion current indicates a turnover rate of 12-14 s^{-1} (Auger and Attwell, 2000; Otis and Jahr, 1998). But, it is unclear whether this estimation reflects the cycling rate of EAAT3 or EAAT4, since both transporters are localized on the Purkinje cell somata (Furuta et al., 1997). In general, a caveat in the patch recordings is that if the capture efficiency for transporters is low, then the cycling rate will be overestimated. Therefore, before we have a complete understanding of transport kinetics, we will not know which technique provides the most accurate value for the EAAT cycling rate.

4. Temperature dependence of glutamate transport

Since glutamate transport requires the EAATs to undergo a series of conformational transitions, significant temperature dependence of transport is expected. Q_{10} values of 1.95 (Schwartz and Tachibana, 1990) and 3.2 (Wadiche and Kavanaugh, 1998) have been measured at steady state for the transporter currents expressed by Muller

cells and EAAT1, respectively. In contrast the thermodynamically uncoupled anion conductance had only a Q_{10} of 0.96 (Wadiche and Kavanaugh, 1998). Rapid glutamate jumps, in the presence of permeant anions, to outside-out patches from hippocampal astrocytes leads to the activation of the anion current. The decay of the anion current to steady-state was temperature sensitive, $Q_{10} \sim 2$, but not the steady-state amplitude. This is consistent with the observations of Wadiche and Kavanaugh (1998). Also, the recovery rate of the peak anion conductance from steady-state had a Q_{10} of 2 (Bergles and Jahr, 1998). Similar results were obtained for the synaptically activated transporter current in Purkinje cells. In the presence of permeant anions the decay kinetics but not the amplitude were temperature sensitive. However, the coupled peak current had a Q_{10} of 3 (Auger and Attwell, 2000). These observations are consistent with the coupled transport current reflecting a multistep process dependent on conformational changes in the transporter protein. In contrast, the small Q_{10} for anion conductance is consistent with anion flux through a pore (Hille, 2001).

G. Structure-Function studies

1. Cation and amino acid binding sites.

Several groups have attempted to identify residues in the transporters that are involved in amino acid and cation recognition (Figure 1). An arginine residue in TM8 (arg^{447} EAAC1; arg^{479} GLAST) originally identified as essential for transport (Conradt and Stoffell, 1995) is now thought to bind glutamate's γ-carboxylate (Bendahan, et al., 2000), since its mutation to a cysteine residue supports transport of the neutral amino acid L-cysteine, but not of glutamate. This mutation also transforms the transporter to an

electroneutral exchanger by eliminating K^+ coupling suggesting a close relationship between the potassium and the amino acid binding sites. Furthermore, conserved mutations of residues tyr^{403} and glu^{404} (GLT-1 numbering; Zhang et al., 1998; Kavanaugh, et al., 1997) to phenylalanine and aspartate, respectively, also convert the transporter to an electroneutral exchanger by eliminating K^+ coupling. In support of glu^{404}, tyr^{403}, and arg^{447} involvement in K^+ coupling, the neutral amino acid transporters ASCT-1 and ASCT-2, which do not support K^+ transport lack these residues. Besides influencing K^+ coupling, the E404D mutant bind aspartate better than glutamate while the Y403F and Y403W have higher Na^+ apparent affinity and broadened cation selectivity (Pines et al., 1995; Zhang et al., 1998). Also, serine residues (S440-S443) found in the second loop between helix 7 and 8 are involved in the discrimination of Na^+ to Li^+ (Zhang et al., 1999; Borre et al., 2001). Finally, chimera studies have demonstrated that the difference in DHK sensitivity and chloride conductance between EAAT1 and EAAT2 is due to differences in the amino acid sequence in the region encompassing the two loops, TM6-TM8 (Mitrovic et al., 1998; Vandenberg et al., 1995).

2. Distinction of glutamate transport from the anion conductance

Replacement of amino acids val^{417}, val^{420}, and iso^{421} (EAAC1 numbering) to cysteine followed by modification by MTSET leads to the elimination of glutamate transport without any effect on the gating of the anion conductance (Seal et al., 2001; Ryan et al., 2002; Borre et al., 2002). After the MTSET modification, the glutamate activated current reversed near E_{cl} irrespective of the substrate used to activate it. However, the apparent affinity for glutamate became higher in the V417C mutant (Seal et

al., 2001), lower in the I421C mutant (Borre et al., 2002), and did not change in the V420C mutant (Ryan et al., 2002). The reason for these differences among the different mutations is unclear. Most importantly, the ability to activate the anion conductance in the absence of transport re-affirms the notion that the major anion conductance is gated when the transporters are bound with glutamate facing outside (Wadiche and Kavanaugh, 1998; Otis and Jahr, 1998).

H. Glutamate transporter modulation.

The emerging picture in the glutamate transporter field is that EAATs are regulated by multiple signaling pathways including, protein kinase C, arachidonate, and tyrosine kinase linked pathways. However, what has become apparent is that the glutamate transporter subtypes are affected to varying degrees by these signaling cascades.

1. Modulation by PKC

Early on, it was shown that application of phorbol esters – PKC activators – to HeLa cells heterologously expressing EAAT2 led to its phosphorylation and, subsequently, to increased amino acid uptake (Cassado et al., 1993). However, Tan et al. (1999) demonstrated that HeLa cells endogenously express EAAT3, which in turn is regulated by PKC activation. These authors suggested that in HeLa cells transfected with EAAT2, PKC upregulates the activity of EAAT3 and not EAAT2, accounting for the finding of increased uptake.

Similar to EAAT2, contradictory results exist in regards to the regulation of EAAT1 by PKC. Cassado et al. (1991) showed that application of 12-O-tetradecanoylphorbol 13-acetate (TPA) to cultured glial cells, which predominantly express EAAT1 (Mennerick et al., 1994), led to increased glutamate uptake (see also Daniels and Vickroy, 1999). However, Gonzalez and Ortega (1997), applying similar methods to chick Bergmann glial cell cultures found a decrease in glutamate uptake. In addition, PKC activation decreased glutamate transport activity in Xenopus oocytes and HEK293 expressing EAAT1 (Conradt and Stoffel, 1997). Furthermore, removal of all putative PKC sites by site-directed mutagenesis did not abolish the inhibition of glutamate transport suggesting that EAAT1 is inhibited by phosphorylation at a non-PKC consensus site. Alternatively, some other protein is the target of PKC and that protein, in turn, leads to glutamate transport inhibition.

The effect of PKC on EAAT3 seems to also depend on the expression system. Trotti et al. (2001) compared the effect of PKC activation on EAAT3 expressed in different systems. Activation of PKC in oocytes expressing EAAT3 decreased membrane capacitance, decreased the transport-induced current, and increased cytosolic accumulation of EAAT3 protein. These authors then suggested that PKC activation inhibits EAAT3 by promoting its retrieval from the plasma membrane. PMA also decreased glutamate uptake in a MDCK cell line stably transfected with EAAT3 but enhanced EAAT3-induced glutamate uptake in the rat C6 glioma cells as shown previously by Robinson and colleagues (Dowd and Robinson, 1996; Davis et al., 1998).

2. Modulation by arachidonic acid

Arachidonic acid (AA) and its metabolic products are important second messengers that can modulate a variety of CNS functions (Meves, 1994). It is believed that activation of PLA_2 leads to the generation of AA, which then, may act as a retrograde messenger. Because of its importance in CNS homeostasis several laboratories have investigated the effect of arachidonate on glutamate transporters. Initially, Rhoads et al. (1983) demonstrated in synaptosomes that there is an inhibition of glutamate uptake in response to cis-unsaturated long chain fatty acids. Subsequently, Volterra et al. (1992) found that arachidonic acid inhibits glutamate uptake in synaptosomes and cultured astrocytes from rat cerebral cortex (see also Barbour et al., 1989; Manzoni and Mennini, 1997; Lundy and McBean, 1995). In addition, Zerangue et al. (1995) showed that EAAT1 is inhibited by arachidonic acid, while in EAAT2 AA increases the apparent affinity for glutamate without modulating the maximum uptake. No effect was seen in EAAT3. Consistent with the EAAT2 data, application of arachidonic acid to outside-out patches from hippocampal astrocytes (expressing predominantly EAAT2) did not affect the transporter kinetics in response to saturating glutamate concentrations (Diamond et al., 1998). In contrast to the previous studies, in cultured Purkinje cells which express EAAT4, application of arachidonic acid leads to a potentiation of the aspartate induced transport current (Kataoka et al., 1997). In Chapter 2 of this dissertation (see also Fairman et al., 1998) we studied the effect of arachidonate to EAAT4 to understand the mechanism of its modulation.

3. Modulation by Tyrosine kinases

A model for studying glutamate transport modulation by different kinases is the C6 glioma cell line, which only expresses EAAT3 (Dowd et al., 1996). In these cells, application of platelet-derived growth factor (PDGF) increases the cell surface expression of EAAT3 (Sims et al., 2000). In particular, the PI3 kinase inhibitor wortmannin inhibits this effect while no effect is seen with PKC inhibitors. Further work is needed as to whether other tyrosine kinases affect transport activity.

4. Modulation by transportable substrates

The pioneering work of Ramamoorthy and Blakely (1999) demonstrated that the trafficking of serotonin transporters is dependent on the substrate (see also Bernstein and Quick, 1999 for GAT1). Subsequently, Duan et al. (1999) demonstrated that application of L-glutamate or D-aspartate, but not L-trans-PDC increases cell surface expression of EAAT1 in astrocytes grown in culture, an effect dependent on the actin cytoskeleton. A similar phenomenon was found for EAAT4, but in that case all transportable substrates could induce the effect (Gegelashvili et al., 2000). To date, no mechanism has been proposed to explain these observations.

SUMMARY

The main aim of this dissertation is to characterize several pertinent aspects of glutamate transport by EAATs. Three sets of experiments are described in the following chapters.

First, we characterized the kinetics of EAAT1-4 under various conditions, with a particular focus on the neuronal transporter EAAT3. This study has led to the description for the first time of an electrogenic alternating access kinetic model of glutamate transport. This model has allowed us to estimate that the capture efficiency of EAAT1-3 is low (~50%, -70 mV), while that of EAAT4 is high (>90%).

Second, we describe the effect of arachidonic acid on the neuronal transporter EAAT4. We determined that arachidonic acid modulates the transporter by gating a proton conductance that is thermodynamically uncoupled from glutamate uptake.

Lastly, we examined whether the neuronal transporter EAAT3 functions as an oligomer or a monomer. As a result, through the use of cross-linking experiments and structure-function studies we propose that EAAT3 is pentamer of functionally independent subunits.

CHAPTER 1

A kinetic model for glutamate uptake

Anastassios V. Tzingounis[1,2], Scott Eliasof[1], Alex Stein[1], and Michael P. Kavanaugh[1]
1. Vollum Institute and 2. Neuroscience Graduate Program, Oregon Health & Sciences University, Portland, OR 97201

Corresponding author:
Michael Kavanaugh
Vollum Institute, L-474
Oregon Health & Sciences University
Portland, OR 97201
phone: 503-494-4602
fax: 503-494-6972
email : kavanaug@ohsu.edu

Acknowledgments:

We thank Drs Dwight Bergles, Craig Jahr, Peter Larsson, John Williams, and Jacques Wadiche for discussions and comments on the manuscript.

ABSTRACT

The microscopic kinetics of glutamate transporters determines the transmembrane glutamate gradient and influence the time course of postsynaptic responses to glutamate. Since the binding order and many pertinent rate constants in the transport cycle are difficult to determine directly, we developed a model constrained by the dependence of the steady-state and pre-steady-state transporter currents on glutamate, H^+, Na^+, K^+, and membrane potential. The data are described by a model with ordered binding of two Na^+ ions preceding binding of glutamate and a proton in a random sequence. A third Na^+ ion then binds and a fast gating transition allows access of the complex to the intracellular compartment. After release, a slower reorientation of the transporter occurs with countertransport of one intracellular K^+ ion in the forward cycle. With intracellular K^+ replaced by Na^+ this reorientation occurs approximately 50 times more slowly, and with intracellular choline the reorientation is not observed. The rate-limiting step in the cycle varied with membrane potential and changes in substrate concentrations. In saturating glutamate at 25°, the cycling time constants of the transporters (EAAT1-EAAT4) in patches ranged from 24 to 100 ms. The glutamate capture efficiency, or probability of transport following binding to the transporter, ranged from 40-50% for the glial transporters EAAT1 and EAAT2 and the neuronal transporter EAAT3 (at –70 mV), suggesting that synaptic glutamate may be buffered by binding and unbinding multiple times at synapses where these transporters are present. In contrast, the Purkinje neuron transporter EAAT4 exhibited a capture efficiency >90%.

key words: glutamate transporter, uptake, kinetics, neurons, astrocytes, postsynaptic.

INTRODUCTION

The amplitude and time course of the synaptic glutamate concentration determines the postsynaptic response (for review see Bergles et al., 1999; Clements, 1996, Danbolt, 2001). In addition to diffusion, glutamate clearance from the synaptic cleft is dependent on glutamate transporter density, location, and kinetics. The slow glutamate transporter cycling rate (~15 s^{-1} at 22° Wadiche et al., 1995a) supported the proposal that, initially, the transporters shape the glutamate concentration time course on the submillisecond scale by rapid binding rather than transporting glutamate to the intracellular space (Diamond and Jahr, 1997; Tong and Jahr, 1994). Recently, several reports have suggested that in addition to binding, other early stages of the transport cycle may also be rapid, leading to the hypothesis that glutamate translocation/sequestration can occur on a fast time scale (Auger and Attwell, 2000; Bergles and Jahr, 1997; Wadiche and Kavanaugh, 1998; Grewer et al., 2000; Mennerick et al., 1999; Otis and Kavanaugh, 2000). In particular, it has been suggested that transporters remove glutamate from the synaptic cleft with high capacity and efficiency at a rate similar to glutamate diffusion from the cleft (Auger and Attwell, 2000). Nevertheless, there is evidence that glutamate in some circumstances can diffuse away from the synaptic cleft ("spillover") to reach either extrasynaptic receptors, transporters, or neighboring synapses (for review see Bergles et al., 1999; Kullman, 2000). The extent of glutamate spillover and sustained elevated glutamate concentration may depend on presynaptic activity, synapse morphology, transporter saturation, and transporter capture efficiency.

To understand the role transporters play in synaptic transmission and glutamate homeostasis, a more complete characterization of transport kinetics is needed, including the determination of substrate binding order as well as the rates and voltage dependencies of various steps in the cycle. Therefore, we used a combination of steady-state and pre-steady state voltage clamp recordings, concentration jump techniques along with computer modeling to characterize the kinetics of glutamate transport under different ionic (Na^+, K^+, H^+) conditions and membrane potentials. Our results suggest that binding of two Na^+ ions precedes the random binding of proton and glutamate to the transporter, and following binding of an additional Na^+ ion the complex is transported in a step separate from K^+ countertransport. In addition, simulations suggest that the slowest step in the transport cycle is the transport of the K^+ to the outside, which involves inward charge movement presumably due to an intrinsic transporter gating charge translocation. In contrast, the faster conformational change that is associated with the transition of the glutamate-bound transporters from outside to inside is voltage independent. Lastly, kinetic modeling of the data suggests that the capture efficiency of EAAT1, EAAT2, and EAAT3 is approximately 50% and strongly dependent on membrane potential, while EAAT4's capture efficiency is greater than 90 % at -70 mV.

MATERIALS AND METHODS

Two electrode voltage clamp recordings. Stage V-VI Xenopus oocytes were injected with capped mRNA (50 ng/oocyte) transcribed from cDNA encoding EAAT1-3 (Arriza et al., 1994). Membrane currents were recorded 2-4 days following injection. The extracellular Ringers solution (ND96) contained: 96 mM NaCl, 2 mM KCl, 1.8 $CaCl_2$, 1 mM $MgCl_2$.

Buffers were present at 5 mM and consisted of MES/HEPES (pH 6.5), Na/HEPES (pH 7.5), or HEPES/Tris (pH 8.5). Solutions containing indicated ion substitutions were changed by bath exchange. Recordings were performed at 22 °C-25 °C with a Geneclamp 500 amplifier. Acquisition was performed with an IBM-compatible PC (Gateway) using a Digidata 1200 A/D controlled with pCLAMP 6.0 program (Axon Instruments, Foster City, CA). The currents were low-pass filtered at 1 kHz and digitized at 5 kHz. Electrodes were filled with 3 M KCl and had tip resistances <1 MΩ. The bath was grounded with a Ag/AgCl electrode. The current-voltage dependence induced by different substrates was estimated by subtracting control currents from currents recorded in the presence of substrate.

Outside-out patch recordings. Prior to patch excision, the vitelline membrane was manually removed. Outside-out patches were obtained using pipettes (0.8-2 MΩ; Warner Instruments, Hamden, CT) that were fire polished. EAAT4 patches were obtained from HEK cells stably expressing rat EAAT4 (Lin et al., 1998; Jackson et al., 2001). The cell line was a generous gift of Dr. Jeff Rothstein. Unless stated the intracellular solutions contained 100 mM KSCN, 10 mM KCl, 3 mM $MgCl_2$, 5 mM Na-HEPES, and 10 mM EGTA adjusted to pH 7.5 with Tris-base. Extracellular solutions contained: 110 mM NaCl, 3 mM $MgCl_2$, and 5 mM Na-HEPES, adjusted to pH 7.5 with Tris-base (Wadiche and Kavanaugh, 1998). Rapid solution changes at the tip of the pipette were made using a glass theta tube (Warner Instruments, Hamden, CT) mounted to a piezo-electric switch (Vernitron, Bedford, OH). Solutions exchange times were monitored regularly by rupturing the patch and recording junction currents across the open tip. Membrane currents were

recorded with an Axopatch 200B voltage clamp (Axon instruments). Records were low pass filtered at 1-2 kHz and digitized at 5-20 kHz. Traces were averaged 3-20 times.

Kinetic modeling. Using ScoP software (Simulation Resources, Berrien Springs, MI; http://www.simresinc.com) we developed a kinetic model to simulate EAAT1-4 (Otis and Jahr, 1998; Otis and Kavanaugh, 2000; Wadiche and Kavanaugh, 1998). In reaction steps the voltage dependence assigned to the forward rate constant has the form $k_{f0}exp^{[-\lambda zVF/RT)]}$ while the backward rate constant has the form $k_{b0}exp^{[(1-\lambda)zVF)/RT)]}$, where k_{f0} and k_{b0} are the forward and backward rate constants at 0 mV; z is the charge moved, λ designates the location of the energy barrier within the electrical field, V is the membrane potential, T = 298 K, and F and R are Faraday's constant and the gas constant (Otis and Kavanaugh, 2000). The sum of charge moved (z) is +2 per forward cycle (Levy et al., 1998; Zerangue and Kavanaugh, 1996b). Capture efficiency was estimated by modeling an ultrashort (10 μs) pulse of saturating glutamate, and monitoring the occupancy of the T_iNa_2 state (modified in this simulation to be an absorbing state).

RESULTS

The proton is transported through the Na^+-hemicycle

The observation that cysteine (pK 8.3) is transported by EAAT3 without intracellular acidification (unlike glutamate or cysteate) along with the suggestion that it is recognized by EAAT3 as a neutral moiety led to the hypothesis that a proton is cotransported as an ion pair with amino acid in the Na^+-hemicycle (Zerangue and Kavanaugh, 1996a,b). However, recent reports have questioned the conclusion that the protonated cysteine is the transported species (Auger and Attwell, 2000; Watzke et al.,

2000), and suggest that a proton is transported through the K^+ countertransport hemicycle (Auger and Attwell, 2000). To explain the lack of intracellular acidification during cysteine transport, such model requires that the transported cysteine species is the deprotonated thiolate ion. Therefore, to test whether L-cysteine is transported as neutral zwitterion (Zerangue and Kavanaugh, 1996a) and in an effort to determine the proton translocation pathway (Na^+-hemicycle or K^+-hemicycle) we examined how proton and substrate concentrations affect steady-state transport currents in EAAT3.

To distinguish whether cysteine is recognized by the transporter as a deprotonated thiolate ion or neutral zwitterion, we studied the effect of extracellular pH on the apparent affinity of EAAT3 for cysteine (see also Zerangue and Kavanaugh, 1996a). As cysteine has a pK_a of 8.3, a change in the extracellular pH from 8.5 to 6.5 will decrease the concentration of the thiolate ion approximately 40 fold. As a result, a proportionate change in the cysteine apparent affinity should take place if the deprotonated thiolate ion is the transported species (Figure 1). The K_m values for cysteine (at -30 mV) were 222 ± 16 μM (n=4) and 279 ± 18 μM (n=4) for pH 8.5 and pH 6.5, respectively. Although the transporter affinity for glutamate, and possibly for the deprotonated thiolate ion, is approximately 3.3-fold higher at pH 6.5 than 8.5 (Figure 4B), this cannot account for the small change in cysteine K_m (1.25 fold) (Figure 1). This result suggests that cysteine cannot be recognized by EAAT3 predominantly in the anionic form as was recently suggested (Auger and Attwell, 2000; Watzke et al., 2000).

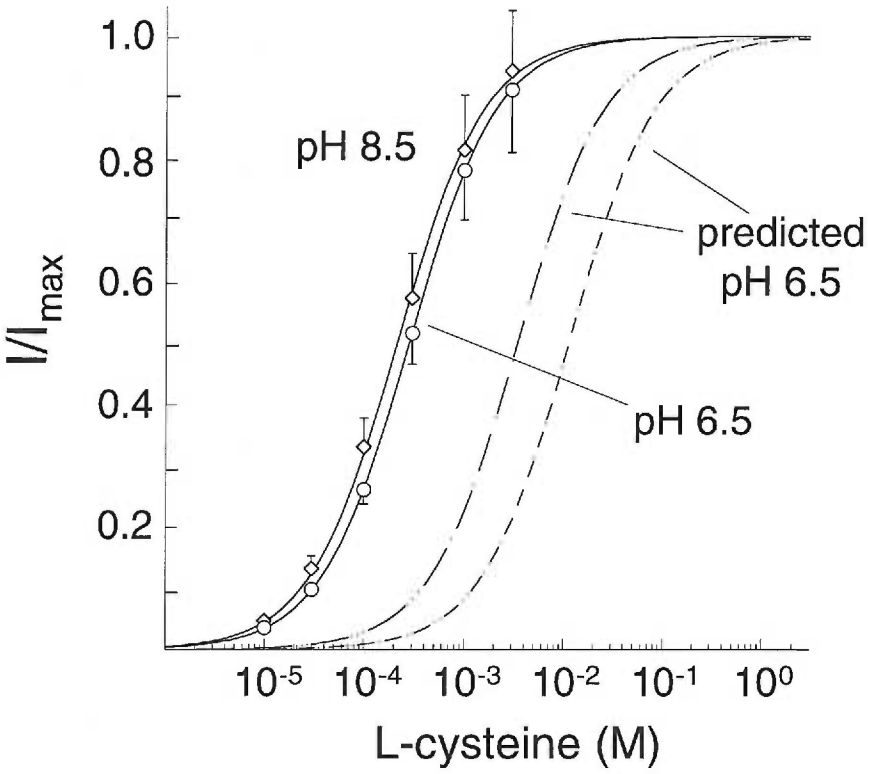
1.0
0.8
0.6
0.4
0.2
I/I_max
pH 8.5
predicted
pH 6.5
pH 6.5
10^-5 10^-4 10^-3 10^-2 10^-1 10^0
L-cysteine (M)

Figure 1. Cysteine is transported by EAAT3 as a neutral zwitterion. Cysteine (pK 8.3) concentration dependence of currents at pH 8.5 and pH 6.5 at –30 mV. Curves are least squares fit of the data (mean ± S.E.; n=5). Currents are normalized to their maximal response obtained at either pH 8.5 or 6.5. The K_m values are 222 μM (pH 8.5) and 279 μM (pH 6.5). Dashed lines curves represent the predicted cysteine concentration dependence had cysteine not be transported as neutral zwitterion. The predicted K_m value at pH 6.5 would then be either 11327 μM (40.6 fold shift; short dashed lines) or 3453 μM (12.35 fold shift; long dashed lines) if we account that the thiolate anion would have higher affinity for the transporter at pH 6.5 (see figure 4B). Data acquired by Scott Eliasof.

Voltage dependence of substrate interactions

To further investigate the interaction of protons with the transporter and whether L-cysteine is transported in a protonated form, we examined the effect of pH and voltage on the substrate evoked transport currents. At pH 7.5, lowering glutamate concentration caused the steady-state current-voltage relationship (I-V) to saturate and develop a negative slope at negative membrane potentials (Figure $2A_1$; see also Kanai et al., 1994). This result is consistent with glutamate binding becoming rate-limiting at these potentials, since it has an opposite voltage-dependence from the net current (Wadiche et al. 1995a). Lowering the proton concentration dramatically reversed this effect at negative potentials (Figure $2B_1$), consistent with proton binding (which has the same voltage-dependence as the net current) becoming limiting at high pH. In contrast to the anionic amino acids glutamate and cysteate (Figure $2A_{1,3}$, $2B_{1,3}$), the cysteine current did not saturate or exhibit a negative slope at low cysteine concentrations (Figure $2A_2$) regardless of extracellular proton concentration (Figure $2B_2$). This supports the proposal that cysteine binds as a neutral moiety since it lacks apparent voltage-dependent binding in contrast to the negatively charged amino acids, glutamate or cysteate. In addition, as with changing extracellular pH the saturation of the glutamate I-V was reversed by altering the extracellular Na^+ concentration (Figure 3A), but not the K^+ concentration (Figure 3B). This is also consistent with the hypothesis that the protons are transported through the Na^+-limb of the cycle. Together with previous data showing that cysteine transport does not result in intracellular acidification (Zerangue and Kavanaugh, 1996b), these data are difficult to reconcile with translocation of a pH-

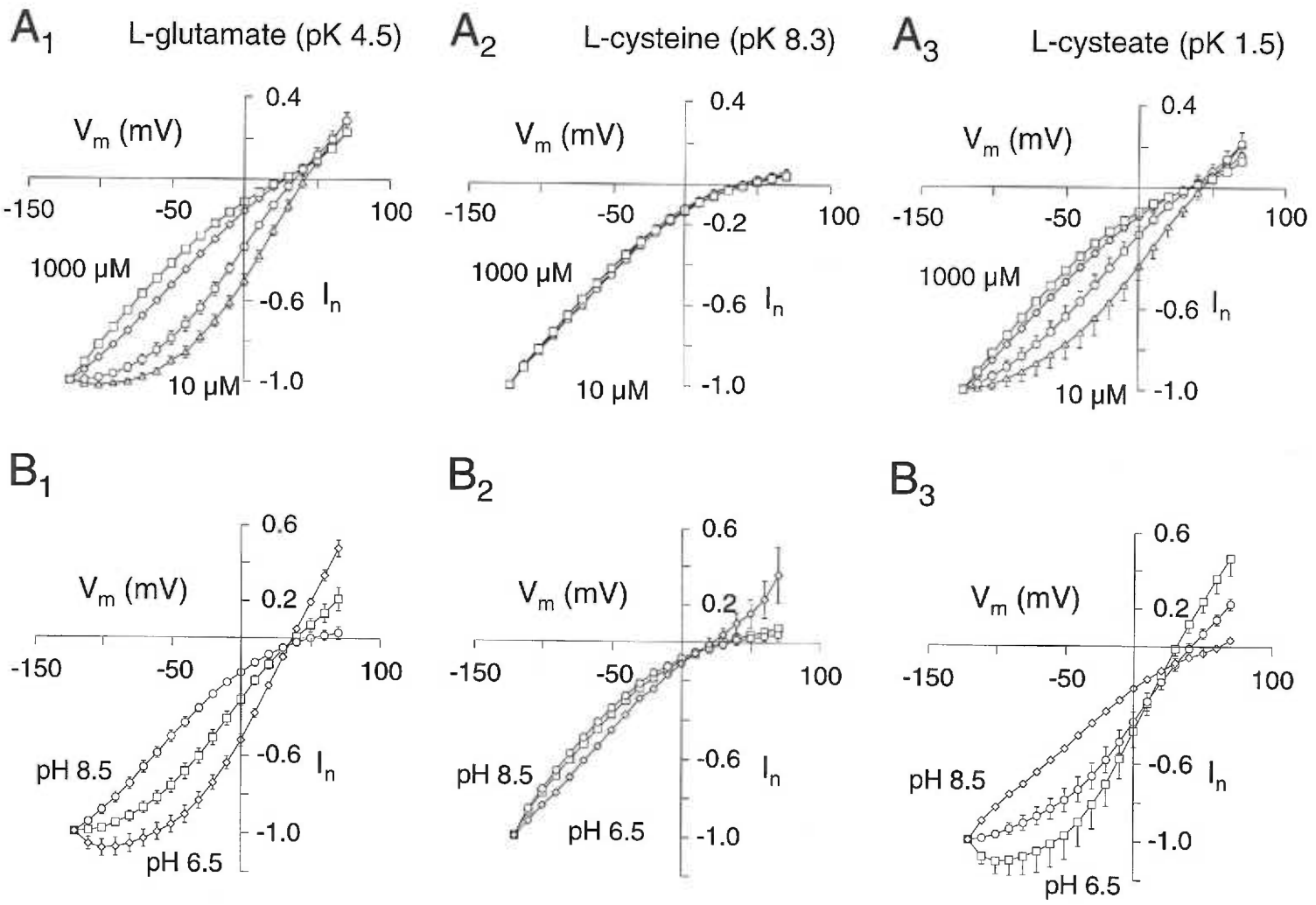
A1
L-glutamate (pK 4.5)
A2
L-cysteine (pK 8.3)
A3
L-cysteate (pK 1.5)
Vm (mV)
0.4
-150
-50
100
1000 µM
-0.6
In
10 µM
-1.0
-0.2
B1
B2
B3
0.6
0.2
pH 8.5
pH 6.5

Figure 2. Electrostatic effects of extracellular proton and substrate concentrations. Voltage-dependence of currents induced by concentrations of: (A_1) glutamate (10, 30, 100, and 1000 μM) at pH 7.5 and (B_1) 10 μM glutamate at pH 8.5, 7.5, and 6.5, (A_2) cysteine (10, 30, 100, and 1000 μM) at pH 7.5 and (B_2) 30 μM cysteine at pH 8.5, 7.5, and 6.5, and (A_3) cysteate (10, 30, 100, and 1000 μM) at pH 7.5 and (B_3) 10 μM cysteate at pH 8.5, 7.5, and 6.5. Each current-voltage relationship was normalized to the current induced by the respective amino acid concentration at –120 mV. The data were acquired in collaboration with Scott Eliasof.

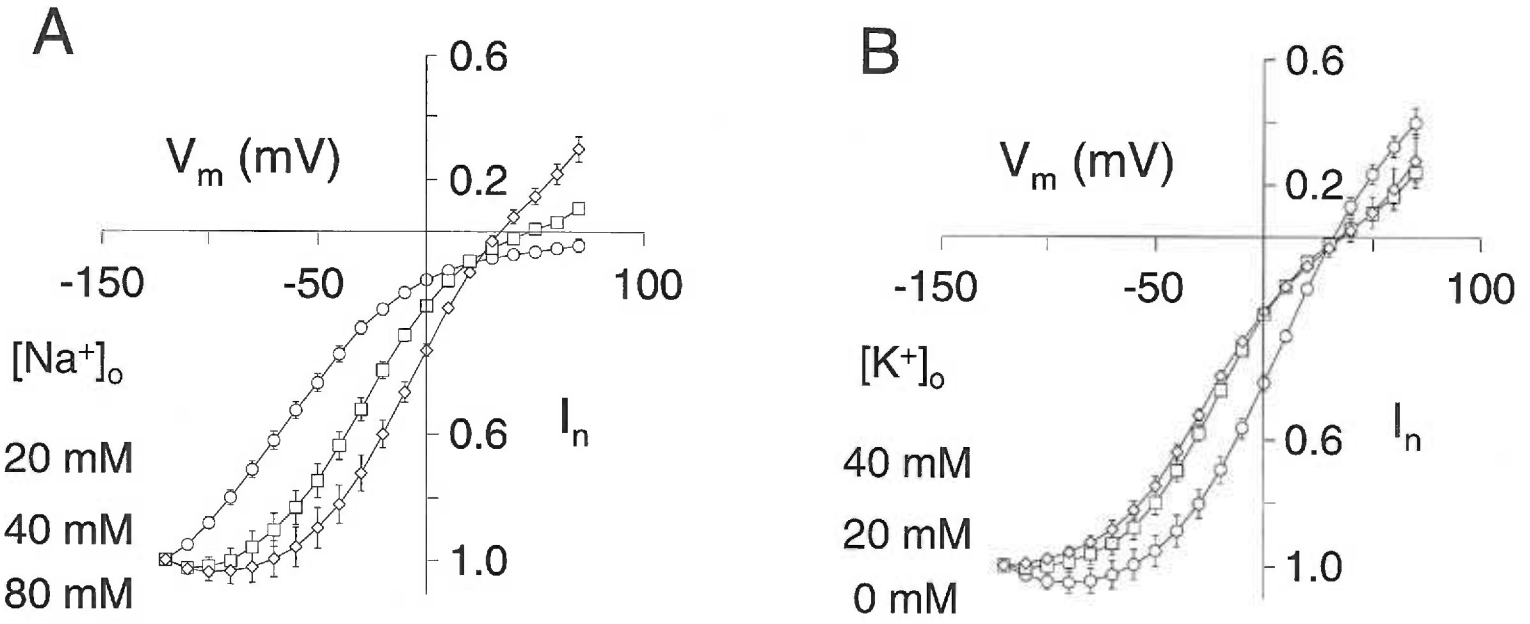
A
0.6
V_m (mV)
0.2
-150
-50
100
$[Na^+]_o$
I_n
20 mM
0.6
40 mM
80 mM
1.0
B
0.6
V_m (mV)
0.2
-150
-50
100
$[K^+]_o$
I_n
40 mM
0.6
20 mM
0 mM
1.0

Figure 3. Electrostatic effects of $[Na^+]_o$, but not $[K^+]_o$, are similar to $[H^+]_o$. (A) Voltage-dependence of currents induced by 10 μM glutamate at different Na^+ concentrations. Each current-voltage relationship was normalized to the current induced by glutamate at –120 mV. (B) Voltage-dependence of currents induced by 10 μM glutamate at different K^+ concentrations. Each current-voltage relationship was normalized to the current induced by glutamate at –120 mV. Data were acquired in collaboration with Scott Eliasof.

changing ion in the K^+-hemicycle and suggest that a proton must be cotransported in the Na^+-hemicycle.

Protons and glutamate bind in a random order

Protons have been proposed to bind either before glutamate (Watzke et al., 2000; Seal et al., 2001) or after glutamate (Otis and Jahr, 1998). An alternative possibility is a random binding order of glutamate and protons. To attempt to distinguish between these binding order models we examined the influence glutamate and protons have on each other's steady-state kinetic parameters. Analytical solutions of a cyclical kinetic scheme with proton binding before glutamate predicts that the glutamate I_{max} would be independent of the external pH while the glutamate K_m is dependent on pH (Stein, 1990; Watzke et al., 2000). However, if the glutamate I_{max} and K_m both depend on extracellular proton concentration and a reciprocal dependence is observed for the proton I_{max} and K_m with respect to extracellular glutamate concentration, a random binding order is predicted (Stein, 1990; see Watzke et al., 2000 for analytical solutions).

Consistent with previous studies (Auger and Attwell, 2000; Barbour and Attwell, 1988; Billups and Attwell, 1996; Billups et al. 1996; Fairman et al., 1998; Zerangue and Kavanaugh, 1996b; but see Watzke et al., 2000), we found that the extracellular proton concentration strongly affected the glutamate-dependent current (Figure 4A). Altering extracellular pH from 8.5 to 6.5 decreased the glutamate K_m between one to five fold depending on the membrane potential, reaching a limiting value as membrane potential becomes more negative (Figure 4B). In addition, a 10-fold increase in extracellular glutamate concentration decreased the proton K_m and increased the I_{max} about three fold

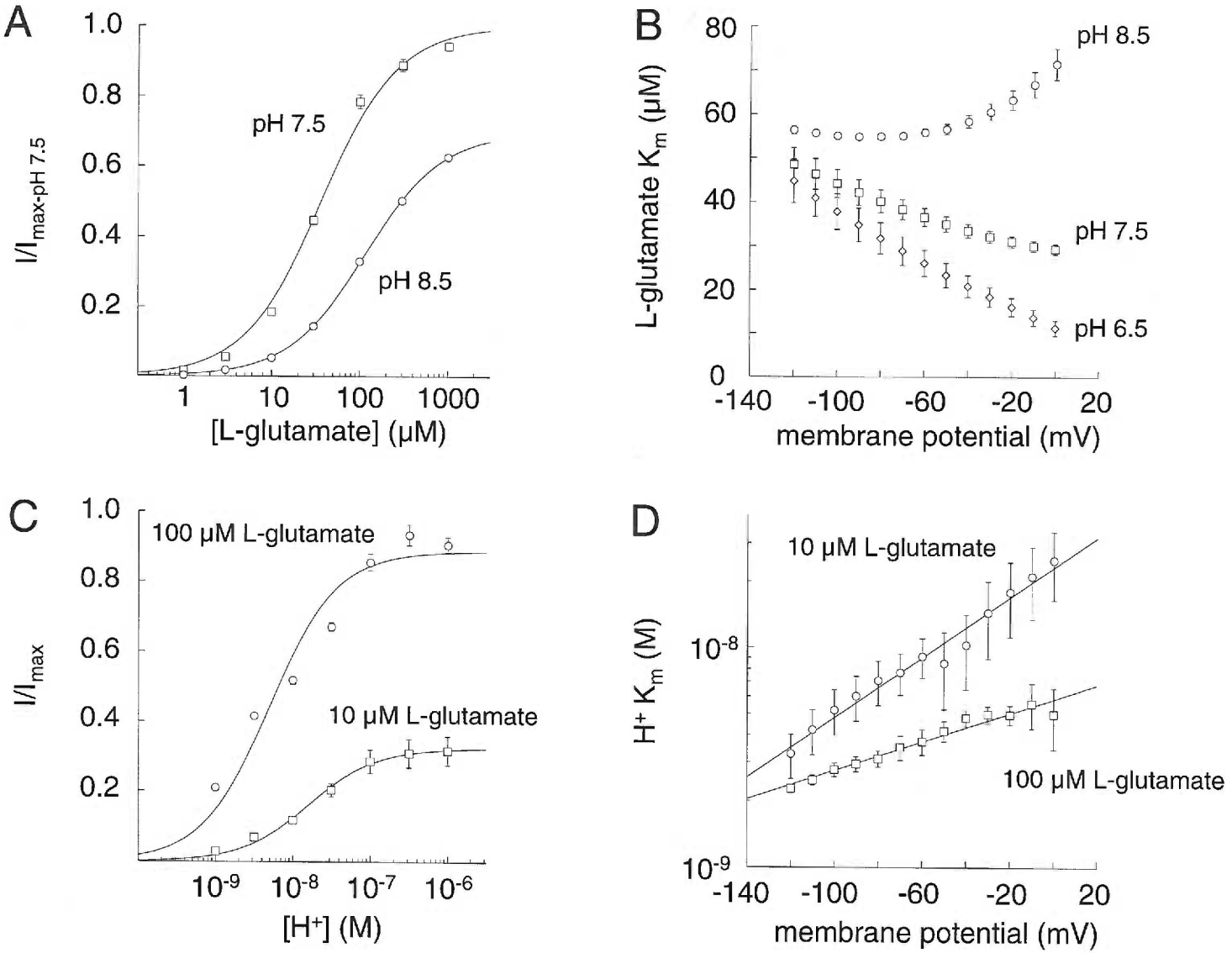
A
1.0
0.8
0.6
0.4
0.2
I/I max-pH 7.5
pH 7.5
pH 8.5
1
10
100
1000
[L-glutamate] (μM)
B
80
60
40
20
0
L-glutamate K m (μM)
pH 8.5
pH 7.5
pH 6.5
-140
-100
-60
-20
20
membrane potential (mV)
C
1.0
0.8
0.6
0.4
0.2
I/I max
100 μM L-glutamate
10 μM L-glutamate
10-9
10-8
10-7
10-6
[H+] (M)
D
10 μM L-glutamate
10-8
H+ K m (M)
100 μM L-glutamate
10-9
-140
-100
-60
-20
20
membrane potential (mV)

Figure 4. Glutamate and protons reciprocally influence both the steady-state kinetic parameters K_m and I_{max}. (A) Glutamate concentration dependence of currents at pH 7.5 and pH 8.5 at –30 mV (gluconate soaked cells). Similar results were obtained with non-dialyzed oocytes (data not shown). Curves are least squares fit of the data (mean ± S.E.; n=5). The K_m values are 36 μM (pH 7.5) and 113 μM (pH 8.5). Currents are normalized to the maximal response obtained at pH 7.5. (B) Effect of membrane potential on glutamate K_m at pH 8.5, pH 7.5, and pH 6.5 (n=5). (C) Proton concentration dependence of currents at 10 μM glutamate and 100 μM glutamate (V_m = –30 mV). Curves are least squares fit of the data (mean ± S.E.; n=5). The K_m values are 16 nM (10 μM glutamate) and 5 nM (100 μM glutamate). Currents are normalized to the response obtained with 1 mM glutamate. (D) Effect of membrane potential on proton K_m in the presence of either 10 μM or 100 μM glutamate (n=5). Data were acquired in collaboration with Scott Eliasof.

(Figure 4C). The proton K_m increased as the membrane potential became more positive (Figure 4D), while the glutamate K_m decreased (Figure 4B). At pH 8.5, the voltage-dependence of the glutamate K_m exhibited more complex behavior. These data are only consistent with a model in which glutamate and a proton can bind to EAAT3 in random order (Stein et al., 1990; Watzke et al., 2000).

Two Na^+ ions bind before and one Na^+ ion binds after glutamate

Uncertainty still exists regarding the extracellular Na^+ binding order. It has been suggested that glutamate binding precedes binding of at least one Na^+ (Kanai et al., 1995; Watzke et al., 2001; but see Mennerick et al., 1999). It is also been proposed that Na^+ ions bind before glutamate (Auger and Attwell, 2000; Billups et al., 1996; Otis and Jahr, 1998; Wadiche et al. 1995a). To determine the Na^+ binding order we studied the effect of different extracellular Na^+ and glutamate concentrations on their respective K_m and I_{max}. Watzke et al. (2001) derived a series of analytical equations that provided testable predictions regarding the Na^+ binding order in respect to glutamate. For instance, for all three Na^+ ions to bind before glutamate, only the glutamate K_m should be dependent on $[Na^+]_o$, and not the glutamate I_{max}. If, on the other hand, both the Na^+ K_m and I_{max} are dependent on $[glutamate]_o$ and likewise the glutamate K_m and I_{max} is dependent on $[Na^+]_o$, then, at least one Na^+ should bind after glutamate (Watzke et al., 2001).

We found that decreasing extracellular glutamate concentration raised the Na^+ K_m and lowered the Na^+ I_{max} (Figure 5A). In particular, at -40 mV and in the presence of 1 mM $[glutamate]_o$ the extracellular Na^+ K_m is 20.2 ± 1 mM (n=3) while at 10 μM $[glutamate]_o$ the Na^+ K_m was 47.1 ± 5 mM (n=3). The relative change in the Na^+ K_m was also dependent on

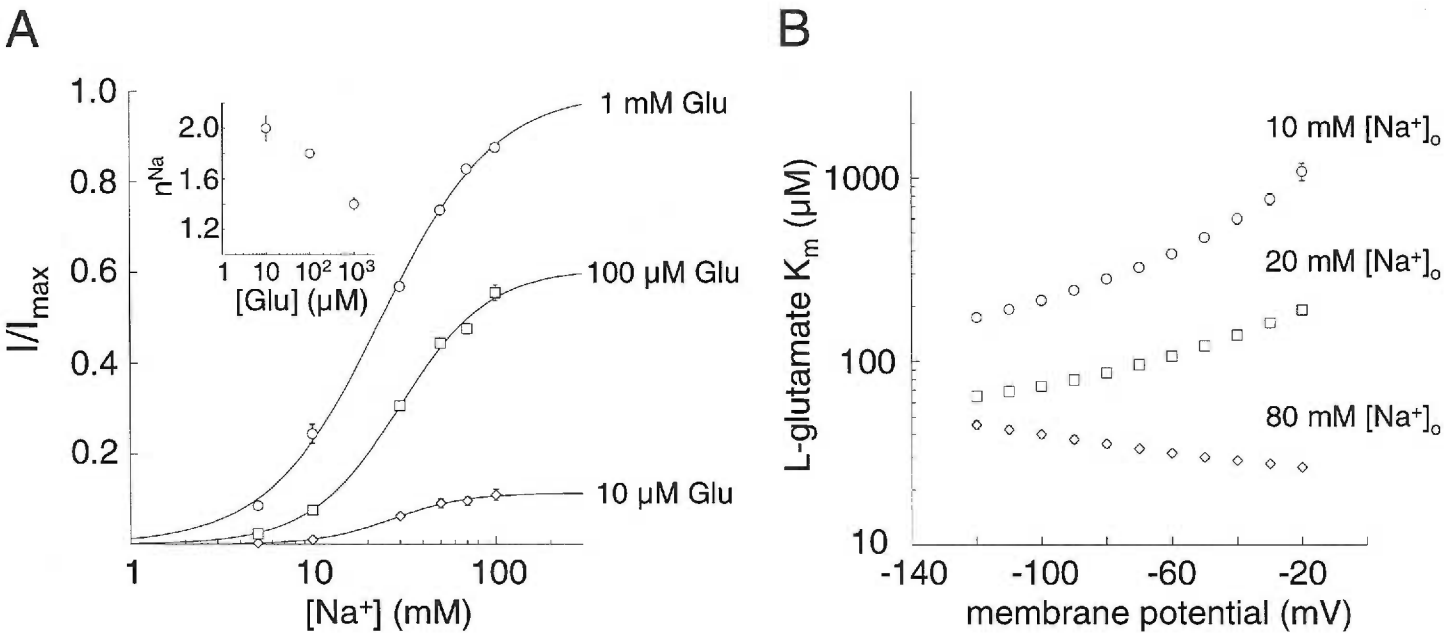
A
1.0
0.8
0.6
0.4
0.2
I/I_max
1 mM Glu
100 μM Glu
10 μM Glu
2.0
1.6
1.2
n^Na
1 10 10² 10³
[Glu] (μM)
1
10
100
[Na+] (mM)
B
1000
100
10
L-glutamate K_m (μM)
10 mM [Na+]_o
20 mM [Na+]_o
80 mM [Na+]_o
-140
-100
-60
-20
membrane potential (mV)

Figure 5. Glutamate and Na^+ reciprocally influence both the steady-state kinetic parameters K_m and I_{max}. (A) Sodium concentration dependence of currents at varying $[glutamate]_o$ (V_m = -80 mV). Curves are least squares fit of the data (mean ± S.E; n=3). The data were fitted to the Hill equation. The K_m and n^{Na} values (inset) are 32 mM and 2.0 (10 μM glutamate), 30 mM and 1.8 (100 μM glutamate), 24 mM and 1.4 (1 mM glutamate). Currents are normalized to the maximal response obtained with 1 mM glutamate. (B) Effect of membrane potential on glutamate K_m at varying $[Na^+]_o$ (n=5). The data in panel A as well as the data mentioned in the text at -40 mV were acquired by Alex Stein. The data for panel B were obtained by Scott Eliasof.

the membrane potential, becoming less pronounced at hyperpolarized potentials (Figure 5A). Also, as was reported previously (Kanai et al., 1995), the Na^+ Hill coefficient, n^{Na}, was depended on $[glutamate]_o$ (Figure 5A inset). In addition, lowering the external $[Na^+]_o$ to 30 mM resulted in a decrease in the glutamate current (67 ± 1 % of control, n=3), while the glutamate K_m was increased and the dependence on membrane potential changed (Figure 5B; Brew and Attwell, 1987; Kanai et al., 1995; Klockner et al., 1993, 1994; Watzke et al., 2001). These data are consistent with a model in which at least one Na^+ binds after glutamate.

As pointed out by Watzke et al. (2001) the aforementioned data do not allow us to determine either the number of Na^+ ions that bind after glutamate nor whether all Na^+ sites are identical to each other. Therefore, in order to investigate the nature of the Na^+ binding sites and the order of binding, we examined the effect of Li^+ on the kinetics of EAAT2 and EAAT3. Consistent with previous reports, replacement of extracellular Na^+ with Li^+ did not support glutamate transport by EAAT2 (Grunewald and Kanner, 1995), but did in EAAT3 (Borre and Kanner, 2001). Also, as with Na^+-coupled glutamate uptake, Li^+-driven glutamate transport in EAAT3 was accompanied by the inward movement of +2 charges (Stein and Kavanaugh, unpublished observations) suggesting that three Li^+ ions kinetically substitute for three Na^+ ions in coupled transport of glutamate (Zerangue and Kavanaugh, 1996b). We observed that while application of glutamate in the presence of Li^+ did not induce steady-state transport currents in EAAT2 (data not shown), glutamate did block a transient capacitive current (Figure 6A, inset; Wadiche and Kavanaugh, unpublished observations). The block of the capacitive current was similar to the one blocked by the non-transportable inhibitor kainate in the presence of extracellular Na^+ (Figure 6A;

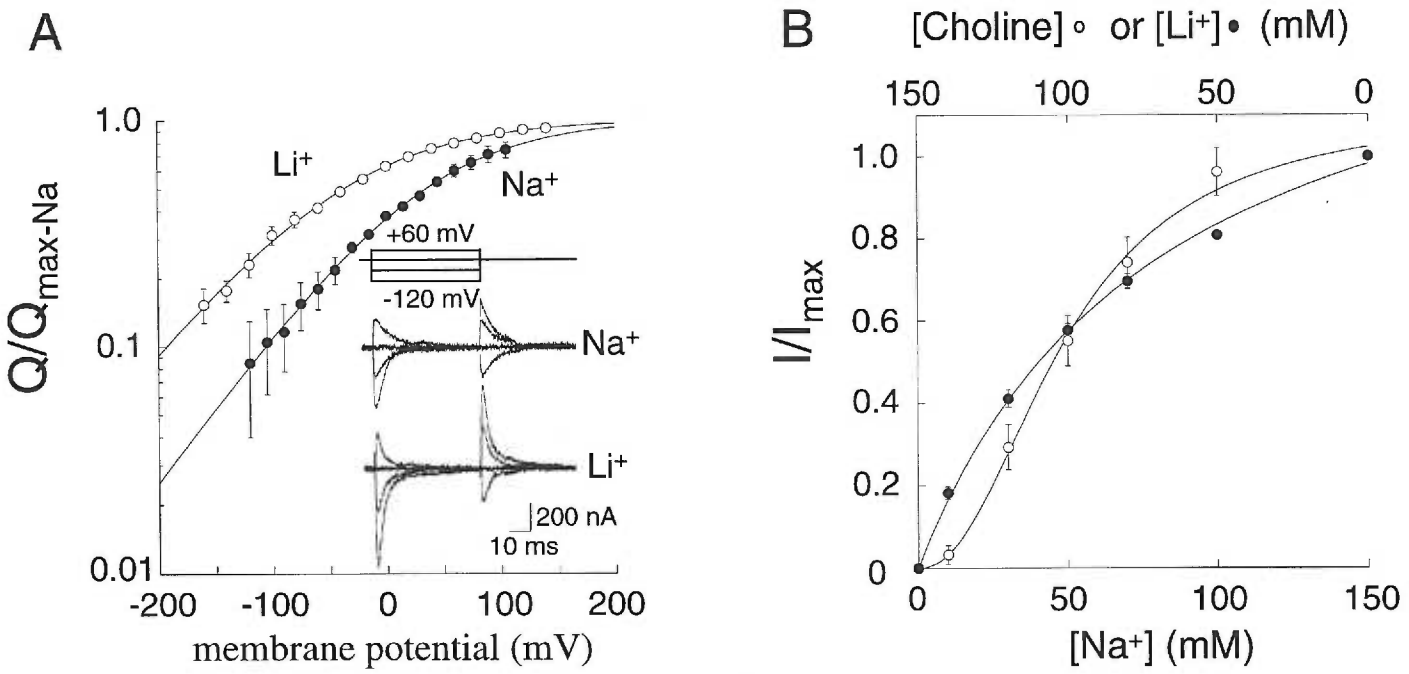
A
1.0
0.1
0.01
Q/Qmax-Na
Li+
Na+
+60 mV
-120 mV
Na+
Li+
200 nA
10 ms
-200
-100
0
100
200
membrane potential (mV)
B
[Choline] ◦ or [Li+] • (mM)
150
100
50
0
1.0
0.8
0.6
0.4
0.2
0
I/Imax
0
50
100
150
[Na+] (mM)

Figure 6. Transporters have one selective sodium-binding site. (A) Log plot of normalized charge movements from oocytes expressing EAAT2 blocked by either kainate in the presence of extracellular Na^+ (300 μM; Q_{max} = 5.5 ± 1.3 nC; n=3) or 3 mM glutamate in the presence of extracellular Li^+ (Q_{max} = 6.6 ± 1.0 nC; n=3). The data were fitted to a Boltzmann function with a $V_{0.5}$ = 43 ± 14 mV and a slope factor of 65 ± 8.4 in the presence of Na^+ (n=3) and a $V_{0.5}$ = -45 ± 7.8 mV and a slope factor of 77 ± 5.2 in the presence of Li^+ (n=3). Inset, Subtracted current records from the same oocyte showing the voltage dependence of transients currents blocked by either 300 μM kainate in 100 mM $[Na^+]_o$ (top traces) or 3 mM glutamate in 100 mM $[Li^+]_o$ (bottom traces). Voltage command pulses in 60 mV from a holding potential of 0 mV (+60 mV to –120 mV). (B) Sodium concentration dependence of glutamate currents (10 μM; V_m = -100 mV) in either partial Li^+ or choline substitution to a total cation concentration of 150 mM. Curves are least squares fit of the data (mean ± S.E.; n=3). Data were fitted to the Hill equation. For choline substitution the n^{Na} = 2.2 ± 0.3 (n=3), while for Li^+ substitution the Hill coefficient was constrained to 1, otherwise the n^{Na} = 0.86 ± 0.06 (n=3). Data acquired by Alex Stein.

Wadiche et al., 1995a). The Li^+ transient current-voltage plot obeyed a Boltzmann function with identical slope as Na^+, but shifted towards hyperpolarized potentials, suggesting that Li^+ occupied the same or similar binding sites as Na^+ but with lower affinity (Figure 6A). The ability of glutamate to block transient capacitive currents, when Li^+ is the extracellular cation, is consistent with the proposal that Li^+ binds prior to glutamate (Grunewald and Kanner, 1995; Zhang et al., 1998). Furthermore, in EAAT2, the concentration dependence of Na^+ binding had an n^{Na} of 2.2 ± 0.3 (n=3) at 10 μM $[glutamate]_o$, but it decreased to 1 (n=3) when Li^+ was used as the background cation instead of choline (Figure 6B; Grunewald and Kanner, 1995). The elimination of Na^+ cooperativity in the presence of Li^+ in EAAT2 suggests that there is one Na^+ selective site and two promiscuous sites i.e. in the presence of Li^+ only one Na^+ selective site is left while, two sites are occupied by Li^+. Since in EAAT2 Li^+ binds to the cation sites preceding glutamate binding, the selective Na^+ site should be on the transporter/glutamate complex. Qualitatively similar Hill coefficient data were obtained for EAAT3 ($n_{choline}$ = 1.9 ± 0.1; n_{Li} =1; n=3; data not shown).

These data suggest that subsequent to glutamate binding there is only one Na^+ selective site. However, we cannot exclude the possibility that there are two Na^+ sites one selective for Na^+ and another that is non-selective. As a result, we attempted to distinguish between these two possibilities. In oocytes expressing EAAT3 a perturbation in the membrane potential led to a transient capacitive current (Figure 7A). To fit the decay of the peak current response to equilibrium required two exponentials, while in uninjected oocytes only one exponential was necessary (Figure 7A). Previously, it was shown that in oocytes expressing EAATs the slow component is due to binding of Na^+ ions to the transporter (Wadiche et al., 1995a). Therefore, to address whether one or two Na^+ ions bind before

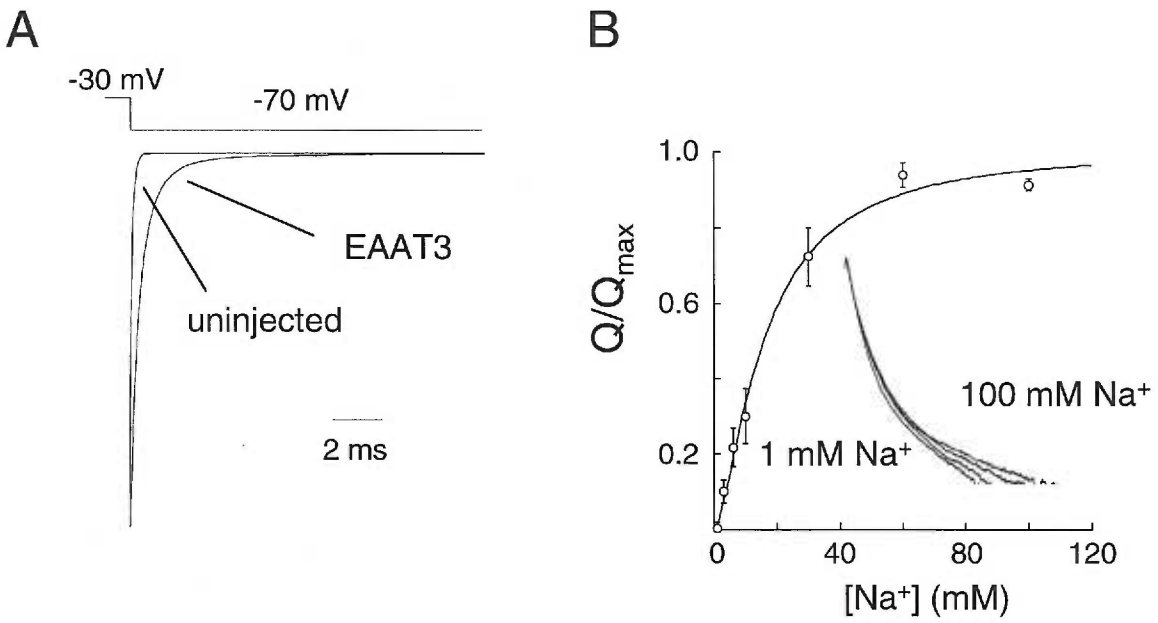
A
-30 mV
-70 mV
EAAT3
uninjected
2 ms
B
1.0
0.6
0.2
Q/Q_max
100 mM Na+
1 mM Na+
0
40
80
120
[Na+] (mM)

Figure 7. Two sodium ions bind before glutamate. (A) Relaxation to equilibrium following a voltage jump from –30 mV to –70 mV for uninjected and injected oocytes with EAAT3. The decay to equilibrium was fitted with one exponential for the uninjected oocytes (τ = 0.14 ± 0.02 ms, n=5), while the EAAT3 expressing oocytes required two exponentials (τ_{fast} = 0.36 ± 0.02 ms, τ_{slow} = 2.3 ± 0.5 ms, 29 ± 4 % slow; n=6). Although the time constants can vary for different batches of oocytes the relative contribution of the slow component stays the same. The extracellular Na^+ concentration was 100 mM. Traces are an average of 10 trials. (B) Na^+ concentration dependence of the slow component. The Na^+ K_m = 20 ± 5 mM and the n^{Na} = 1.8 ± 0.2 (n=9). Inset, representative trace showing the effect of extracellular Na^+ on the slow component (1 mM, 10 mM, 30 mM, 100 mM Na^+). Currents are plotted in a log scale.

glutamate we determined the Na^+ concentration dependence and Hill coefficient of the slow component (Figure 7B). If the n^{Na} of the slow component is one, then, at least one Na^+ binds before glutamate. However, we found that the $n^{Na} = 1.64 \pm 0.2$ with a Na^+ $K_m = 20 \pm 5$ mM (n=10) suggesting that two Na^+ ions bind before glutamate.

In summary, the collected steady-state data are consistent with an ordered binding scheme with binding of two Na^+ ions preceding H^+/glutamate binding followed by a third Na^+ ion.

Transporter hemicycle kinetics

Yet another parameter critical to our understanding of glutamate transport kinetics is the identity of the rate-limiting step. Recent studies suggested that the rate-limiting step is associated with the glutamate bound steps (Auger and Attwell, 2000; Grewer et al., 2000; Otis and Jahr, 1998; Wadiche and Kavanaugh, 1998), while earlier work had concluded that the K^+-bound steps are the slowest in the cycle (Erecinska and Nelson, 1987; Kanner and Bendahan, 1982). In order to resolve this controversy we investigated the influence intracellular ions have on the kinetics of glutamate transport. Therefore, we analyzed the kinetics of the anion current induced by rapid glutamate application to excised outside-out patches from EAAT3 expressing oocytes with either intracellular K^+ or Na^+. This allowed us to compare the kinetics of the complete cycle to the kinetics of the Na^+-hemicycle (Billups et al., 1996; Kanner and Bendahan, 1982; Otis and Jahr, 1998; Otis and Kavanaugh, 2000; Watzke et al., 2001).

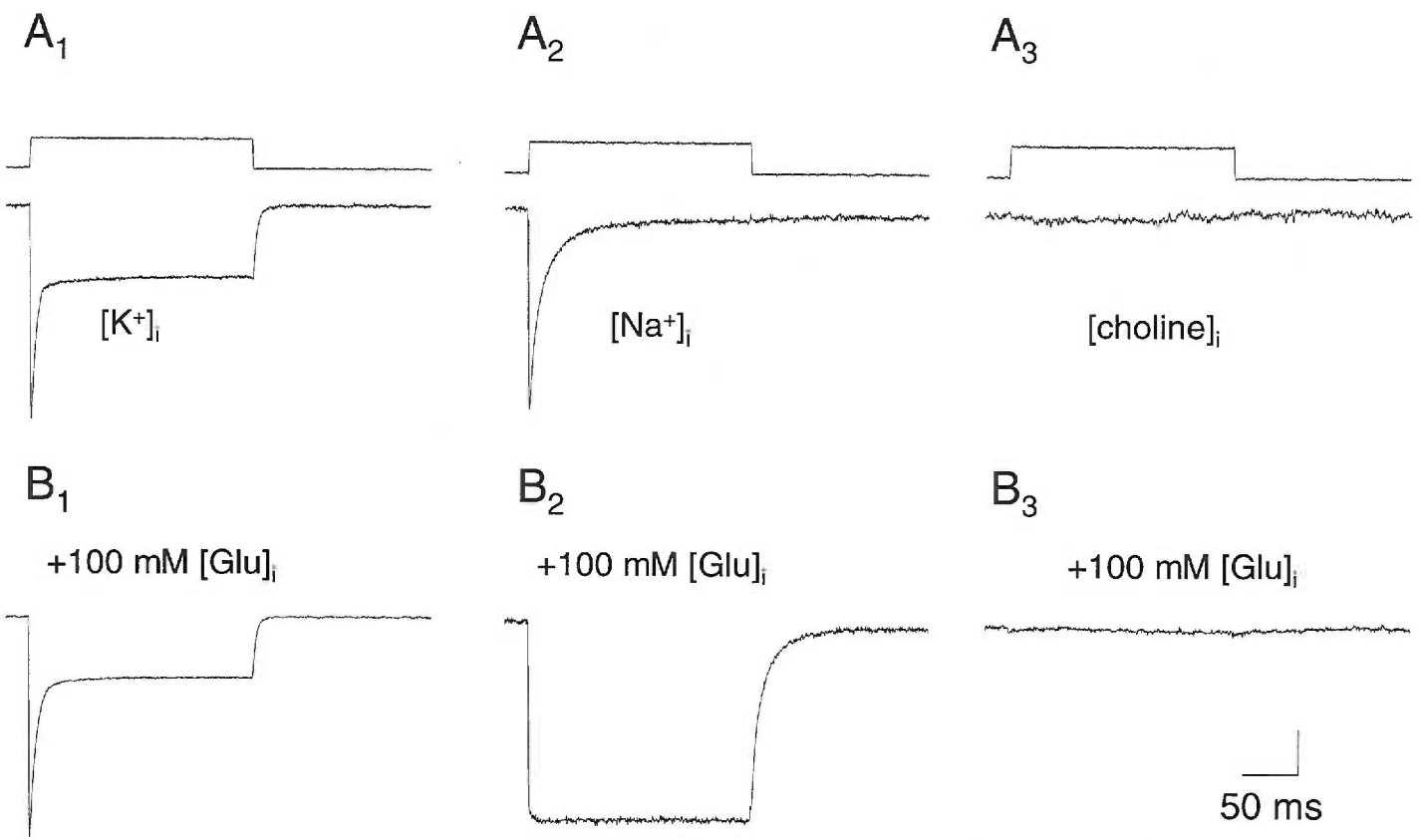
A1
A2
A3
[K+]i
[Na+]i
[choline]i
B1
B2
B3
+100 mM [Glu]i
+100 mM [Glu]i
+100 mM [Glu]i
50 ms

Figure 8. Intracellular ions affect the EAAT3 macroscopic kinetics. Rapid application of 10 mM glutamate to outside-out patches (200 ms, -70 mV) in which the major intracellular ions were: (A_1) K^+ ions (scale bar=10 pA), (B_1) with 100 mM glutamate (scale bar=6 pA), (A_2) Na^+ ions (scale bar=5 pA), (B_2) with 100 mM glutamate (scale bar=4 pA), and (A_3) choline ions (scale bar=10 pA), (B_3) with 100 mM glutamate (scale bar=6 pA).

Rapid application of saturating glutamate (10 mM) with K^+ the major internal cation resulted in a fast activating anion current (Figure $8A_1$; $\tau = 0.40 \pm 0.04$ ms, n=15, -70 mV) that decayed to a steady-state level in the continuous presence of glutamate (peak-to-steady state ratio = 3.4. ± 0.3, n=22, -70 mV). The peak response can be viewed as the synchronous entrance of the glutamate bound transporters to the conducting state, while the steady-state component reflects the desynchronized transporters (Bruns et al., 1993). The decay to steady-state (desychronization) was well described by a single exponential time constant of 3.5 ± 0.4 ms (n=22, -70 mV), as was the decay to baseline (deactivation) following the rapid removal of glutamate ($\tau = 3.0 \pm 0.3$ ms; n=21, -70 mV). Similar to previous studies on other EAAT subtypes, the desychronization, but not the deactivation time constant was voltage-dependent (data not shown; Mennerick et al., 1999; Otis and Kavanaugh, 2000; Wadiche and Kavanaugh, 1998). Inclusion of 100 mM glutamate with K^+ in the pipette (Figure $8B_1$) affected the desychronization time constant modestly ($\tau = 6.9 \pm 0.5$ ms; n=8; $p<0.005$). In contrast, the peak-to-steady state ratio and the deactivation time constant were similar to experiments (3.4 ± 0.3; $\tau = 4.2 \pm 0.5$ ms, n=8) where no glutamate was included in the pipette (Figure $8A_1$). The lack of change to the peak-to-steady state ratio in the presence of intracellular glutamate is consistent with a kinetic model in which glutamate is not the first substrate to unbind following translocation to the inside (see also Otis and Jahr, 1998). If glutamate were the first ion to unbind and if we assume that the major anion conductance is gated from a glutamate-bound state, high intracellular glutamate concentration will drive the transporters back into the anion conducting state and, thus, change the peak-to-steady state ratio.

To isolate the Na^+ hemicycle kinetics we measured the currents in the presence of different intracellular glutamate concentrations with Na^+ as the major intracellular cation. Rapid extracellular application of 10 mM glutamate with Na^+ as the main internal cation activated an anion conductance with different kinetics than intracellular K^+ (Fig. $8A_2$; see also Bergles et al., submitted). The peak current decayed to a smaller steady-state level with a $\tau = 17 \pm 2$ ms (n=26), a value significantly different from the one obtained with K^+ inside the pipette (3.5 ms; $p<0.0001$). The peak-to-steady state ratio was 8.1 ± 0.9 (n=26). Inclusion of 100 mM glutamate in the pipette dramatically affected the behavior of the anion conductance (see also Otis and Jahr, 1998; Otis and Kavanaugh, 2000). The peak-to-steady state ratio decreased to 1.01 ± 0.05 (n=4; Figure $8B_2$), and following the rapid removal of glutamate the current decay to baseline required two exponentials to fit the data. The slow component was $\tau = 30 \pm 2$ ms and the fast component was $\tau = 7.5 \pm 0.5$ ms (n=4; 63 ± 8 % fast). Table I summarizes the effect of varying intracellular glutamate concentration in the presence of Na^+ ions on the anion current kinetics. Although it was initially suggested that a glutamate-bound state transition might be the slowest step in the cycle (Wadiche and Kavanaugh, 1998), the relatively fast desychronization kinetics of these Na^+-hemicycle currents (Table I) make it unlikely that this part of the transport cycle is rate-limiting.

The cycling rate is dependent on the intracellular cation and membrane potential

In contrast to K^+ or Na^+, intracellular choline did not support currents in response to glutamate concentration jumps in patches (Figure $8A_3$, n=3; see also Grewer et al., 2000; Wadiche and Kavanaugh, 1998), even in the presence of 100 mM intracellular glutamate

Table I. Kinetic Parameters when Na^+ is the major intracellular cation.

	$[Na^+]_i$ + 0 mM $[L\text{-glutamate}]_i$	$[Na^+]_i$ + 1 mM $[L\text{-glutamate}]_i$	$[Na^+]_i$ + 10 mM $[L\text{-glutamate}]_i$	$[Na^+]_i$ + 100 mM $[L\text{-glutamate}]_i$
Peak-to-steady state	8.1 ± 0.9 (26)	2.1 ± 0.1 (9)	1.5 ± 0.1 (6)	1.01 ± 0.05 (4)
τ desychron. fast (ms)	17 ± 2 (26)	6.4 ± 1.3 (5)	2.8 ± 0.1 (6)	N.D.
% amplit. fast	100	78 ± 2	76 ± 4	N.D.
τ desychron. slow (ms)	N.D.	56 ± 14 (5)	39 ± 7 (6)	N.D.
τ deactivation fast (ms)	N.D.	4.6 ± 0.4 (9)	6.4 ± 0.4 (6)	7.5 ± 0.5 (4)
% amplit. fast	N.D	61 ± 4	60 ± 4	63 ± 8
τ deactivation. slow (ms)	N.D.	53 ± 4 (9)	43 ± 4 (6)	30 ± 2 (4)
τ recovery (ms,-80 mV)	1300 ± 80 (6)	70 ± 3 (3)	75 ± 7 (3)	N.D.

The kinetic parameters, unless stated otherwise, were obtained at -70 mV. All values are expressed as mean ± SEM (number of observations). N.D.: not able to measure it.

(Figure $8B_3$, n=4). The absence of anion conductance activation when intracellular choline was in the pipette suggests the transporters may have been forced into "inward facing" states unavailable to bind glutamate from the outside. This would imply that external Na^+ can re-orient transporters to the intracellular states in the absence of any extracellular glutamate (i.e. slippage; Kanai et al., 1995). However, since the anion conductance is activated by extracellular application of glutamate when the internal cation is Na^+, then, Na^+ should substitute for K^+ to reorient the transporters outside. To test the possibility that there might be pathways by which Na^+-bound transporters can equilibrate between extracellular and intracellular facing conformations, we analyzed the recovery kinetics of the peak anion current in the presence of intracellular Na^+ using a paired-pulse protocol (Bergles and Jahr, 1997) (Figure 9). The recovery time constant of the peak anion current with intracellular K^+ was 25 ± 1 ms (n=15), similar to previous measurements (Bergles and Jahr, 1998; Otis and Kavanaugh, 2000). With Na^+ in the pipette, the peak current also recovered, although the kinetics were remarkably prolonged, τ =1.3 ± 0.08 s (n=6). This slow cycling rate suggests that either Na^+ is a poor substrate for the intracellular K^+ binding site or that the conformational change that allows the transporters to return outside is slow. Our modeling suggested the latter, but we cannot unequivocally exclude the former possibility (see Kinetic model section).

Furthermore, the recovery rate of the peak current ($1/\tau_{recovery}$) with K^+ in the pipette was also voltage-dependent (e-fold/79 mV; Figure 10). This is comparable to the voltage dependence of the glutamate transport rate (e-fold/76-89 mV; Wadiche et al., 1995a; Wadiche and Kavanaugh, 1998). However, the recovery rate was significantly faster (40 s^{-1} at -80 mV) than the estimated glutamate turnover rate (14-16 s^{-1}; Wadiche et al., 1995a;

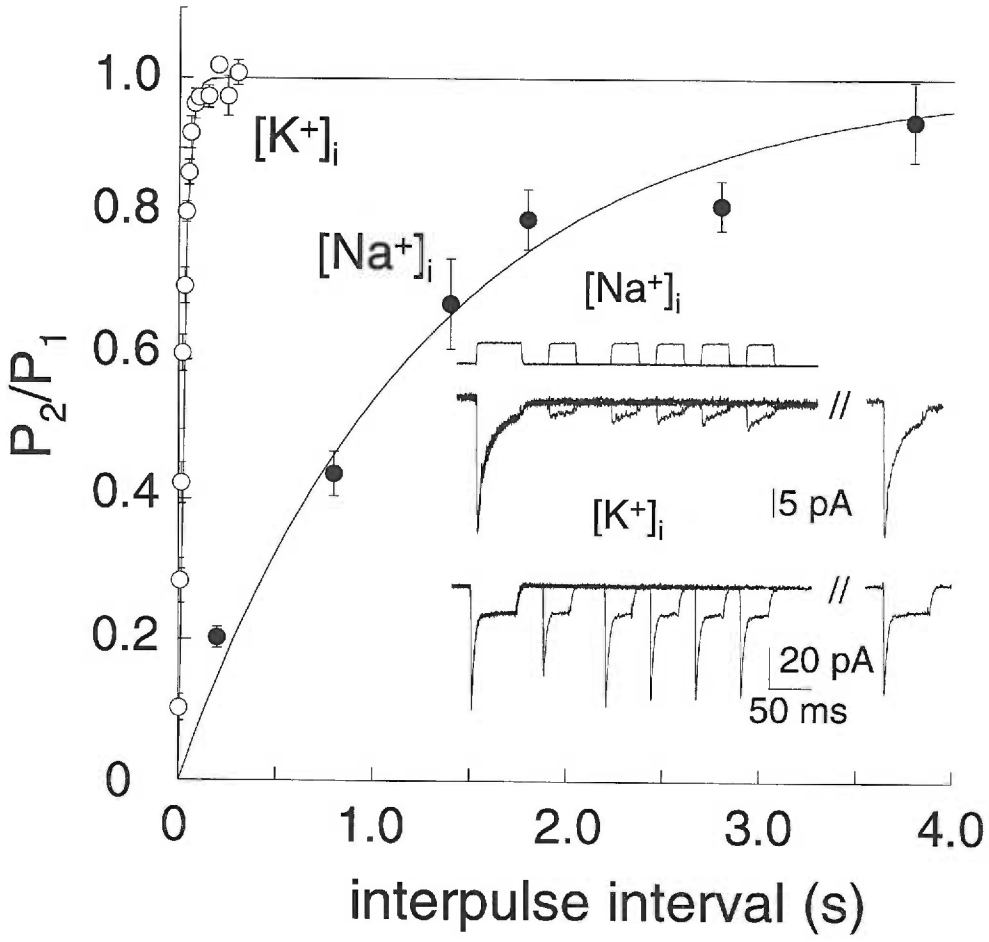
1.0
0.8
0.6
0.4
0.2
0
P_2/P_1
$[K^+]_i$
$[Na^+]_i$
$[Na^+]_i$
//
5 pA
$[K^+]_i$
//
20 pA
50 ms
0
1.0
2.0
3.0
4.0
interpulse interval (s)

Figure 9. Replacement of intracellular potassium by sodium slows the recovery of the peak anion current from steady-state. Recovery from steady-state (V_h = -80 mV, n=6) following a 200 ms conditioning pulse (10 mM glutamate). For intracellular Na^+, a test pulse of 200 ms (10 mM glutamate) was applied at various intervals after the conditioning pulse while for K^+ see below. The ratio of the 2nd peak (P_2, conditioning pulse) to the 1st peak (P_1, test pulse) following the subtraction of the steady-state current against the interval time is plotted. The time constant (τ = 1.3 ± 0.08 s; 0.77 s^{-1}) for the recovery was obtained by fitting the data with a first order exponential. *Inset*, A comparison of the peak anion current recovery with either intracellular Na^+ or K^+ ions using the same protocol (50 ms conditioning pulse followed by a 30 ms test pulse).

Wadiche and Kavanaugh 1998). One possible explanation for this discrepancy is that the recovery kinetics may be faster than the overall cycling rate if the transporters are significantly less than 100% efficient at transporting an initially bound glutamate molecule (see Discussion; Bergles and Jahr, 1998; Otis and Jahr, 1998; Wadiche and Kavanaugh, 1998).

Kinetic model

To understand the role transporters play in synaptic transmission, a characterization of the microscopic rates is needed, including the identity of the voltage steps in the cycle. Since many of these rates are difficult to measure directly, we developed a kinetic model (Figure 11) to simulate both the anion and coupled current kinetics (see also Bergles et al., submitted). The model proposed by Wadiche and Kavanaugh (1998) and Otis and Jahr (1998) provided the framework for the current model. To model our experimental results we suggest a kinetic scheme in which two Na^+ ions bind first, followed by the random binding of glutamate and a H^+. Then, the third Na^+ binds (see previous Result sections for binding order) triggering a voltage independent transition of bound $Na^+/H^+/Glu^-$ transporters from outside to inside. Following translocation to the inside, one Na^+ unbinds followed by the ordered unbinding of the H^+, glutamate, and the remaining two Na^+ ions. Lastly, K^+ binds to the empty transporter and the K^+-bound transporter reverts to the outside in a voltage dependent manner completing the cycle. To simulate the anion conductance, channel states in the extracellular side of the transporters were included (Auger and Attwell, 2000; Grewer et al., 2000; Otis and Jahr, 1998; Wadiche and Kavanaugh, 1998; Watzke et al., 2001). The major conducting state, $T_oNa_3GH^*$, is in a

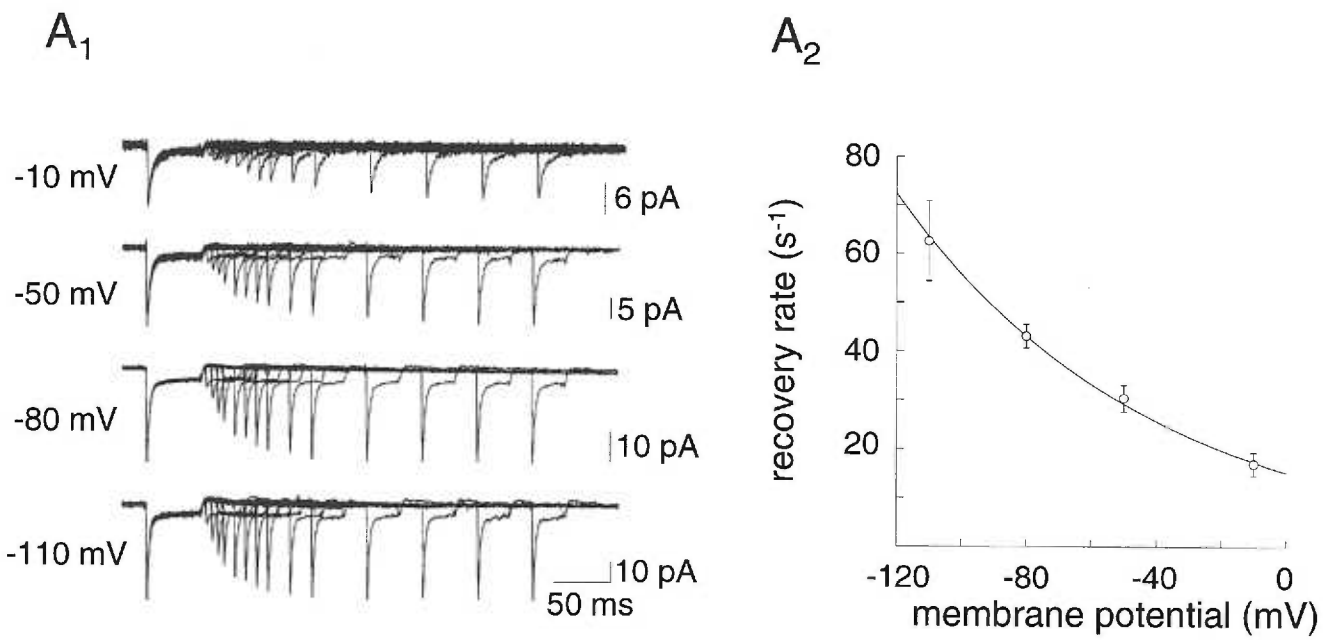
A1
-10 mV
6 pA
-50 mV
5 pA
-80 mV
10 pA
-110 mV
10 pA
50 ms
A2
recovery rate (s-1)
80
60
40
20
-120
-80
-40
0
membrane potential (mV)

Figure 10. The recovery rate of the anion current from steady-state depends on the membrane potential. (A_1) Recovery of the peak anion current from steady-state at different membrane potentials following a 50 ms conditioning pulse (10 mM glutamate). A test pulse of 30 ms (10 mM glutamate) was applied at various intervals after the conditioning pulse. Traces are from the same patch. (A_2) The recovery rate against the membrane potential is plotted (e-fold/79 mV). At -110 mV the recovery rate was 63 ± 8 s^{-1} (16 ± 2 ms, n=5), whereas at -80 mV the rate was 43 ± 2 s^{-1} (24 ± 2 ms, n=9), 31 ± 3 s^{-1} (33 ± 3 ms, n=5) at –50 mV, and 17 ± 0.5 s^{-1} at -10 mV (57 ± 8 ms, n=5).

rapid equilibrium with T_oNa_3GH and was placed on the extracellular limb of the model due to the submillisecond activation of the anion current (Auger and Attwell, 2000; Bergles et al., 1997; Bergles and Jahr, 1997; Otis and Kavanaugh, 2000; Otis et al., 1997; Wadiche and Kavanaugh, 1998; Watzke et al., 2001; Watzke and Grewer, 2001). A "leak" conductance, $T_oNa_1^*$, $T_oNa_2^*$, and $T_oNa_2H^*$ from the T_oNa_1, T_oNa_2, and T_oNa_2H was introduced to explain the anion conductance seen in the absence of any glutamate (Bergles and Jahr, 1997; Grewer et al., 2000; Otis and Jahr, 1998; Otis and Kavanaugh, 2000; Wadiche and Kavanaugh, 1998; Watzke et al., 2001). In addition, conducting states gated from the intracellular states have been included in order to simulate the small steady state anion current seen in the presence of intracellular Na^+ (Figure 9; see also Bergles et al., in press).

We only applied few constraints on the model: (a) it was previously shown that the binding of the Na^+ ion(s) preceding glutamate binding contributes 0.41-0.46 charges (Wadiche et al., 1995a; Wadiche and Kavanaugh, 1998). Thus, we assigned 0.46 charges for the binding of the first Na^+. We cannot exclude the possibility that the binding of the second Na^+ is also voltage dependent. However, assigning voltage dependence to the second Na^+ binding did not affect the simulations (data not shown). (b) The sum of the moved charge (z) is +2, due to the +2 net charges moved per one forward transport cycle (Levy et al., 1998; Zerangue and Kavanaugh, 1996b). (c) The anion channel P_o increases as the membrane potential becomes more negative and (d) the glutamate binding rate was set ~6 $\bullet 10^6$ $M^{-1}s^{-1}$ for all EAATs (Wadiche and Kavanaugh, 1998).

Simulations of the model were consistent with previous experimental results as well as our results. The model reproduced the steady-state glutamate I-V (Figure 12A), as

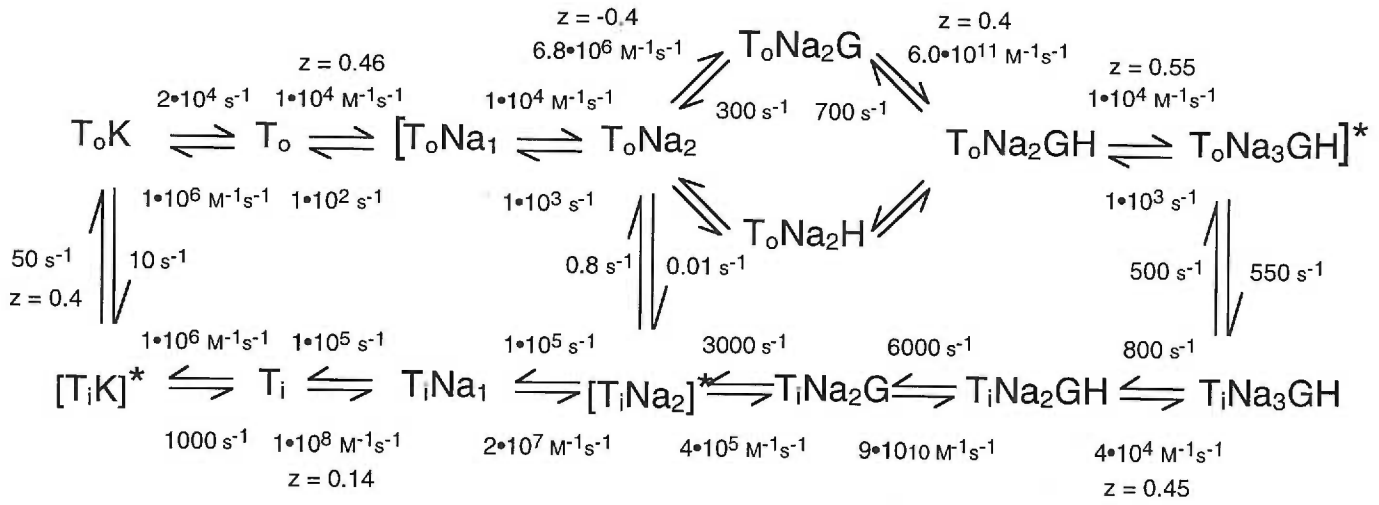
z = -0.4
6.8•10^6 M^-1s^-1
ToNa2G
z = 0.4
6.0•10^11 M^-1s^-1
z = 0.46
2•10^4 s^-1
1•10^4 M^-1s^-1
1•10^4 M^-1s^-1
300 s^-1
700 s^-1
z = 0.55
1•10^4 M^-1s^-1
ToK
To
[ToNa1
ToNa2
ToNa2GH
ToNa3GH]*
1•10^6 M^-1s^-1
1•10^2 s^-1
1•10^3 s^-1
1•10^3 s^-1
50 s^-1
z = 0.4
10 s^-1
ToNa2H
0.8 s^-1
0.01 s^-1
500 s^-1
550 s^-1
1•10^6 M^-1s^-1
1•10^5 s^-1
1•10^5 s^-1
3000 s^-1
6000 s^-1
800 s^-1
[TiK]*
Ti
TiNa1
[TiNa2]*
TiNa2G
TiNa2GH
TiNa3GH
1000 s^-1
1•10^8 M^-1s^-1
z = 0.14
2•10^7 M^-1s^-1
4•10^5 M^-1s^-1
9•1010 M^-1s^-1
4•10^4 M^-1s^-1
z = 0.45

Figure 11. Alternating access computer model. Asterisk denotes states from which the anion conductance is gated. For the $T_oNa_1^*$, $T_oNa_2^*$, $T_oNa_2H^*$, $T_oNa_2GH^*$ states $\alpha = 8094\ s^{-1}$ and $\beta = 5\ s^{-1}$. For the $T_oNa_3GH^*$ state $\alpha = 12600\ s^{-1}$ and $\beta = 700\ s^{-1}$. For the $T_iNa_2^*$ $\alpha = 4700\ s^{-1}$ and $\beta = 10\ s^{-1}$, while for the T_iK^* state $\alpha = 4700\ s^{-1}$ and $\beta = .001\ s^{-1}$ (α denotes closing rate while β denotes opening rate). The z values are noted on the model while the λ values are (see methods): 0.5 for the binding of the first Na^+ ion, the H^+ binding, the glutamate binding, and the binding of the third Na^+ ion. While the λ values for the intracellular release of the first Na^+ ion is 0.1, 0.5 for the release of the third Na^+ ion, and 0.9 for K^+ countertransport. The displayed rates are for V_h =-70 mV.

well as the effect extracellular alkalization had on both the current-voltage relationship at low glutamate concentrations (Figure 12B) and the glutamate K_m (Figure 12C-D). To simulate the saturation seen in the steady-state I-Vs at low glutamate concentrations (Figure $2A_1$) and the decrease in the glutamate K_m at depolarized membrane potentials (Figure 4B), it was necessary to assign voltage dependence to the binding of glutamate to EAAT3. Our model also simulated the major changes seen in the macroscopic kinetics of the anion conductance with the different intracellular solutions (Figure 13A) as well as the voltage dependence of the paired-pulse recovery rate (Figure 13B). In addition, the model predicts that the return of the transporter from inside to outside moves a net negative charge outwards, implying that there are uncompensated negative charges on EAAT3 during its return outside. Since there are -0.4 charges on the K^+-bound transporter moving outwards (Figure 11) the total intrinsic transporter gating charge should be at least -1.4 (K^+ must compensate for 1 charge).

We, also, extended our model to EAAT1, EAAT2 as well as EAAT4 (Figure 14; Bergles et al., in press). To constrain the models, we measured the recovery rate of the anion current for EAAT1, EAAT2, and EAAT4. The recovery time constant for either EAAT1 or EAAT2 (see also Otis and Kavanaugh, 2000) was not different from the one obtained for EAAT3 (Figure 9), suggesting a similar rate value for the rate-limiting step among EAAT1, EAAT2, and EAAT3. The slow kinetics of EAAT4 suggested (Figure $14C_{1-2}$) that either the relocation rate is significantly different compared to the other EAATs or another step in the cycle is rate limiting. To simulate EAAT1, EAAT2, and EAAT4 several rates had to be changed (Figure 14 legend).

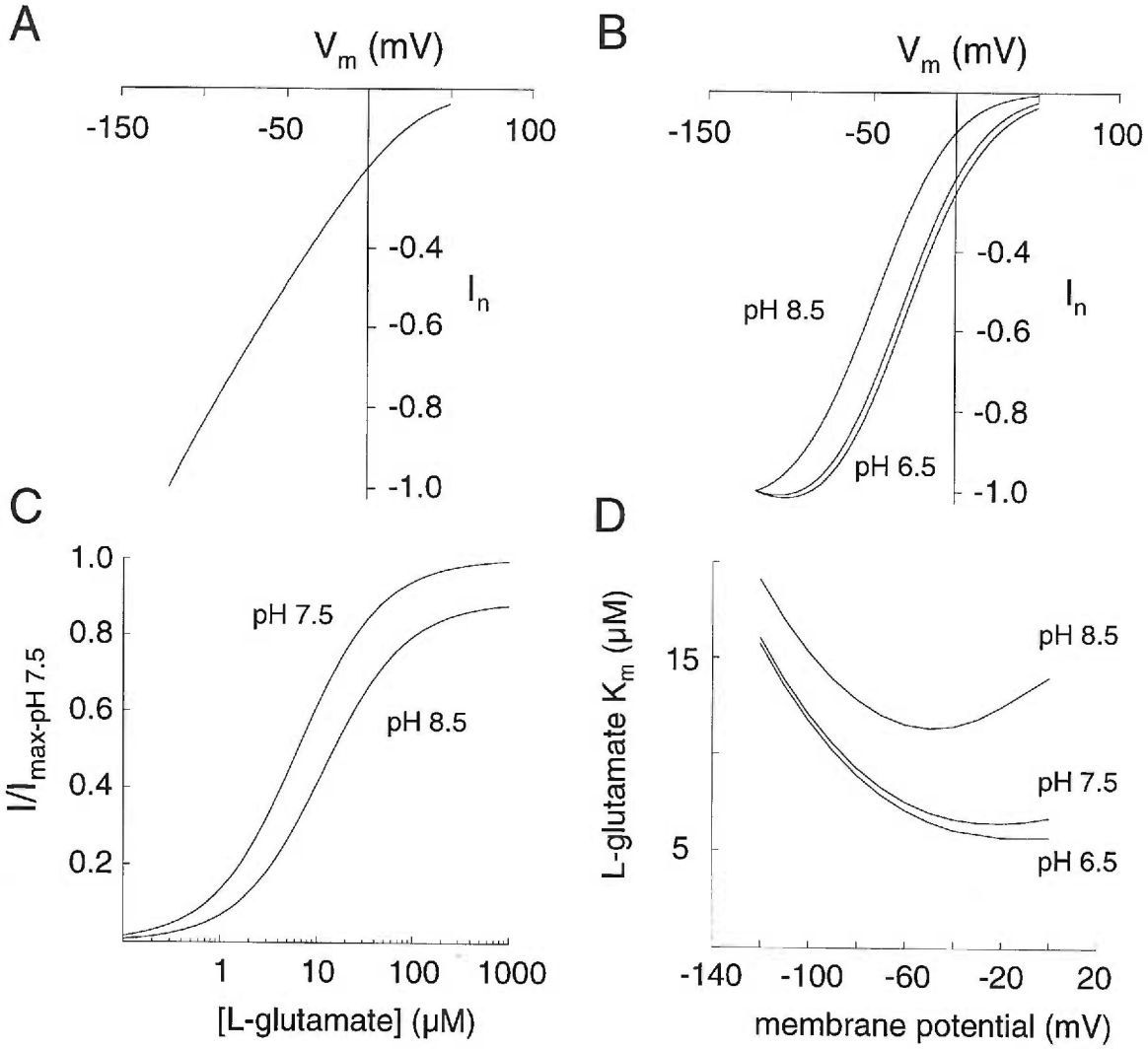
A
V_m (mV)
-150
-50
100
-0.4
-0.6
-0.8
-1.0
I_n
B
V_m (mV)
-150
-50
100
pH 8.5
pH 6.5
-0.4
-0.6
-0.8
-1.0
I_n
C
$I/I_{max\text{-}pH\ 7.5}$
1.0
0.8
0.6
0.4
0.2
pH 7.5
pH 8.5
1
10
100
1000
[L-glutamate] (μM)
D
L-glutamate K_m (μM)
15
5
pH 8.5
pH 7.5
pH 6.5
-140
-100
-60
-20
20
membrane potential (mV)

Figure 12. Simulations of steady-state glutamate induced currents. (A) Model derived I-V induced by 1 mM glutamate. For the model the extracellular ionic conditions are the same as in regular Ringers (see methods). We also assume that the intracellular K^+ concentration is 110 mM, while the intracellular Na^+ and glutamate concentrations are 10 mM (Zerangue and Kavanaugh, 1996b). (B) Simulation of the effect extracellular proton concentration has on the current-voltage relationship at low glutamate concentrations. To simulate this effect we used 1 μM instead of 10 μM glutamate since the model has a higher affinity for glutamate (8.3 μM; -70 mV) compared to the one measured in our experiments (30-40 μM; -70 mV). (C) Simulation of the glutamate concentration dependence of currents at pH 7.5 and pH 8.5 (V_h = –30 mV). Curves are least squares fit of the data. The K_m values are 6.5 μM (pH 7.5) and 11.8 μM (pH 8.5). (D) Simulation of the effect membrane potential has on the glutamate K_m at pH_o 8.5, pH_o 7.5, and pH_o 6.5.

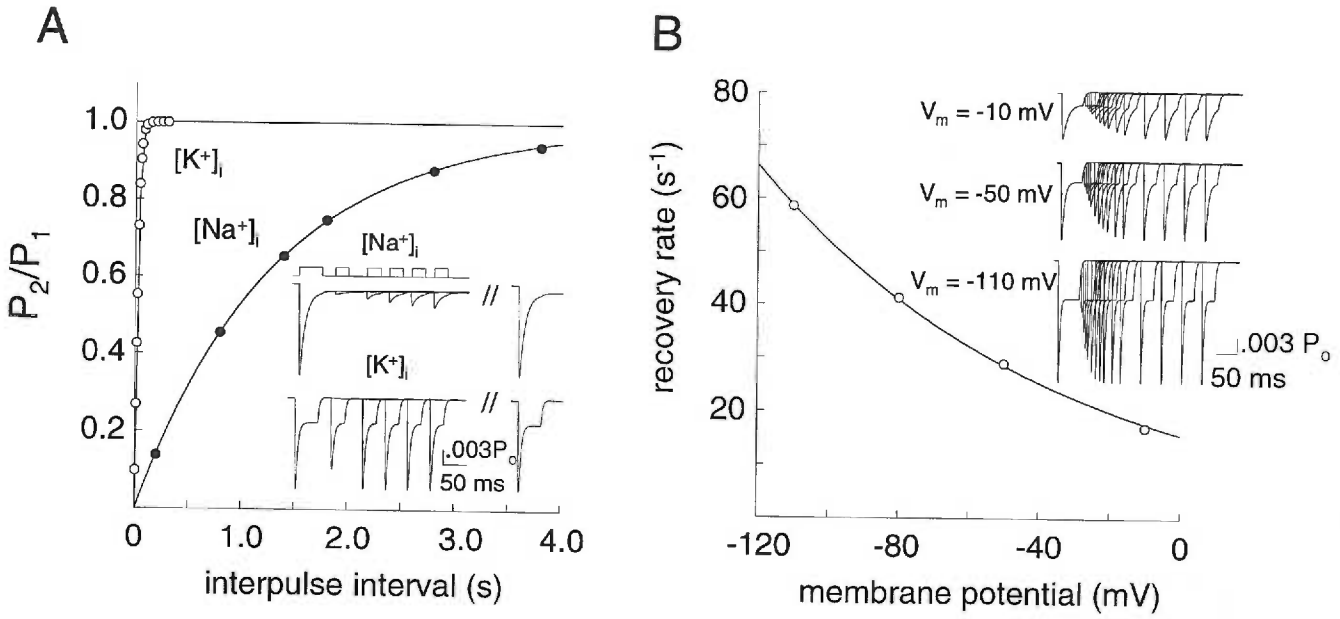
A
1.0
0.8
0.6
0.4
0.2
P_2/P_1
$[K^+]_i$
$[Na^+]_i$
$[Na^+]_i$
//
$[K^+]_i$
//
.003P_o
50 ms
0
1.0
2.0
3.0
4.0
interpulse interval (s)
B
80
60
40
20
recovery rate (s^{-1})
V_m = -10 mV
V_m = -50 mV
V_m = -110 mV
.003 P_o
50 ms
-120
-80
-40
0
membrane potential (mV)

Figure 13. Simulation of the EAAT3 outside-out patch kinetics. (A) Simulation of the recovery of the peak anion current from steady-state (V_h = -80 mV) with either intracellular K^+ (peak-to-steady state = 3.4, $\tau_{desych.}$= 4.9 ms, $\tau_{deac.}$= 3.4 ms, $\tau_{recov.}$= 24.2 ms) or intracellular Na^+ (peak-to-steady state = 8.5, $\tau_{desych.}$= 12 ms, $\tau_{recov.}$= 1.3 s). *Inset*, paired-pulse protocol simulation (see figure 9 legend for protocols). (B) The recovery rate of the model against the membrane potential is plotted (e-fold/83 mV). At -110 mV the recovery rate was 58.5 s^{-1} (17 ms) whereas at -80 mV the rate was 41.3 s^{-1} (24.2 ms), 28.9 s^{-1} (34.6 ms) at –50 mV, and 17.1 s^{-1} (58.5 ms) at -10 mV. *Inset*, paired-pulse protocol simulation at different membrane potentials.

DISCUSSION

The basic features of glutamate transport energetics depend on the gradients for Na^+, K^+ and pH (Bendahan and Kanner, 1982; Erecinska et al., 1983 Kanner and Sharon, 1978; Nelson et al., 1983). An overall stoichiometry of cotransport of 3 Na^+, 1 H^+, and countertransport of 1 K^+ was determined from reversal potential measurements for EAAT3 (Zerangue and Kavanaugh 1996b) and EAAT2 (Levy et al 1998). However, many aspects of glutamate transport kinetics are still unclear (see for review Danbolt, 2001). Therefore, we examined the kinetics of several EAATs under a variety of experimental conditions in order to develop a kinetic model of the glutamate cycle. This model successfully simulated a multitude of experimental parameters, suggesting that it is robust and may be used to reliably predict parameters that are difficult to determine experimentally.

The Na^+ binding steps

One controversy regarding glutamate transport is the substrate binding order (see for review Danbolt, 2001). Based on the following experimental data, we propose that two Na^+ ions bind to the transporter followed by the random binding of glutamate and proton, before a third Na^+ binds. First, in the presence of Li^+, glutamate blocks non-linear capacitance transients in EAAT2, as does kainate in the presence of Na^+ (Figure 6A). Thus, at least one cation must bind prior to glutamate (Wadiche et al., 1995a; Watzke et al., 2001). Second, like Watzke et al. (2001) we found that extracellular Na^+ and glutamate reciprocally affect each other's K_m and I_{max} values (Figure 5 and Result

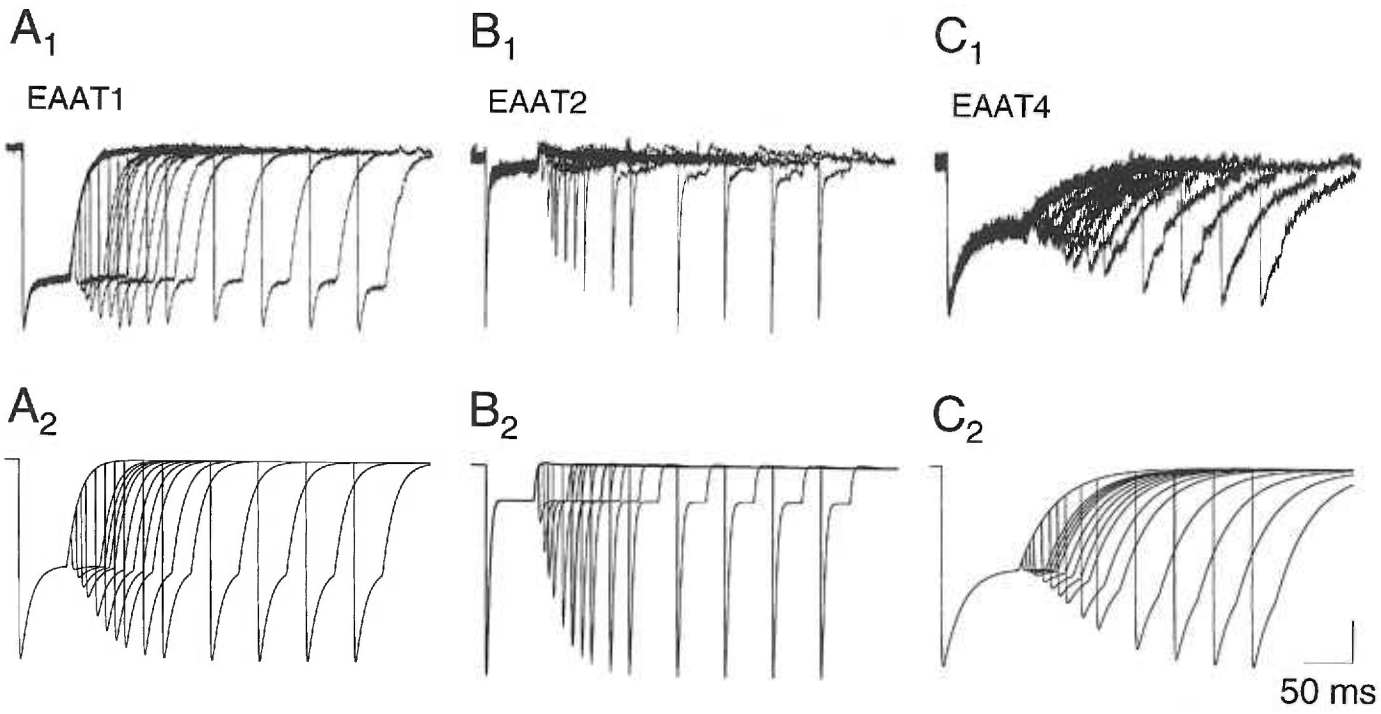
A1
EAAT1
B1
EAAT2
C1
EAAT4
A2
B2
C2
50 ms

Figure 14. Kinetic data and model simulations for EAAT1, EAAT2, and EAAT4. (A_1) EAAT1 recovery of the peak anion current from steady-state ($\tau = 25 \pm 2$ ms; n=9; -80 mV). Scale bar is 30 pA. (A_2) To simulate the EAAT1 data the translocation rate was changed from 550 s^{-1} to 100 s^{-1} and the extracellular unbinding rate was changed from 300 s^{-1} to 80 s^{-1}. Thus, for EAAT1 $\tau_{recov.}$= 28.5 ms. Scale bar is .006 P_o. (B_1) EAAT2 recovery of the peak anion current from steady-state ($\tau = 24 \pm 4$ ms; n=4; -80 mV). Scale bar is 6 pA. (B_2) EAAT2 simulation, (rates are from Bergles et al., submitted). Thus, for EAAT2 $\tau_{recov.}$= 21.4 ms. Scale bar is .003 P_o. (C_1) EAAT4 recovery of the peak anion current from steady-state ($\tau = 98 \pm 14$ ms; n=4; -80 mV). Also $\tau_{desychron.}$= 26 ± 2 ms and $\tau_{deactivat.}$ = 49 ± 3 ms (n=12). (C_2) To simulate the EAAT4 data the translocation rate was changed from 550 s^{-1} to 60 s^{-1} and the extracellular unbinding rate was changed from 300 s^{-1} to 2 s^{-1}, while the relocation rate was altered from 50 s^{-1} to 20 s^{-1}. Thus, for EAAT4 $\tau_{recov.}$= 85 ms, $\tau_{desychron.}$= 26.1 ms, and $\tau_{deactivat.}$ = 51.5 ms. Scale bar is .006 P_o. The channel's opening and closing rates for EAAT1, EAAT2, and EAAT4 are the same as for EAAT3 (see Figure 11 legend). We, currently, do not assign any voltage dependence to either glutamate or proton binding for EAAT1, EAAT2, or EAAT4.

section). As a result, we also conclude that at least one Na^+ binds after glutamate (Watzke et al., 2001). Third, the shift in the n^{Na} from 2 to 1 in EAAT2 and EAAT3 when Li^+ is used as the background cation (Figure 6B) suggests that there is only one selective Na^+ binding site on the transporters (Grunewald and Kanner, 1995). Since Li^+ binds before glutamate the selective Na^+ binding occurs to the transporter/glutamate complex, in agreement with the hypothesis that at least one Na^+ binds after glutamate. Fourth, the Hill coefficient for the Na^+ dependent slow capacitance transient is 1.6 (Figure 7B) indicating two Na^+ ions bind before glutamate.

Proton binding and transport

Our data suggest that the H^+ is not countertransported with K^+ (Auger and Attwell, 2000), but is transported along with Na^+ and glutamate in a distinct step. This conclusion is based on the observation that cysteine is transported as a neutral zwitterion (see also Zerangue and Kavanaugh, 1996a). At low glutamate concentrations the I-V saturates at negative potentials, reflecting the voltage-dependence of glutamate binding (Figure $2A_1$). However, when cysteine is a substrate, no saturation of the I-V at negative potentials is observed, regardless of the cysteine and proton concentration (Figure $2A_2$, $2B_2$). Along with the pH-independence of the cysteine K_m (Figure 1) these results unequivocally support the conclusion that cysteine is binding as a neutral moiety. In addition, the K_m and I_{max} of glutamate and proton are dependent on each other (Figure 4), an effect most easily simulated by a kinetic model with a random binding order (Stein et al., 1990; Watzke et al., 2000). However, Auger and Attwell (2000) found that the

activation kinetics of synaptically evoked Purkinje cell transporter currents were not significantly different between pH 7.5 and 8.5, which they took as evidence against proton/glutamate cotransport in a closely coupled step. Consistent with these results and those of Watzke et al. (2000), we also found that the rise time of the current activated by a pulse of glutamate in excised outside-out patches from oocytes expressing EAAT3 was not greatly affected by the extracellular pH (Apendix I Figure 1; τ_{rise} = 0.16 ± 0.02 ms, pH 7.5; τ_{rise} = 0.19 ± 0.03 ms, pH 8.5; n=4; paired Student's t test p>0.4). However, our model with the proton contransported in the Na^+-hemicycle also predicts relatively modest changes in activation kinetics when the extracellular pH is changed from 7.5 to 8.5 (τ_{rise} = 0.40 ms, pH 7.5; τ_{rise} = 0.57 ms, pH 8.5). Therefore, a small change in rise kinetics is not inconsistent with $Na^+/H^+/Glu^-$ cotransport. Lastly, due to the high microscopic affinity of the EAATs for protons the model suggests that the transporters are predominantly in a protonated state (T_oNa_2H). This ensures that the transporters are in a glutamate-competent state. Otherwise, in the absence of protons, the transporters will be distributed among multiple states (T_o, T_oNa_1, and T_oNa_2) some of which cannot bind glutamate. In agreement to this prediction, preliminary results using voltage clamp fluoremetry (see for review Tzingounis et al., 2002) demonstrated that the occupancy of the empty transporter is modulated by extracellular pH (Appendix I Figure 2).

The rate limiting step

A parameter paramount to our understanding of glutamate transport kinetics is the identity of the rate-limiting step. Recently, a step in the Na^+ hemicycle is usually set as rate-limiting (Auger and Attwell, 2000; Otis and Jahr, 1998; Wadiche and Kavanaugh,

1998). This was based on the observation that the EAAT turnover rate is dependent on the identity of the substrate (Wadiche et al., 1995a; Wadiche and Kavanaugh, 1998). However, to model our data we suggest that the K^+ driven countertransport is the slowest step in the cycle. This was necessary in order to model the change in the peak-to-steady state ratio and speeding of the desychronization kinetics of EAAT3 when Na^+ was used as the intracellular cation (Table I and Figure $8A_2$, $8B_2$). In agreement, replacement of intracellular K^+ with Na^+ slowed the transporter cycling rate over 50 fold (Figure 9). Therefore, in our model the rate-limiting step in the cycle is independent of the substrate. However, our model still predicts a substrate dependent turnover rate since the relative concentration of the state that triggers transporter reorientation, T_iK, is proportional to the rates that are dependent on the substrate (Figure 11).

Unlike previous models (Watzke et al., 2001) we assign voltage dependence in the K^+ countertransport step. In particular, we propose that there is an intrinsic gating charge on the transporter (-1.4; see Kinetic model section) that is partially compensated by K^+. This was necessary to simulate that the glutamate steady-state I-V (>100 μM; Figure $2A_1$ and 12A) and the recovery rate of the anion current in patches (Figure 10 and 13B) do not saturate at hyperpolarized potentials. Such lack of saturation in the I-V is suggestive that the rate-limiting step of the cycle is electrogenic (Lauger, 1991).

Capture efficiency

A property that kinetic transport models can estimate is the capture efficiency or the percentage of whether a molecule of glutamate will be transported rather than released following binding (Otis and Jahr, 1998; Wadiche and Kavanaugh, 1998; Bergles

et al., in press). The determination of capture efficiency is significant because it is a key factor in the decline of extracellular glutamate concentration following synaptic release. According to our model the capture efficiency for EAAT3 ($[Na^+]_o$ and $[K^+]_i$ = 140 mM) at -70 mV is 52 % while at +50 mV it is only 14 %. The low transport efficiency is partly the outcome of having similar rates for the forward (550 s^{-1}) and reverse (500 s^{-1}) glutamate translocation step. As a result, the transporter ricochets between the T_oNa_3GH and T_iNa_3GH states before glutamate is released inside, thus, increasing the probability for glutamate and Na^+ to unbind outside.

The capture efficiency for EAAT1 ($[Na^+]_o$ is 140 mM) is 48 % at -70 mV. However, in oocyte Ringer solution ($[Na^+]_o$ = 98.5 mM) the capture efficiency is only 39 % (-70 mV; see also Wadiche and Kavanaugh, 1998). In addition, although the glutamate translocation rate of EAAT2 (2000 s^{-1}; Bergles et al., in press) is 20 fold faster than EAAT1's (100 s^{-1}), EAAT2 exhibits a capture efficiency of 51 % at -70 mV in the presence of 140 mM $[Na^+]_o$. This is because the EAAT2 glutamate unbinding rate is faster (500 s^{-1}; Bergles et al., in press) than that of EAAT1 (80 s^{-1}), which decreases the probability a glutamate molecule is transported inside instead of unbinding outside. The only EAAT with high capture efficiency is EAAT4, with a capture efficiency of 93 % (-70 mV). This is because EAAT4 has a slow unbinding rate (2 s^{-1}). It was necessary to assign such slow unbinding rate in order to simulate EAAT4' slow deactivation kinetics (see Figure 14 legend).

Significance in synaptic transmission

The low capture efficiency of EAAT1-3 indicates that these transporters would decrease the synaptically released glutamate mainly via rapid binding (Diamond and Jahr,

1997; Tong and Jahr, 1994) leading to buffered diffusion (Rusakov and Kullmann, 1998). In addition, the diminished efficiency of EAAT1 and EAAT2 may lead to their prolonged and asynchronous activation, which, in turn, may contribute to the slow decay kinetics of synaptically activated glial transporter currents (Bergles and Jahr, 1997; Clark and Barbour, 1997). Furthermore, the low capture efficiency of EAAT3 at positive membrane potentials is consistent with the recent finding by Diamond (2001) that spillover in CA1 is pronounced when the neuronal transporters are blocked by holding the membrane potential at a depolarized value (+50 mV). Our model suggests that at this potential (+50 mV), EAAT3 acts more like a glutamate binding protein than a transporter. Unlike the other transporters, however, EAAT4 exhibits remarkable high capture efficiency (>90%) consistent with the proposal by Brasnjo and Otis (2001) that EAAT4 creates a barrier to mGluR1 activation. EAAT4 seems ideal to play such role, since EAAT4 binds glutamate with high affinity (~1-2 μM; Fairman et al., 1995; Lin et al., 1998) and allows minimal unbinding.

In summary, we have developed a comprehensive model for glutamate transport by EAATs. The model simulates the kinetics of glutamate transport at different membrane potentials and ionic conditions. Most importantly, using the model we can estimate the capture efficiency of EAAT1, EAAT2, EAAT3, as well as EAAT4. We hope this model will be a tool in elucidating the role of transporters in synaptic transmission.

CHAPTER 2

Arachidonic acid activates a proton current in the rat glutamate transporter EAAT4

A.V. Tzingounis*, C.L. Lin#, J.D. Rothstein#, and M.P. Kavanaugh*§
*Vollum Institute, Oregon Health Sciences University and #Department of Neurology, Johns Hopkins University

§Author for correspondence
Michael Kavanaugh
Vollum Institute
Oregon Health Sciences University
3181 SW Sam Jackson Pk. Rd.
Portland, OR 97201
tel 503 494 4601
fax 503 494 6972
internet: kavanaug@ohsu.edu

abbreviations: EAAT1-5, excitatory amino acid transporters 1-5

ABSTRACT

The excitatory amino acid transporter EAAT4 is expressed predominantly in Purkinje neurons in the rat cerebellum (Furuta et al., 1997; Nagao et al., 1997; Yamada et al., 1996) and it participates in postsynaptic reuptake of glutamate released at the climbing fiber synapse (Otis et al., 1997). Transporter-mediated currents in Purkinje neurons are increased more than three-fold by arachidonic acid, a second messenger that is liberated following depolarization-induced Ca^{++} activation of PLA_2 (Kataoka et al., 1997). In this study we demonstrate that application of arachidonic acid to oocytes expressing rat EAAT4 increased glutamate-induced currents to a similar extent. However, arachidonic acid did not cause an increase in the rate of glutamate transport or in the chloride current associated with glutamate transport, but rather activated a proton-selective conductance. These data reveal a novel action of arachidonate on a glutamate transporter and suggest a mechanism by which synaptic activity may decrease intracellular pH in neurons where this transporter is localized.

INTRODUCTION

Glutamate transporters play critical roles in synaptic transmission and in maintaining glutamate homeostasis in the brain (Takahashi et al., 1996). They are encoded by genes belonging to a family of acidic and neutral amino acid transporters (Malandro et al., 1996), and they exhibit specific localization patterns. Glutamate transporters found on glia include EAAT1/GLAST and EAAT2/GLT-1 (Lehre et al., 1995; Rothstein et al., 1994) and transporters found on neurons include the widely expressed EAAT3/EAAC1 (Rothstein et al., 1994), the cerebellar-specific EAAT4 (Furuta et al., 1997; Nagao et al., 1997; Yamada et al., 1996), and the retinal EAAT5 (Eliasof et al., 1998).

Arachidonate is released following activation of postsynaptic glutamate receptors (Dumuis et al., 1988). In synaptosomal preparations, arachidonate inhibits glutamate uptake (Chan et al., 1983; Rhoads et al., 1982; Volterra et al., 1992). However, it exerts differential effects on cloned glutamate transporter subtypes, enhancing EAAT2 and inhibiting EAAT1 transport (Zerangue et al., 1995). Arachidonate inhibits uptake in salamander retinal glial cells (Barbour et al., 1989). These cells predominantly express an EAAT1 homolog (sEAAT1) that is similarly inhibited by arachidonate when it is exogenously expressed in oocytes (Eliasof et al., 1998; Zerangue et al., 1995). Because arachidonate is released during synaptic activity and can modulate synaptic transmission (Linden, 1995; Williams et al., 1989), understanding its effects on various glutamate transporter subtypes is important. Recently, Kataoka et al. (1997) reported an activity-dependent enhancement of glutamate transporter currents in rat cerebellar Purkinje neurons that was mediated by arachidonate (Kataoka et al., 1997). The present study was

designed to examine the effects of arachidonate on the cloned rat EAAT4 transporter, which is expressed at high levels in Purkinje neurons.

EXPERIMENTAL PROCEDURES

Electrophysiology and radioflux measurements of rEAAT4. The rat EAAT4 cDNA (Lin et al., 1998) was subcloned into pOG, a vector derived from pBSTA (Goldin et al., 1992) that contains a multiple cloning site between flanking *Xenopus* β-globin 5' and 3' untranslated sequences. Capped mRNA was transcribed using T7 polymerase and injected into stage V or VI oocytes (approx. 50 ng/oocyte). Recordings and radiolabel uptake assays were made 4-7 days later as described (Zerangue et al., 1995). Extracellular Ringer's solution contained (in mM) 100 NaCl, 2 KCl, 1.8 $CaCl_2$, 1 $MgCl_2$. Buffers were present at 5 mM and consisted of MES/HEPES (pH 6.5), Na/HEPES (pH 7.5), or HEPES/TRIS (pH 8.5). Solutions containing indicated ion substitutions were changed by bath exchange. Recordings were made using a two-microelectrode voltage clamp circuit (Wadiche et al., 1995a), and records were analyzed using pCLAMP 6.0 software (Axon Instruments). [^{3}H]L-glutamate (1 Ci/mmol; Amersham) uptake assays were performed at 25°. Following a 5 minute incubation in the indicated concentration of [^{3}H]L-glutamate (10 μCi/mL), oocytes were rapidly washed 3x in cold Ringer, lysed in 1% SDS, and scintillation spectroscopy was performed. Arachidonic acid (Calbiochem) was stored at -20° in 100 mM stock solutions in DMSO and dissolved in recording solution by sonication immediately prior to use. All other compounds were from Sigma.

RESULTS

Three to four days following injection of RNA transcribed from the rat excitatory amino acid transporter EAAT4 cDNA (Lin et al., 1998) *Xenopus* oocytes displayed >30-fold increased uptake of 1μM [^{3}H]L-glutamate. In oocytes voltage-clamped at -60 mV, currents generated by 30 μM L-glutamate were reversibly increased upon co-application of 100 μM arachidonate (Figure 1A). Application of 100 μM arachidonate alone in oocytes expressing rEAAT4 resulted in a small inward current (Figure 1B; -2.2 nA ± 0.6, n=4). This inward current was not observed in uninjected oocytes (1.1 nA ± 0.9, n=9). At -60 mV, arachidonate increased the magnitude of the steady-state current induced by 30 μM glutamate to 324 ± 41 % of its control value (n=11). Currents elicited by glutamate in the presence and absence of arachidonate at a series of membrane potentials showed that arachidonate enhanced the current amplitude to a greater extent at more negative potentials (Figure 1C, D; also see Figure 4). A recent report on the human EAAT4 transporter described a similar increase in inward current in the presence of arachidonate, although the maximal rate of uptake was reduced (Fairman et al., 1997). The glutamate-elicited currents were carried in large part by chloride ions (Fairman et al., 1995; Otis et al., 1997; Wadiche et al., 1995), as the outward current was abolished when chloride was substituted by gluconate (n=4; data not shown).

The arachidonate concentration-dependence in the presence of a saturating concentration of glutamate (30 μM) revealed that the archidonate effect on the current was saturable, with an EC_{50} of 135 ± 21 μM (n=3; Figure 2A). In the presence of arachidonate, the apparent affinity of the transporter for glutamate was unaffected; the EC_{50} of the current was 1.5 ± 0.2 μM and 1.5 ± 0.3 μM in control and with 100 μM

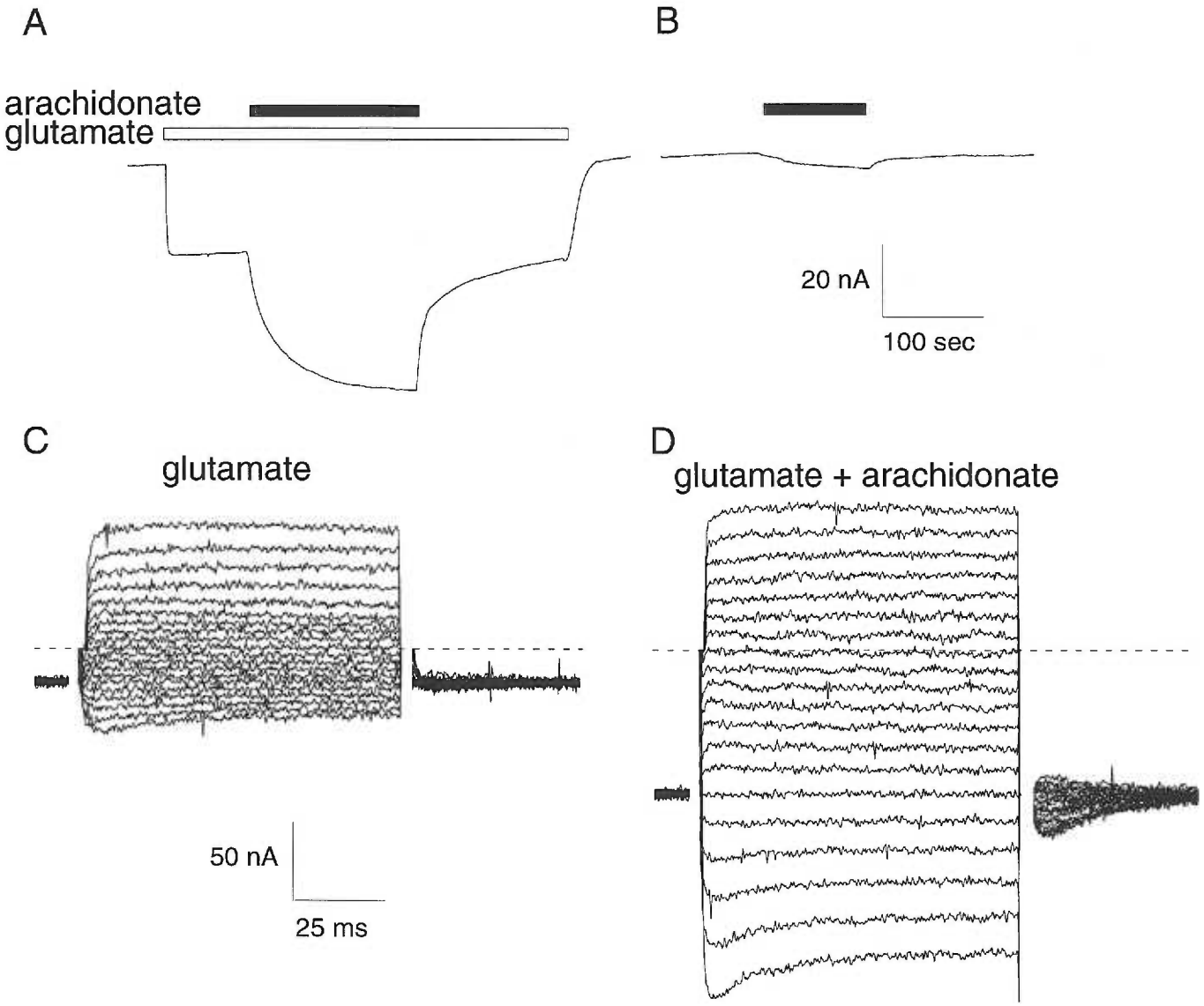
A
arachidonate
glutamate
B
20 nA
100 sec
C
glutamate
50 nA
25 ms
D
glutamate + arachidonate

Figure 1. Arachidonic acid enhances the magnitude of glutamate-induced currents recorded in voltage-clamped oocytes expressing rat EAAT4. A. Representative cell clamped at -60 mV; compounds were superfused for the times indicated by open (30 μM L-glutamate) and closed (100 μM arachidonic acid) bars. B. Application of arachidonate alone induced a current much smaller than observed with co-application of L-Glu. C. Subtracted (30 μM glutamate-control) currents recorded during 90 ms voltage jumps between -120 mV and +70 mV. D. Currents recorded in the same cell as (C) with 100 μM arachidonic acid present. Dashed line indicates zero current; capacitive artifacts have been removed for clarity. Holding potential = -70 mV

arachidonate, respectively (n = 6). The effects of arachidonate on the transport current seemed to be direct rather than through a metabolite, as coapplication of the cyclooxygenase inhibitor indomethacin (100 μM) and the lipoxygenase inhibitor nordihydroguaretic acid (50 μM) had no effect on the potentiation induced by arachidonic acid (96 ± 2 % of control enhancement, n = 3). To examine whether arachidonate affected the transport of L-glutamate in oocytes expressing rEAAT4, uptake of 1 μM or 30 μM [^{3}H] L-glutamate was assayed in the presence or absence of 300 μM arachidonate (Figure 2C and 2D). In marked contrast to its effects on the currents, arachidonate had no significant effect on the uptake of L-glutamate into oocytes. Uptake of 1μM [^{3}H] L-glutamate was 524 ± 152 fmoles/min in control conditions and 468 ± 86 fmoles/min in (n=6; P=0.74). Uptake of 30 μM L-glutamate uptake was also not significantly changed by 300 μM arachidonate (1753 ± 506 fmol/min and 1477 ± 271 fmol/min in control and arachidonate, respectively; n=5; P=0.64). Arachidonate also had no effect on L-glutamate uptake in uninjected oocytes (Figure 2C, D).

These results demonstrate that arachidonate increased a glutamate-dependent rEAAT4 current without affecting glutamate uptake. This is in contrast to arachidonate's effects on the EAAT1 and EAAT2 subtypes, in which L-glutamate uptake and currents are decreased or increased in parallel (Zerangue et al., 1995). Hence, the ionic nature of the rEAAT4 conductance increased by arachidonate was investigated further. Similar to the human EAAT1-EAAT4 subtypes (Fairman et al., 1995; Wadiche et al., 1995b), rat EAAT4 mediates an uncoupled Cl^- conductance in addition to the Na^+-coupled glutamate transport current. To examine whether arachidonate selectively increased the uncoupled Cl^- conductance, the voltage-dependence of the current induced by glutamate was

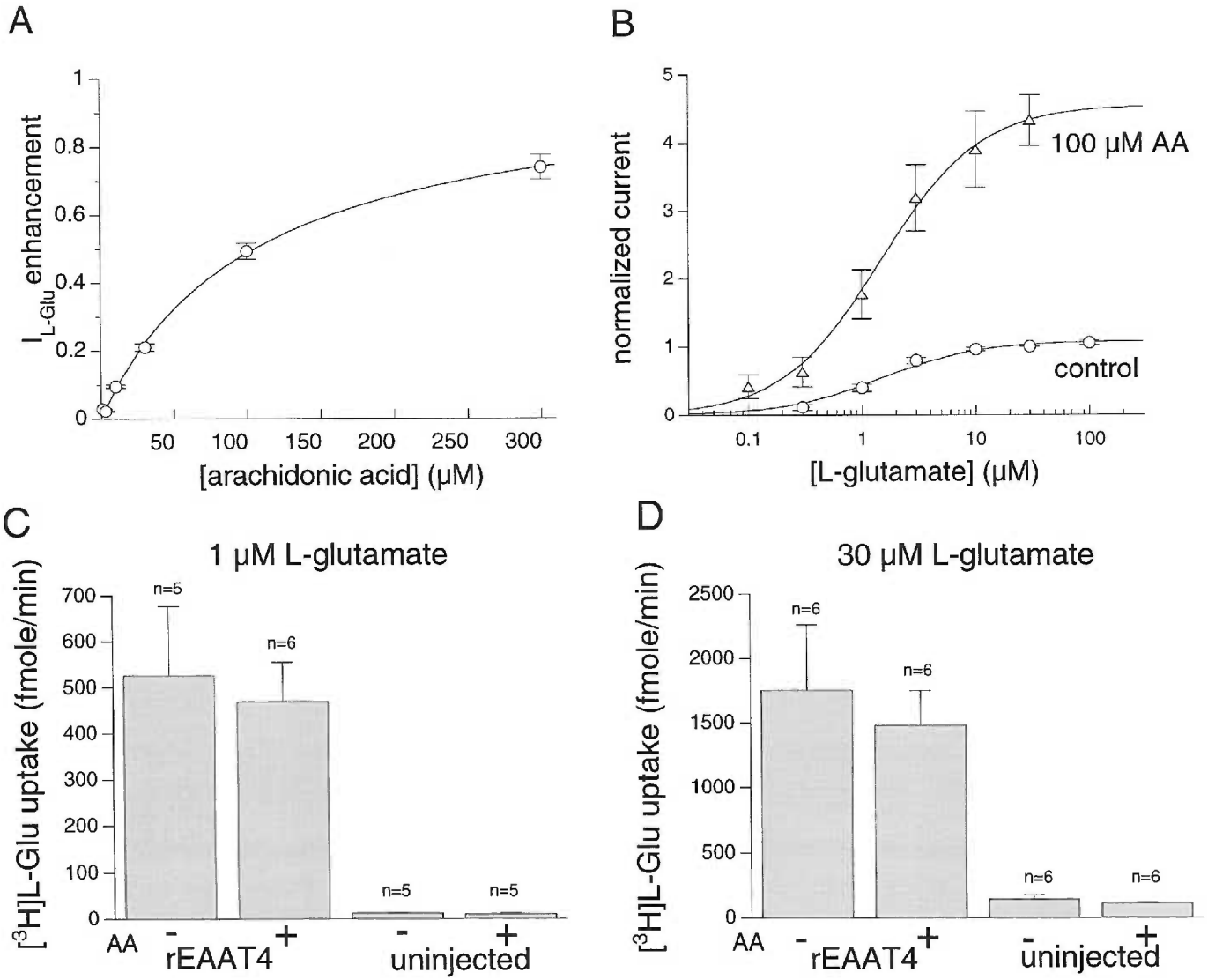
A
$I_{L\text{-}Glu}$ enhancement
[arachidonic acid] (μM)
B
normalized current
100 μM AA
control
[L-glutamate] (μM)
C
1 μM L-glutamate
[^{3}H]L-Glu uptake (fmole/min)
n=5
n=6
n=5
n=5
AA
rEAAT4
uninjected
D
30 μM L-glutamate
[^{3}H]L-Glu uptake (fmole/min)
n=6
n=6
n=6
n=6
AA
rEAAT4
uninjected

Figure 2. Arachidonate dose-dependently increases the transport current without increasing glutamate flux. (A) Arachidonate concentration dependence of transporter currents activated by 30 μM glutamate (normalized to the maximal current at V_m=-70 mV). Points (mean ± s.e.m., n=3) are fitted to the Michaelis-Menten equation with a $K_{0.5}$ of 135 μM. (B) L-glutamate concentration dependence of currents in the presence and absence of 100 μM arachidonate. Currents (mean ± s.e.m., n=6) were normalized to the maximum current in the absence of arachidonate and fitted to the Michaelis-Menten equation. Arachidonate increased the I_{max} without changing the glutamate $K_{0.5}$ value (1.5 μM). (C) Incubation of 100 μM arachidonate along with 1 μM L-glutamate or (D) 30 μM L-glutamate does not affect the [^{3}H] L-glutamate uptake in oocytes expressing rat EAAT4.

examined in the presence and absence of arachidonate. The arachidonate-dependent current was inwardly rectifying, and did not reverse at the Cl^- equilibrium potential (~-20 mV), indicating that the conductance increased by arachidonate was not Cl^- -selective (Figure 3A). To further rule out an action of arachidonate on the transporter-mediated anion conductance, extracellular Cl^- was substituted by the more permeant ion NO_3^- (Otis et al., 1997; Wadiche et al., 1995b). Similar to results with the human EAAT4 transporter (Otis et al., 1997) NO_3^- was more permeant than Cl^-. Relacement of extracellular Cl^- by NO_3^- increased the glutamate-induced outward current and shifted the reversal potential to more negative potentials, from -14.8 mV ± 1.1 to -81.8 mV ± 1.1 (n=3; Fig. 3b). Coapplication of 100 μM arachidonate with glutamate slightly inhibited the outward NO_3^- current, further supporting that conclusion that the conductance increased by arachidonate was not anion selective (Figure 3B). The reversal potential of the glutamate-induced current was shifted approximately +10 mV by arachidonate (from -14.8 +/- 1.1mV to - 4.7 +/- 2.4, n=3), and this shift was not influenced by changing the Na^+ gradient by substitution of 48 mM Na^+ with choline (n=3; data not shown). Hence, the arachidonate mediated increase of the L-glutamate current was selective for ions other than sodium or chloride.

Glutamate transporters mediate a coupled flux of protons with glutamate (Zerangue et al., 1996b). To examine whether a proton-selective current was involved in the arachidonate potentiation of the L-glutamate current, currents were measured with varying extracellular pH between 6.5 and 8.5. Altering the extracellular proton concentration markedly influenced voltage-dependence of the arachidonate-dependent current. As the extracellular proton concentration increased, the potential at which the

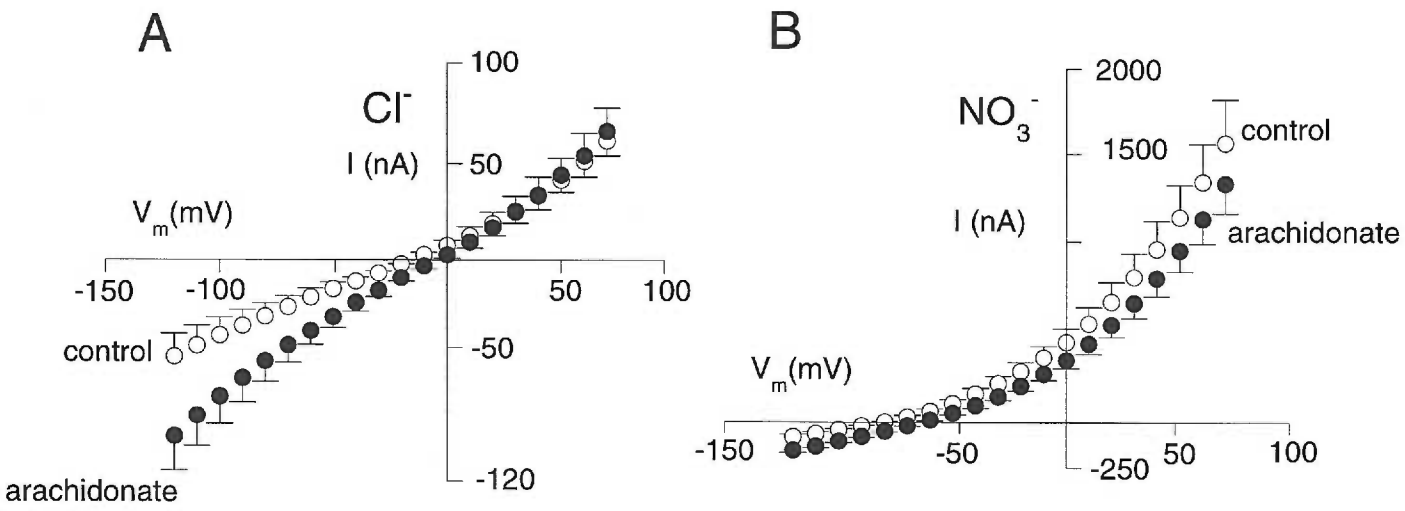
A
Cl-
I (nA)
100
50
-50
-120
Vm(mV)
-150
-100
50
100
control
arachidonate
B
NO3-
2000
1500
control
I (nA)
arachidonate
Vm(mV)
-150
-50
-250
50
100

Figure 3. Arachidonate did not enhance the NO_3^--selective transporter anion conductance. A. Voltage-dependence of glutamate transport currents recorded in Cl^--containing Ringer and B. Glutamate transport currents in the same group of cells with NO_3^- substituted for Cl^-. Note different scales. Open circles, control; closed circles 100 μM arachidonate. Currents represent mean ± s.e.m. n = 3.

glutamate current recorded in the presence of arachidonate crossed the control glutamate current shifted to more positive potentials (Figure 4). With extracellular pH at 7.5, close to the value of the intracellular pH (Webb and Nuccitelli, 1981) the arachidonate-dependent current crossed the control current at 2.3 ± 3.9 mV (n = 11), and this reversal potential changed 53 mV/pH unit (Figure 4D). These results indicate that the major component of the conductance amplified by arachidonate was proton-selective.

DISCUSSION

The present results show that arachidonic acid activates a proton-selective conductance during EAAT4-mediated transport of L-glutamate, extending the recognized types of currents associated with glutamate transporters. In addition to the current associated with the $Na^+/H^+/K^+$ coupled translocation of glutamate (Zerangue et al., 1995), thermodynamically uncoupled Cl^- currents (Billups et al., 1996; Eliasof and Jahr, 1996; Fairman et al., 1995; Picaud et al., 1995; Wadiche et al.,1995b) as well as cation leak currents (Schwartz and Tachibana, 1990; Vandenberg et al., 1995) have been associated with glutamate transport. Different subtypes exhibit variability in both their anion (Wadiche et al., 1995b) and cation conductances (Vandenberg et al., 1995). Several other neurotransmitter transporters mediate uncoupled proton currents (Cao et al., 1997; Sonders et al., 1997), but EAAT4 is the first glutamate transporter reported to exhibit this property.

Rat EAAT4 is predominantly localized to the cerebellum, where it is found on Purkinje cell bodies and dendrites (Furuta et al., 1997; Nagao et al., 1997; Yamada et al., 1996). Transporter-mediated reuptake of glutamate released at climbing and parallel fiber

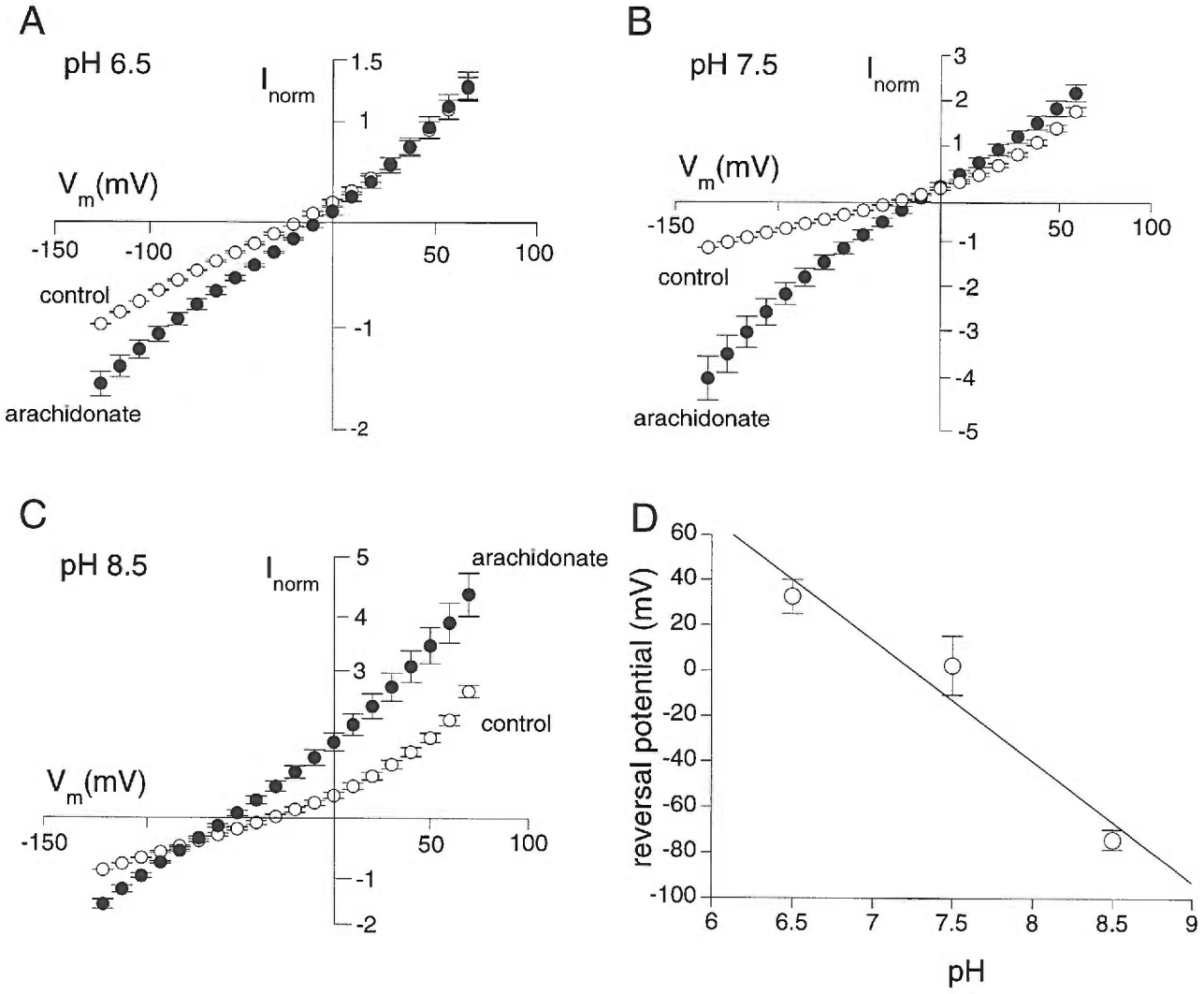
A
pH 6.5
I norm
1.5
1
V m(mV)
-150
-100
50
100
control
-1
arachidonate
-2
B
pH 7.5
I norm
3
2
1
V m(mV)
-150
50
100
control
-1
-2
-3
-4
arachidonate
-5
C
pH 8.5
I norm
5
arachidonate
4
3
control
V m(mV)
-150
50
100
-1
-2
D
reversal potential (mV)
60
40
20
0
-20
-40
-60
-80
-100
6
6.5
7
7.5
8
8.5
9
pH

Figure 4. Arachidonate enhances a proton-selective current. Voltage dependence of currents induced by 30 μM glutamate in the presence and absence of 100 μM arachidonate at pH 6.5 (A), 7.5 (B), and 8.5 (C). D. Extracellular pH shifted the potential at which currents in the presence of arachidonate crossed over the control transport currents. Line shows least squares fit with slope of -53.4 mV/pH unit.

synapses onto Purkinje cells plays an important role in speeding the decay of postsynaptic responses (Barbour et al., 1994; Takahashi et al., 1995). The transporters participating in this process are located both in glial cells surrounding the synapse (Bergles et al., 1997; Clark and Barbour, 1997), as well as in the postsynaptic dendrites and cell body (Otis et al., 1997; Takahashi et al., 1996). The pharmacological and electrophysiological properties of the synaptically activated transport current in Purkinje cells suggest that it is mediated in large part by EAAT4 (Otis et al., 1997).

Arachidonic acid is liberated by activation of phospholipase A_2 during neuronal activity (Dumuis et al., 1990; Kataoka et al., 1997), and it can modulate activity-dependent changes in synaptic strength in Purkinje cells (Linden, 1995). Whether exogenously applied or generated by depolarization, arachidonic acid increased the amplitude of glutamate transporter-mediated currents in rat Purkinje cells (Kataoka et al., 1997). The amplitude of the increase seen in Purkinje cells was similar to that reported here with the exogenously expressed EAAT4. Together these results suggest that synaptic activity may lead to activation of a glutamate transporter-mediated proton influx in neurons which express EAAT4. Because pH strongly influences the activity of many types of ion channels (for review see Takahashi and Copenhagen, 1996) this property of the transporter could provide an additional mechanism to modulate postsynaptic responses.

Acknowledgments

We thank Yuqin Yang for oocyte preparation and T. Otis and J. Wadiche for discussions and comments on the manuscript.

CHAPTER 3

The neuronal glutamate transporter EAAT3 functions as a pentamer of independent subunits

Anastassios V. Tzingounis[1,2*], Navid Madani[1*], and Michael P. Kavanaugh[1]
1. Vollum Institute and 2. Neuroscience Graduate Program, Oregon Health & Sciences University, Portland, OR 97201

Corresponding author:
Michael Kavanaugh
Vollum Institute, L-474
Oregon Health & Sciences University
Portland, OR 97201
phone: 503-494-4602
fax: 503-494-6972
email : kavanaug@ohsu.edu

*: These authors contributed equally to this work.

Acknowledgments: We thank Hans Koch and Jacques Wadiche for discussions and comments on the manuscript.

ABSTRACT

Glutamate transporters are responsible for the reuptake of L-glutamate following its release from excitatory terminals. Several lines of evidence indicate that both glial and neuronal glutamate transporters assemble into an aggregate of multiple subunits. Estimates from radiation inactivation experiments suggest that glutamate transporters contain at least two but no more than four subunits. We have examined the subunit stochiometry of the neuronal glutamate transporter EAAT3 first, by cross-linking EAAT3 transporters expressed on oocytes and, two, by coexpressing a wild type EAAT3 along with a point mutant with altered amino acid selectivity. The results from this study support a model where EAAT3 is a homopentamer of functionally independent transporters.

INTRODUCTION

Upon fusion of synaptic vesicles to presynaptic excitatory terminals, glutamate is released where it rapidly diffuses within the synaptic cleft activating glutamate receptors. The termination of its action is dependent on diffusion and reuptake by a distinct family of transporters known as excitatory amino acid transporters (EAATs; see for review Danbolt, 2001). The role of glutamate transporters in synaptic transmission and in general normal brain homeostasis is still controversial. Various groups have reported different effects of blocking glutamate uptake on the time course of synaptic transmission. In hippocampus, for instance, blocking transporters with substrate inhibitors had no effect on AMPA and NMDA mediated synaptic transmission (Isaacson and Nicoll, 1993; Sarantis et al., 1993). Recently, however, it was demonstrated that application of the non-selective competitive inhibitor TBOA (Shimamoto et al., 1998) results in a slight enhancement of the NMDA mediated response (Diamond, 2001). Because the time constant of a transport cycle for glutamate transporters is significantly slower (10-70 ms; Bergles and Jahr, 1998; Wadiche et al., 1995a; Wadiche and Kavanaugh, 1998) than the time constant for glutamate decay in a hippocampal synapse (~1-2 ms; see for review Bergles et al., 1999), the current notion regarding the role of transporters during fast synaptic transmission is to rapidly bind glutamate and, then to slowly transport it into the cell. This hypothesis has been slightly modified, recently, with the suggestion that the early parts of the glutamate cycle are rapid (Auger and Attwell, 2000; Bergles et al., 1997; Grewer et al., 2000; Otis and Jahr, 1998; Otis and Kavanaugh, 2000). As a result, glutamate transporters have been suggested to bind and transport glutamate on a faster time scale than was previously expected even though the cycling rate is slow. Glutamate

transporters do set the lower limit for ambient levels of glutamate in the brain (see for review Danbolt, 2001). Since basal glutamate levels (~200 nM; Jabaudon et al., 1999) are at the threshold for activating NMDA-type glutamate receptors, one parameter that influences synaptic receptor activity is the transporter density (Iino et al., 2001; Oliet et al., 2001).

Based on quantitative electron microscopy measurements, it has been estimated that the density of transporters surrounding the synapse varies between 740-8500 molecules/μm^2 depending on the transporter subtype and brain region (Dehnes et al., 1998; Lehre et al. 1998). However, such estimations assume that transporters are primarily assembled as monomers. To date, there is a lack of consensus regarding the stoichiometry of glutamate transporters (Beliveau et al., 1990; Dehnes et al., 1998; Eskandari et al., 2000; Haugeto et al., 1996). Chemical crosslinking of homogenised rat brains followed by SDS gel electrophoresis suggested that transporters might associate as homomultimers. It was shown that EAAT1, EAAT2, and EAAT3 could form either dimers or trimers, while EAAT4 forms only dimers (Dehnes et al., 1998; Haugeto et al., 1996). Recently, using freeze-fracture electron microscopy, Eskandari et al. (2000) reported that EAAT3 is a pentamer. The reason for the discrepancy between the conclusions of Eskandari et al. (2000) and Haugeto et al. (1996) is unknown.

Furthermore, there is still no conclusive evidence as to whether multimer formation is required for transporter function. Radiation inactivation experiments have suggested a functional unit that is 2-4 times the monomer size (Beliveau et al., 1990; Haugeto et al., 1996). However, the discovery of EAAT specific interacting proteins confounds these estimations. To resolve the issue of whether EAATs function as

multimers, we have used an approach that was originally developed to determine the subunit stiochiometry of K^+ channels (MacKinnon, 1991).

MATERIALS AND METHODS

Modification of membranes with glutaraldehyde. Stage V-VI Xenopus oocytes were injected with capped mRNA (50 ng/oocyte) transcribed from cDNA encoding EAAT1-3 (Arriza et al., 1994). Three to four days later, oocyte membranes were prepared by homogenizing 6-10 oocytes in disruption buffer (50 mM Tris [pH 8.0] 10 mM EDTA [pH 8.0], 10% glycerol, 100 mM PMSF) at 4 °C. The homogenates were spun using a table top microfuge at 4,000 rpm for 5 min. The supernatant was removed and spun at 14,000 rpm for 30 min. Oocyte yolk was removed from each tube and the membrane pellets were then dissolved in 1% triton X-100 in phosphate buffered saline (PBS), pH 7.5. Increasing concentrations of glutaraldehyde were mixed with membrane detergent extracts for 1 min prior to quenching with glycine. The cross-linked proteins were dissolved in sodium dodecyl sulfate (SDS)-polyacrylamide gel electrophoresis sample buffer (62.5 mM Tris-HCl [pH 6.8], 10% glycerol, 2% SDS, 0.1% bromophenol blue, 10% 2-mercaptoethanol), heated at 37 °C for 10 min, then loaded onto a 6% polyacrylamide gel in the presence of 0.1% SDS and subjected to electrophoresis. The resolved proteins were transferred to nitrocellulose membranes, which were used for subsequent immunoblotting. Cross-linked proteins were detected by incubating the membranes with human EAAC1 antiserum (generous gift of Dr. Jeffery Rothstein). The antiserum was diluted at a 1:1000 dilution in 5% milk-0.1% Tween 20-Tris buffered

saline (Bio-Rad laboratories; Hercules, Calif.). This incubation was followed by incubating with protein A-conjugated horseradish peroxidase (HRP) (Bio-Rad) at a 1:10,000 dilution. Antibody binding was then detected with a Phototope-HRP Western blot detection kit (New England Biolabs, Mass). For albumin cross-linking, bovine albumin (Sigma, St. Louis, Mo) was dissolved in PBS at a concentraion of 20 mg/mL. 20 *m*L samples of albumin were used for cross-linking with varied concentrations of glutaraldehyde. The samples were then quenched with glycine, dissolved in SDS-sample buffer, run on a 6% polyacrylamide gel as described before. Coommassie staining was used to detect cross-linked proteins. P300 (generous gift of Dr. Richard Goodman) was used as a molecular weight marker. 1-ethyl-3-(3-dimethylaminopropyl) carbodiimide hydrochloride was purchased from Molecular Probes (Eugene, OR).

Two electrode voltage clamp recordings. Oocytes were injected with EAAT3 cRNA as described above. In co-expression experiments EAAT3 and R443C cDNA were quantified by spectroscopy then mixed in given ratios followed by cRNA synthesis (Kavanaugh et al., 1992). Membrane currents were recorded 2-4 days following injection. The extracellular Ringers solution (ND96) contained: 96 mM NaCl, 2 mM KCl, 1.8 $CaCl_2$, 1 mM $MgCl_2$ and 5 mM Na/HEPES. Tris base was used to pH the solution at 7.5. Recordings were performed at 22°C-25 °C with a Geneclamp 500 amplifier. Acquisition was performed with an IBM-compatible PC (Gateway) using a Digidata 1200 A/D controlled with pCLAMP 6.0 program (Axon Instruments, Foster City, CA). The currents were low-pass filtered at 1 kHz and digitized at 5 kHz. Electrodes were filled with 3 M KCl and had tip resistances <1 MΩ. The bath was grounded with an Ag/AgCl electrode.

The current-to-voltage dependence induced by different substrates was estimated by subtracting control currents from currents recorded in the presence of substrate.

Uptake assays. [^{3}H] L-amino acid (1 Ci/mmol; Amersham Pharmacia Biotech) uptake assays were performed at 25 °C. Following a 10-min incubation in 1 mM of [^{3}H]-amino acid (10 μM/ml), oocytes were rapidly washed three times in cold Ringer and lysed in 1% SDS, and scintillation spectroscopy was performed.

RESULTS

Glutaraldehyde modification of bovine albumin and EAAT3.

Freeze-fracture electron microscopy on oocytes expressing EAAT3 resolved particles that were pentagonal in shape and size. As a result, it was concluded that EAAT3 forms homomultimers each consisting of five subunits (Eskandari et al., 2000). To biochemically verify this result we determined the number of glutamate transporter subunits in EAAT3 by using cross-linking reagents.

To avoid experimental artifacts due to slowed mobility of cross-linked EAAT3 on polyacrylamide gel we first compared the relative mobility of molecular weight standards to cross-linked albumin (Figure 1A). Albumin has a similar molecular weight to EAAT3, thus, can serve as a good control. Consistent with previous reports (Steele et al., 1978; Sukharev et al., 1999) the mobility between the molecular weight standards for monomers and dimers to the cross-linked polypeptides coincide (Figure 1A). However, higher molecular weight oligomers have a tendency to migrate faster than their molecular

A.

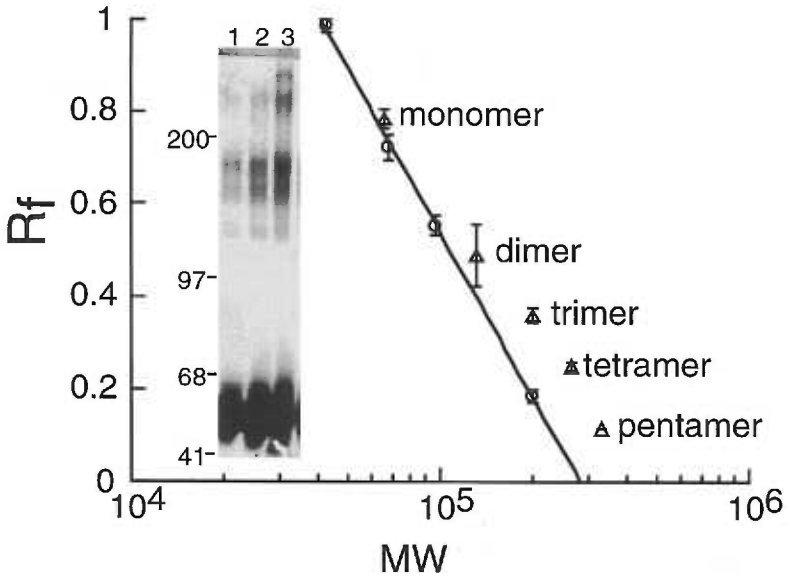
1
0.8
0.6
0.4
0.2
0
Rf
1 2 3
200
97
68
41
monomer
dimer
trimer
tetramer
pentamer
10^4
10^5
10^6
MW

B.

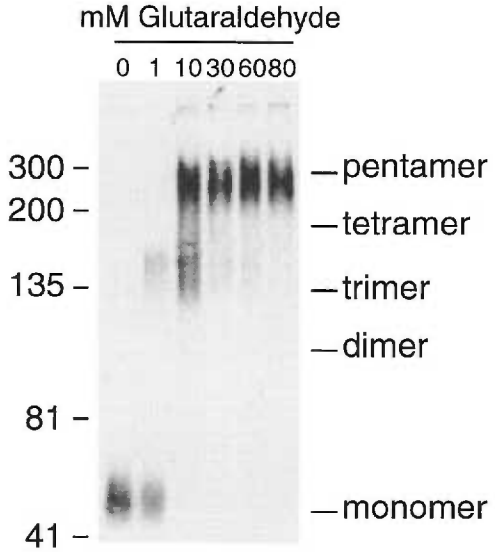
mM Glutaraldehyde
0 1 10 30 60 80
300
200
135
81
41
pentamer
tetramer
trimer
dimer
monomer

Figure 1. Cross-linking of bovine serum albumin and neuronal specific glutamate transporter, EAAT3: (A) Bovine serum albumin was cross-linked with glutaraldehyde. The relative mobility of crossed-linked albumin is plotted against the molecular weight of standards on a log scale. Standard proteins are shown as open circles. The oligomers of albumin are plotted as open triangles. Each point is the mean of 3 independent experiments and the error bars represent standard errors. Inset: coommassie stained gel of cross-linked albumin, lane 1, 2, 3 are 30, 60, and 100 mM glutaraldehyde, respectively. (B) Oocytes were injected with EAAT3 cRNA, oocyte membranes were purified and cross-linked with different concentrations of glutaraldyde as described in Materials and Methods. Data acquired by Navid Madani.

weight counterparts (Figure 1A; Steele et al., 1978; Sukharev et al., 1999). Based on our results with albumin, there is 10-20% deviation of cross-linked oligomers to that of molecular weight standard monomers.

Once this deviation in mobility of cross-link vs. monomeric polypeptides was established, we examined the homo-multimerization of EAAT3. Oocyte membranes from cells expressing EAAT3 were prepared and cross-linked as described in Materials and Methods. Figure 1B is a representative experiment of 8 different determinations demonstrating that increasing concentrations of glutaraldehyde results in formation of higher molecular weight complexes. The slowest running band migrates at approximately 300,000 daltons, slightly less than expected for an EAAT3 pentamer (330,000). However, according to our previous data (Figure 1A), and published work of others (Steele et al., 1978; Sukharev et al., 1999), oligomers of polypeptides larger than dimers have a tendency to migrate faster in SDS gels. Therefore the 300 kDa value for an EAAT3 pentamer falls within the previously described deviation. Similar results were obtained using 1-ethyl-3-(3-dimethylaminopropyl) carbodiimide hydrochloride (EDAC) as a cross-linking agent (data not shown).

Arg^{443} affect EAAT3's amino acid selectivity

The C-terminal domain of the EAAT subunits participates in the cation and substrate selectivity (Kanner et al., 2001). In agreement, Bendahan et al. (2000) demonstrated that arg^{447} located at transmembrane domain 8 of the rat EAAT3 plays an important role in the binding and transport of acidic amino acids. Therefore, we engineered a cysteine point mutation of arg^{447} at the equivalent position in the human

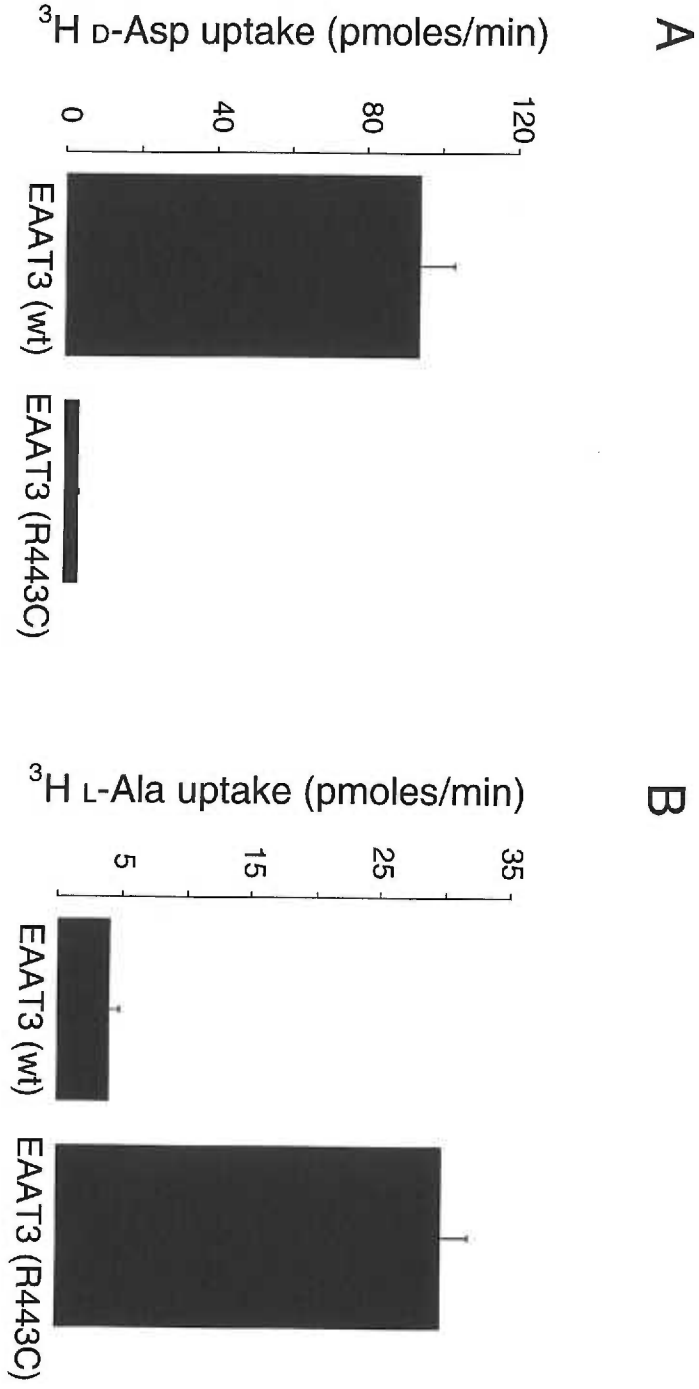
A
^{3}H D-Asp uptake (pmoles/min)
0
40
80
120
EAAT3 (wt)
EAAT3 (R443C)
B
^{3}H L-Ala uptake (pmoles/min)
5
15
25
35
EAAT3 (wt)
EAAT3 (R443C)

Figure 2. Substitution of Arg^{443} to Cys changes the amino acid selectivity of EAAT3. Uptake of oocytes expressing wild type EAAT3 and mutant EAAT3 R443C. Each experiment is an average of 5 oocytes. Oocytes were incubated in 1 mM L-alanine or 1 mM D-aspartate (see Methods). Data acquired by Navid Madani.

EAAT3 (arg^{443}). Figure 2 shows the effect of the R443C mutation to the amino acid uptake. Compared to the wild type, the mutant transporter shows significant levels of L-alanine uptake (Figure 2B), while the D-aspartate uptake is severely diminished (Figure 2A). Similar results were obtained for L-glutamate. Furthermore, Figure $3A_1$ shows that application of 1 mM L-alanine to oocytes expressing R443C EAAT3 elicits an outwardly rectifying current, while application of 1 mM L-glutamate does not induce any response (Figure $3B_1$), in sharp contrast to the L-glutamate responses obtained with wild type EAAT3 (Figure $3B_3$). Previously, Bendahan et al. (2000) demonstrated that the R to C mutation also eliminates K^+ countertransport, as a result, the transporters are transformed to exchangers. Thus, the current induced by L-alanine might reflect the activation of the thermodynamically uncoupled anion current (Bendahan et al., 2000; Wadiche et al., 1995b).

EAAT3 functions as an independent subunit

To assess whether EAATs function as multimers, we co-expressed wild type and mutant transporter cRNAs in varying ratios. The rationale for this experiment is that, if the subunits comprising the functional transporter are greater than one, then some transporters will have only wild type subunits, some will have only mutant subunits, while some others will have both subunit types. If the transporter subtypes were to interact, the concentration dependence of L-glutamate would follow a model in which L-glutamate would activate a current to a distribution of multimeric transporter forms with a variable L-glutamate affinity. By assuming a random association of wild type and mutant subunits, the ratios of multimeric species can be predicted based on a binomial

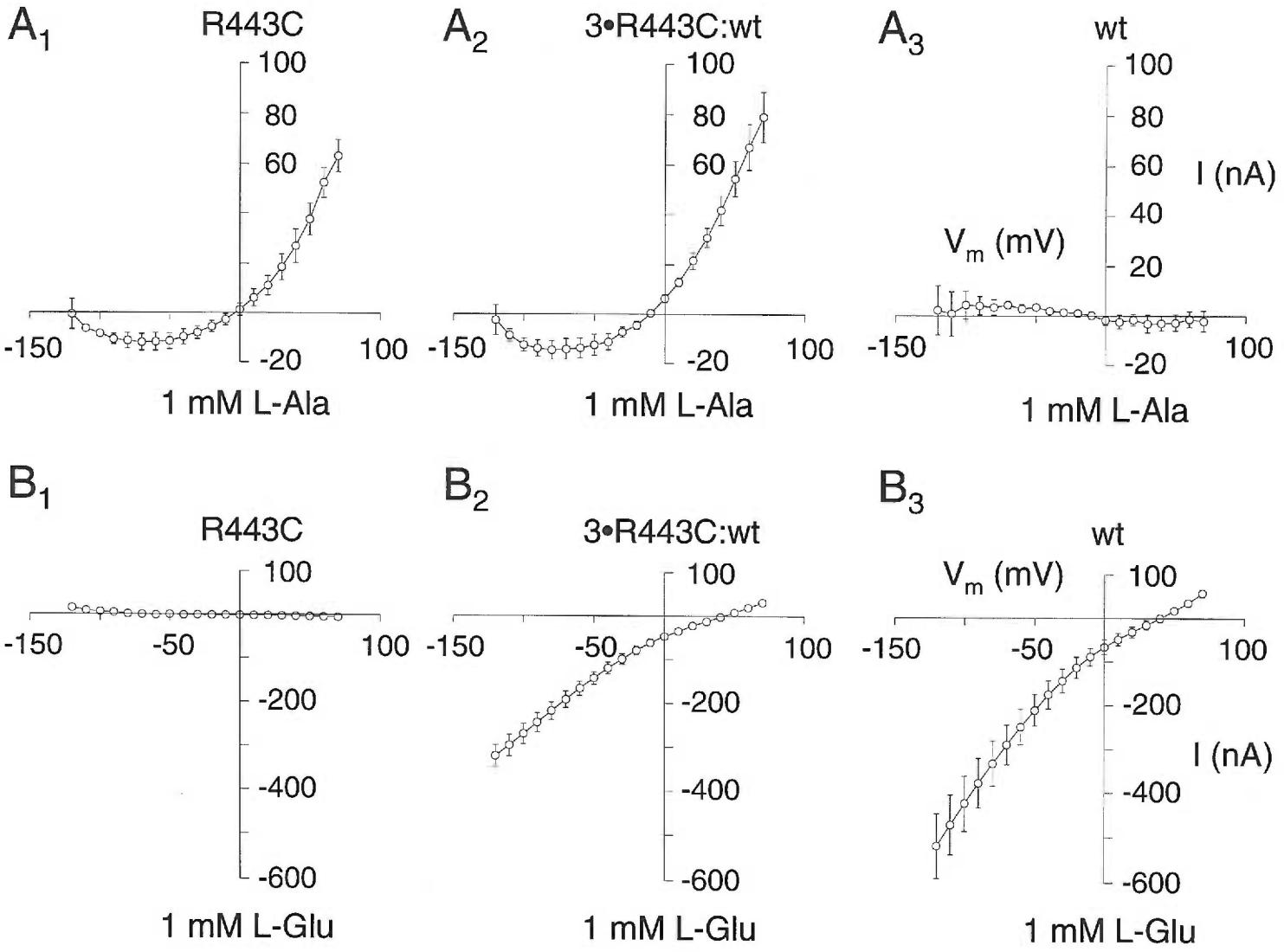
A1
R443C
100
80
60
-150
-20
100
1 mM L-Ala
A2
3•R443C:wt
100
80
60
-150
-20
100
1 mM L-Ala
A3
wt
100
80
60
40
20
I (nA)
Vm (mV)
-150
-20
100
1 mM L-Ala
B1
R443C
100
-150
-50
100
-200
-400
-600
1 mM L-Glu
B2
3•R443C:wt
100
-150
-50
100
-200
-400
-600
1 mM L-Glu
B3
wt
Vm (mV)
100
-150
-50
100
-200
I (nA)
-400
-600
1 mM L-Glu

Figure 3. R443C co-expresses with wild type EAAT3. (A_1) Application of 1 mM L-alanine induces a current in oocytes expressing EAAT3 R443C, while (B_1) 1 mM L-alanine does not. (A_2) Application of 1 mM L-alanine or (B_2) 1 mM L-glutamate induces currents at oocytes expressing both wild type EAAT3 and EAAT3 R443C. (A_3) Application of 1 mM L-alanine induces a response in oocytes expressing only EAAT3 R443C, while (B_3) application of 1 mM L-glutamate does not.

distribution. This type of analyses is based on the assumption that the L-glutamate insensitive subunit is expressed along with the wild type EAAT3 and in equal manner. We could verify expression of the mutant subunit by application of 1 mM L-alanine to oocytes injected with mutant cRNA, since L-alanine will only elicit a current on the mutant subunits (Figure $3A_1$). For instance, unlike the oocytes expressing only mutant or wild type subunits, when the mutant subunits are coexpressed at different ratios with the wild type subunits, application of either L-alanine or L-glutamate induces a steady-state current (Figure $3A_2$, B_2). Figure $3A_2$-B_2 shows the current induced by L-alanine and L-glutamate in oocytes expressing both R443C and wild type EAAT3 in a ratio of 3:1. Similar results were obtained when the ratio of R443C to wild type EAAT3 was 10:1 (data not shown).

An added complication is that the apparent affinity of EAAT3 for L-glutamate varies with its expression level. In particular, the glutamate apparent affinity decreases with transporter expression. This becomes important when we compare the affinity of wild type EAAT3 to the affinity of oocytes co-injected with the mutant subunit along with either 3 or 10 fold lower levels of wild type EAAT3 cRNA. As a result, to avoid any expression artifacts we compared oocytes with low to intermediate expression of wild type EAAT3 to oocytes co-injected with mutant and wild type EAAT3.

The results of coexpressing wild type and mutant EAAT3 are shown in Figure 4. Surprisingly, the L-glutamate apparent affinity did not shift with changes in the mutant to wild type co-injection ratios of 3:1 and 10:1 (Figure 4). In particular, the K_m values were 18.6 ± 2 μM (n=5) for the wild type EAAT3, 22.7 ± 1 μM (n=4) for the oocytes expressing 3 times more R443C EAAT3, and 13.4 ± 1 μM (n=5) for oocytes expressing

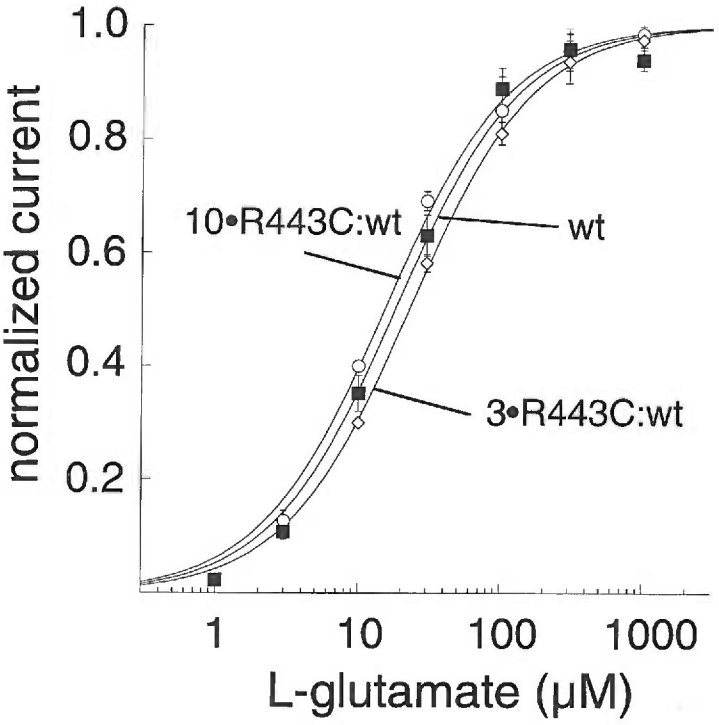
normalized current
1.0
0.8
0.6
0.4
0.2
10•R443C:wt
wt
3•R443C:wt
1
10
100
1000
L-glutamate (μM)

Figure 4. EAAT3 is functionally a monomer. L-glutamate concentration dependence of currents from oocytes either expressing wild type EAAT3 or differing ratios of wild type EAAT3 and mutant EAAT3 R443C. Curves are least squares fit of the data (mean ± S.E). The K_m values are 18.6 ± 2 μM (n=5; wt EAAT3), 22.7 ± 1 μM (n=4; wt: 3•R443C), and 13.4 ± 1 μM (n=5; wt: 10•R443C). Currents are normalized to the maximal response.

10 times more R443C EAAT3 than wild type EAAT3. The simplest interpretation of these data is that EAAT3 functions as an independent subunit even though it exists in a multimeric complex. Otherwise, a shift in the L-glutamate affinity to lower values should have been seen as we express higher proportion of mutant cRNA. We were not able to perform the reciprocal experiment of measuring the L-alanine K_m, because of high variability in the responses induced by L-alanine. However, a similar conclusion has been suggested by co-expressing a different mutant subunit (E375C), which exhibits a higher apparent L-glutamate affinity in conjunction to sensitivity to MTSEA. Application of MTSEA to oocytes co-injected with wild type EAAT3 and E375C mutant blocked a fraction of current that was consistent with independent transporter populations (Hubbard and Kavanaugh, unpublished observations).

DISCUSSION

Results of our study suggest that EAAT3 contains five subunits that are functionally independent from each other. Cross-linking of oocytes expressing EAAT3 with either glutaraldehyde or EDAC clearly demonstrates that EAAT3 is an oligomer, and consistent with Eskandari et al. (2000), a pentamer. Our results differ from previous reports using cross-linking reagents suggesting EAAC1 or EAAT3 is a trimer (Haugeto et al., 1996). However, these authors did observe transporter bands of higher molecular weight than a trimer.

An important question that our study addresses is whether transporters also function as oligomers. We took advantage of a point mutant (R443C) that decreased the

sensitivity of the transporters to D-aspartate and L-glutamate (Figure 2; Bendahan et al., 2000). Application of 1 mM L-glutamate to oocytes expressing R443C EAAT3 did not elicit a glutamate dependent current (Figure $3B_1$), while 1 mM L-alanine activated an outwardly rectifying current (Figure $3A_1$). This allowed us to confirm that R443C EAAT3 is expressed in oocytes in the presence of the wild type EAAT3. Therefore, we could determine the number of subunits in a functional transporter by estimating the affinity of L-glutamate in oocytes that contained different proportions of wild type EAAT3 and mutant cRNAs. If the transporters were functioning as pentamers, assuming random association of subunits, injection of the two cRNAs (R443C and wild type) will result in transporters that contain one to five mutant subunits with the relative amount of each species dictated by the proportion of cRNA injected (Kavanaugh et al., 1992; MacKinnon, 1991; Tzounopoulos et al., 1995; Wang and Goldstein, 1995). The L-glutamate affinity, then, is determined by fitting the sum of several logistic functions to concentration-response data (Kavanaugh et al., 1992). Since L-glutamate application does not activate a current in R443C EAAT3, a transporter that contains this mutant subunit along with the wild type EAAT3 should have lower apparent affinity for L-glutamate than wild type EAAT3. However, by injecting either wild type EAAT3 alone or co-expressing it with the mutant subunit in different cRNA ratios resulted in L-glutamate dose responses that were fitted with one component Michaelis-Menten equation with similar K_m values (Figure 4). This finding suggests that EAAT3 functions as an independent subunit and not as a multimer as was previously suggested (Beliveau et al., 1990; Haugeto et al., 1996). Our results are also consistent with earlier work demonstrating that the removal of glycosylation sites from GLAST/EAAT1 eliminate the

ability of the transporter to homodimerize, but retained its transport activity (Conradt et al., 1995).

An assumption inherent to this work is that the wild type EAAT3 and the mutant subunits form heteromultimers. One can argue that the mutant subunit could have a dominant negative effect when co-assembled with wild type EAAT3. As a result, only homomultimers of either wild type EAAT3 or R443C EAAT3would be functional. We think this is an unlikely possibility, particularly, since preliminary results with a different mutant subunit points to similar conclusions (Hubbard and Kavanaugh, unpublished observations). Furthermore, it is also possible that the mutant subunit does not express to the same level as the wild type EAAT3, biasing our results towards the wild type EAAT3. However, the lack of shift in the L-glutamate K_m when we injected 10 times more mutant cRNA than wild type EAAT3 makes it unlikely that the conclusions are an expression artifact.

Our result leads to the following question, why are transporters oligomers and yet function as independent subunits? One suggestion has been that oligomers are required for the formation of the thermodynamically uncoupled anion conductance that is associated with the EAATs (Borre et al., 2002; Eskandari et al., 2000; Ryan and Vandenberg, 2002). However, there is as of yet no experimental evidence to support such claim. Another possibility is that oligomerization may allow for high-density packing. Lehre and Danbolt (1998) estimated that in hippocampus the concentration of glutamate transporters surrounding the synapse is approximately ~100–300 μM (Lehre et al., 1998). If transporters are functionally pentamers then their concentration would be 20-60 μM and as a result the uptake capacity through glutamate transporters in the brain would be

significantly impaired. To date no quantitative data exist regarding the concentration of EAAT3 in the brain. Such estimation is now important due to the recent demonstration in hippocampus that neuronal transporters, presumably EAAT3, may control the extent of cross-talk among synapses (Diamond, 2001) as well as GABA synthesis (Sepkuty et al., 2002).

DISCUSSION AND CONCLUDING REMARKS

A. Kinetic mechanism for glutamate transport

The work presented in this dissertation has led us to propose a kinetic model for the glutamate cycle. We suggest that two Na^+ ions bind first followed by the binding of either a proton or a glutamate, before a third Na^+ ion binds to the transporter. Then, a voltage independent transition moves the transporter from an outward facing to an inward facing conformation allowing Na^+, H^+, and glutamate to unbind. First, one Na^+ unbinds followed by the ordered unbinding of a proton and glutamate. Then, the cycle is completed, by the unbinding of the remaining Na^+ ions, the binding of K^+, and the K^+-driven countertransport. We also propose that in addition to the first Na^+ the binding of the third Na^+ outside and inside along with K^+-countertransport are the major charge moving steps in the cycle. This model successfully simulates the majority of our experimental findings as well as the kinetics of the coupled current in patches (Bergles et al., in press), further supporting its predictability. In addition, although the kinetic scheme is the same for EAAT1-4, there are some variations between the EAAT1-4 models in the rates entering and leaving several states. In summary, I believe this model can serve as a tool in understanding the complex kinetic behavior of glutamate transport.

For example, using the model we estimated EAATs (EAAT1-4) capture efficiency: the probability that a glutamate molecule when bound to the transporter will be sequestered inside instead of unbinding back outside. This is a property that has not been measured otherwise experimentally. According to the model, the capture efficiency for EAAT1-EAAT3 ranges at ~50 % (V_m = -70 mV), while EAAT4's is greater than ~90

%. This indicates EAAT1-3 will clear the synaptically released glutamate initially via rapid binding leading to buffered diffusion (Rusakov and Kullman, 1998). In contrast to EAAT1-3, the Purkinje cell specific transporter EAAT4 has high capture efficiency and glutamate affinity but slow kinetics. Actually, while the cycling time constant of EAAT1-3 in patches is ~ 25 ms, EAAT4 has a cycling time constant of 100 ms. This means that EAAT4 will reach saturation at lower glutamate concentrations in comparison to the other EAATs. EAAT4's high capture efficiency ensures that no or little glutamate will spill in back into the synapse. In summary, EAAT1-3's low capture efficiency reaffirms the notion that rapid glutamate binding by transporters along with high transporter density determines the fidelity and speed by which EAATs will clear synaptically released glutamate from the extracellular space.

B. Proton transport

Early studies showed that glutamate uptake is coupled to the translocation of a pH-changing ion (Ererecinska et al., 1983; Nelson et al., 1983). However, only recently it was resolved that the pH-changing ion is a H^+ and not an OH^- ion (see for review Danbolt, 2001). Although there is an acceptance regarding the nature of the pH-changing ion, its binding order in respect to glutamate has been controversial. Our results were consistent with a model in which a proton and glutamate can bind to the transporter in a random fashion. Like Zerangue and Kavanaugh (1996a,b), we also concluded that L-cysteine binds to the transporter primarily as a neutral zwitterion. Unlike L-glutamate, the transport of L-cysteine is not accompanied with an intracellular acidification (Zerangue and Kavanaugh, 1996b). Therefore, the transport of L-glutamate requires the independent

binding of a proton from the extracellular solution, while L-cysteine gives up its proton to the transporter. Based on this observation, it was postulated that EAATs transport amino acids as a carboxylate-proton ion pair (Zerangue and Kavanaugh, 1996b). However, this hypothesis would be plausible only if the pKa of the amino acid and proton binding site is low enough to promote the protonation of acidic amino acids. For instance, the pKa for the transportable substrates L-glutamate, L-cysteate, and L-serine-O-sulfate is 4.3, 1.5, and less than < 0, respectively (Vandenberg et al., 1998). As a result, the pKa of the amino acid-proton binding site has to be significantly less than 5 to allow protonation of some of the acidic amino acids. This prediction, is in contrast to recent conclusions of Watzke et al. (2000), who suggested that the pKa for the proton binding site should be greater than 8. In addition, to model our experimental findings we also had to set the pKa for proton binding greater than 8. If the pKa of the proton site is greater than 8, then it is likely that the proton of L-cysteine with its pKa of 8.3 will be shared by L-cysteine and the transporter. In contrast, acidic amino acids will be transported in their anionic form since they would not be protonated. Inherit to this mechanism is that L-cysteine binds to an unprotonated transporter. Therefore, a prediction of this model would be that the apparent affinity for L-cysteine would be lower when the extracellular pH is shifted from 8.5 to 6.5, since a smaller fraction of transporters will be in an unprotonated state. Indeed, at hyperpolarized potentials, which further promote proton binding to the transporter, the affinity for L-cysteine decreases almost two fold (see also Zerangue and Kavanaugh, 1996a), while at depolarized potentials which favor proton unbinding, the affinity changes slightly (Eliasof and Kavanaugh, unpublished observations). This data then are consistent with the suggestion that amino acid binding to EAATs can proceed in an

unprotonated transporter. Therefore, I postulate that the transport of neutral or acidic amino acids that have pKa's similar to the substrate-proton binding site will not be associated with an intracellular acidification.

Furthermore, an issue of interest that has not been addressed adequately is as to why would glutamate transporters be coupled to the H^+ gradient? The difference between the extracellular and intracellular pH is ~0.2 units (Attwell et al., 1993), a contribution that is negligible compared to Na^+ coupling ($3Na^+$ ions and a 10 fold concentration gradient). Watzke et al. (2000) have proposed that the proton might act as a gate for glutamate transport. Transporters are modeled as having two gates, one from the outside and one from the inside, which open in an alternating fashion (Jardetsky, 1966; Lauger, 1979; Vidaver, 1966). Watzke et al. (2000) proposed that the pKa for proton binding from the outside is greater than 8, while from the inside is less than 6.5. They also observed that the glutamate affinity of the transporter for either the outward or inward facing conformation is dependent on pH becoming higher at low pH. As a result, they suggested that a change in the proton affinity between the two conformations triggers the release of glutamate inside.

Similar to the hypothesis by Watzke et al. (2000), in our model, having the proton to bind after the first two Na^+ ions ensures the transporter is in a state available to bind glutamate. However, a parameter paramount to this suggestion is that the extracellular proton affinity is high. In our model, at pH_o 7.5, the proton site is close to saturation. This is consistent with the lack of change in the glutamate K_m in EAAT1 and EAAT2 when the extracellular pH is changed from 7.5 to 6.0 (Klockner et al., 1993; Seal et al., 2001; Vandenberg et al., 1998). Furthermore, besides controlling the occupancy of certain

transport states, the fast proton kinetics might also play a neuroprotective role during pathological conditions. For instance, the thermodynamic equilibrium equation for uptake predicts that the EAATs during severe ischemia will reverse and reach an equilibrium when the extracellular concentration of glutamate reaches ~100 μM instead of the less than 1 μM under normal conditions (Rossi et al., 2000; Szatkowski and Attwell, 1990; see for review Takahashi et al., 1997). What is more important, however, is how quickly the transporters can reach this equilibrium. Since both the extracellular and intracellular pH decreases to ~ 6 during ischemia (Attwell et al, 1993; Billups and Attwell, 1996) the transporters will be locked in the glutamate bound states seesaw between an outward and inward facing conformation. As a result, the time constant for reaching the new equilibrium value will be significantly slowed (see also Billups and Attwell, 1996). In summary, the coupling of protons to glutamate uptake might be of a kinetic rather than of a thermodynamic value.

C. EAATs voltage sensitivity

The stochiometry for glutamate transport is coupled to the cotransport of 3 Na^+, 1 H^+, and countertransport of 1 K^+ (Levy et al., 1998; Zerangue and Kavanaugh, 1996b). Due to the unequal quantities of charge transported in opposite directions glutamate transport leads to the net movement of positive charge (+2) into the cell. A recurrent concept in the glutamate transport field is that the major charge-moving step in the cycle is the transition of the $Na^+/H^+/Glu^-$ from outside to inside. To model our experimental findings we concluded that the binding and release of the third Na^+ is the major electrogenic step in the Na^+-hemicycle, while the conformational change is voltage

independent. We also propose that charge translocates when the inward facing K^+-bound transporter reverts to the outward facing conformation.

The suggestion that the ion-binding reactions in the Na^+-hemicycle are the major charge moving steps is not unique to glutamate transporters. In the Na^+-K^+ ATPase (Gadsby et al., 1993; Hilgenman, 1994; Holmgren et al., 2000), Na^+-Ca^{2+} exchanger (Hilgemann et al., 1991), Na^+-dependent glucose transporter (Panayotova-Heiermann et al., 1995), and the GABA transporter GAT-1 (Hilgemann and Lu, 1999) the transition associated with the conformation change of the Na^+-bound transport from outside to inside is modeled as voltage independent, while a Na^+ binding reaction is voltage dependent. However, our work cannot distinguish whether the movement of Na^+ to its binding site located inside the electric field or the occlusion of Na^+ into the transporter is the actual charge-moving step. Occlusion is defined as the conformational change, which makes Na^+ inaccessible to the extracellular solution without changing its affinity and not yet transport it inside (Lauger, 1991). It is likely that a combination of both processes contribute to the rheogenicity of the Na^+-binding steps. One would expect that the diffusion of Na^+ to its binding site will be almost instantaneous, thus, the charge movement will be limited by the occlusion and de-occlusion reactions in a fashion similar to GAT1 (Lu and Hilgenmann, 1999; Hilgenmann and Lu, 1999) and Na^+-K^+ ATPase (Holmgren et al., 2000).

D. Modulation by arachidonic acid

Besides the coupled charges, glutamate transporters are associated with a thermodynamically uncoupled anion conductance (Fairman et al., 1995; Wadiche et al.,

1995b). Here we demonstrate that glutamate in the presence of arachidonate in EAAT4 gates a thermodynamically uncoupled proton conductance (see also Fairman et al., 1998). Arachidonate does not affect either the EAAT4's apparent glutamate affinity or magnitude of the anion conductance. The effect of arachidonate on EAAT4 is in contrast to its effect on EAAT1 and EAAT2, where it only modulated parameters associated with glutamate transport (Zerangue et al., 1995). Recently, Poulsen and Vandenberg (2002) showed that application of niflumic acid on oocytes expressing EAAT4 also elicits an uncoupled proton flux. However, application of arachidonate in the presence of niflumic acid still elicited the proton conductance. This indicates that the site of action of niflumic acid differs from arachidonate's. The physiological significance of the proton flux is unknown. However, the presence of a proton flux along with an anion flux, independent of each other raises several biophysical questions. Do both fluxes use the same pore? And, what is their relationship to the glutamate transport pathway? Further work and probably a glutamate transporter crystal structure will be needed before an answer to these questions is provided.

E. Oligomerization

An important parameter for our understanding of glutamate uptake in synaptic transmission is the concentration of transporters encapsulating the synapse. Danbolt and colleagues have recently estimated that the density of transporters around the synaptic cleft varies between 740 – 8500/μm^2 depending on the brain region and EAAT subtype (Dehmes et al., 1998; Lehre and Danbolt, 1998). As a result, the effective concentration of transporters around the cleft is 0.1-0.3 mM (Lehre et al., 1998). However, this estimate

depends on whether the transporters are functioning as oligomers or monomers. If the transporters function as oligomers, then, their effective concentration should be divided by the number of subunits that compose a functional transporter. In chapter 3 we proposed that transporters associate as an aggregate of five subunits. However, it seems that each subunit acts independently from each other. Therefore, transporters can form high-density clusters around the synapse. This property might be beneficial to neuronal transporters located on the post-synaptic spine in the peri-synaptic region. Recently, it was shown that neuronal transporters can limit spillover from one synapse to another (Diamond, 2001) or can shield receptors from activation by glutamate (Brasnjo and Otis, 2001). By associating in a five subunit aggregate transporters can be packed at high densities in a very small area such as a postsynaptic spine ensuring efficient glutamate removal.

REFERENCES

Amato A, Barbour B, Szatkowski M, Attwell D (1994) Counter-transport of potassium by the glutamate uptake carrier in glial cells isolated from the tiger salamander retina.J Physiol. 479:371-80.

Arriza, JL, Eliasof S, Kavanaugh MP, Amara SG (1997) Excitatory amino acid transporter 5, a retinal glutamate transporter coupled to a chloride conductance. Proc Natl Acad Sci U S A 94: 4155-60.

Arriza JL, Fairman WA, Wadiche JI, Murdoch GH, Kavanaugh MP, Amara SG (1994) Functional comparisons of three glutamate transporter subtypes cloned from human motor cortex. J Neurosci 14: 5559-69

Arriza JL, Kavanaugh MP, Fairman WA, Wu YN, Murdoch GH, North RA, Amara SG (1993) Cloning and expression of a human neutral amino acid transporter with structural similarity to the glutamate transporter gene family. J Biol Chem. 268:15329-32.

Attwell D, Barbour B, Szatkowski M (1993) Nonvesicular release of neurotransmitter. Neuron 11:401-7.

Auger C and Attwell D (2000) Fast removal of synaptic glutamate by postsynaptic transporters. Neuron 28:547-58.

Barbour B (2001) An evaluation of synapse independence. J Neurosci. 21:7969-84.

Barbour B, Brew H, Attwell D (1988) Electrogenic glutamate uptake in glial cells is activated by intracellular potassium. Nature 335:433-5.

Barbour B, Brew H, Attwell D (1991) Electrogenic uptake of glutamate and aspartate into glial cells isolated from the salamander (Ambystoma) retina. J Physiol. 436:169-93.

Barbour B, Keller BU, Llano I, Marty A (1994) Prolonged presence of glutamate during excitatory synaptic transmission to cerebellar Purkinje cells. Neuron 12: 1331-43.

Barbour B, Szatkowski M, Ingledew N, Attwell D (1989) Arachidonic acid induces a prolonged inhibition of glutamate uptake into glial cells. Nature 342:918-20.

Beckman ML, Bernstein EM, Quick MW (1998) Protein kinase C regulates the interaction between a GABA transporter and syntaxin 1A. J Neurosci 18: 6103-12.

Beliveau R, Demeule M, Jette M, Potier M (1990) Molecular sizes of amino acid transporters in the luminal membrane from the kidney cortex, estimated by the radiation-inactivation method. Biochem J 268: 195-200.

Bendahan A, Armon A, Madani N, Kavanaugh MP, Kanner BI (2000) Arginine 447 plays a pivotal role in substrate interactions in a neuronal glutamate transporter. J Biol Chem 275: 37436-42.

Bergles DE, Diammond JS, Jahr CE (1999) Clearance of glutamate inside the synapse and beyond. Curr Opin Neurobiol 9:293-8.

Bergles DE, Dzubay JA, Jahr, CE (1997) Glutamate transporter currents in bergmann glial cells follow the time course of extrasynaptic glutamate. Proc Natl Acad Sci 94:14821-5.

Bergles DE, Jahr CE (1998) Glial contribution to glutamate uptake at Schaffer collateral-commissural synapses in the hippocampus. J Neurosci 18:7709-16.

Bergles DE, Jahr CE (1997) Synaptic activation of glutamate transporters in hippocampal astrocytes. Neuron 19:1297-308.

Bernstein EM and Quick MW (1999) Regulation of gamma-aminobutyric acid (GABA) transporters by extracellular GABA. J Biol Chem 274: 889-95.

Billups B, Attwell D (1996) Modulation of non-vesicular glutamate release by pH. Nature 379:171-4.

Billups B, Rossi D, Attwell D (1996) Anion conductance behavior of the glutamate uptake carrier in salamander retinal glial cells. J Neurosci 16:6722-31.

Billups, B, Rossi D, Oshima T, Warr O, Takahashi M, Sarantis M, Szatkowski M, Attwell D (1998) Physiological and pathological operation of glutamate transporters. Prog Brain Res 116: 45-57.

Borre L and Kanner BI (2001) Coupled, but not uncoupled, fluxes in a neuronal glutamate transporter can be activated by lithium ions. J Biol Chem. 276:40396-401.

Borre L, Kavanaugh MP, Kanner BI (2002) Dynamic equilibrium between coupled and uncoupled modes of a neuronal glutamate transporter. J Biol Chem 277:13501-7.

Bouvier M, Miller BA, Szatkowski M, Attwell D (1991) Electrogenic uptake of sulphur-containing analogues of glutamate and aspartate by Muller cells from the salamander retina. J Physiol. 444:441-57.

Bouvier, Szatkowski M, Amato A, Attwell D (1992) The glial cell glutamate uptake carrier countertransports pH-changing anions. Nature 360: 471-4.

Brasnjo G and Otis TS (2001) Neuronal glutamate transporters control activation of postsynaptic metabotropic glutamate receptors and influence cerebellar long-term depression. Neuron 31: 607-16.

Brew H and Attwell D (1987) Electrogenic glutamate uptake is a major current carrier in the membrane of axolotl retinal glial cells [published erratum appears in Nature 1987 328:742]. Nature 327: 707-9.

Bridges RJ, Kavanaugh MP, Chamberlin AR (1999) A pharmacological review of competitive inhibitors and substrates of high-affinity, sodium-dependent glutamate transport in the central nervous system. Curr Pharm Des 5: 363-79.

Bridges RJ, Stanley MS, Anderson MW, Cotman CW, Chamberlin AR (1991) Conformationally defined neurotransmitter analogues. Selective inhibition of glutamate uptake by one pyrrolidine-2,4-dicarboxylate diastereomer. J Med Chem. 34:717-25.

Brocke L, Bendahan A, Grunewald M, Kanner BI (2002) Proximity of Two Oppositely Oriented Reentrant Loops in the Glutamate Transporter GLT-1 Identified by Paired Cysteine Mutagenesis. J Biol Chem 277: 3985-92.

Campiani G, De Angelis M, Armaroli S, Fattorusso C, Catalanotti B, Ramunno A, Nacci V, Novellino E, Grewer C, Ionescu D, Rauen T, Griffiths R, Sinclair C, Fumagalli E, Mennini T (2001) A rational approach to the design of selective substrates and potent nontransportable inhibitors of the excitatory amino acid transporter EAAC1 (EAAT3). new glutamate and aspartate analogues as potential neuroprotective agents. J Med Chem 44: 2507-10.

Cao Y, Mager S, Lester HA (1997) H+ permeation and pH regulation at a mammalian serotonin transporter. J.Neurosci. 17:2257-2266

Casado M, Bendahan A, Zafra F, Danbolt NC, Aragon C, Gimenez C, Kanner BI (1993) Phosphorylation and modulation of brain glutamate transporters by protein kinase C. J Biol Chem. 268:27313-7.

Chan PH, Fishman RA, Chen S, Chew S (1983) Effects of temperature on arachidonic acid-induced cellular edema and membrane perturbation in rat brain cortical slices. J Neurochem. 41:1550-7.

Clark BA and Barbour B (1997) Currents evoked in Bergmann glial cells by parallel fibre stimulation in rat cerebellar slices. J Physiol 502:335-50.

Clements JD (1996) Transmitter timecourse in the synaptic cleft: its role in central synaptic function. Trends Neurosci 19:163-71.

Conradt M and Stoffel W (1995) Functional analysis of the high affinity, Na(+)-dependent glutamate transporter GLAST-1 by site-directed mutagenesis. J Biol Chem 270: 25207-12.

Conradt M and Stoffel W (1997) Inhibition of the high-affinity brain glutamate transporter GLAST-1 via direct phosphorylation. J Neurochem 68: 1244-51.

Conradt M, Storck T, Stoffel W (1995) Localization of N-glycosylation sites and functional role of the carbohydrate units of GLAST-1, a cloned rat brain L-glutamate/L-aspartate transporter. Eur J Biochem. 229:682-7.

Danbolt NC, Pines G, Kanner, BI (1990) Purification and reconstitution of the sodium- and potassium-coupled glutamate transport glycoprotein from rat brain. Biochemistry 29: 6734-40.

Danbolt NC (2001) Glutamate uptake. Prog Neurobiol 65:1-105.

Daniels KK and Vickroy TW (1999) Reversible activation of glutamate transport in rat brain glia by protein kinase C and an okadaic acid-sensitive phosphoprotein phosphatase. Neurochem Res. 24:1017-25.

Davis KE, Straff DJ, Weinstein EA, Bannerman PG, Correale DM, Rothstein JD, Robinson MB (1998) Multiple signaling pathways regulate cell surface expression and activity of the excitatory amino acid carrier 1 subtype of Glu transporter in C6 glioma. J Neurosci 18: 2475-85.

Dehnes Y, Chaudhry FA, Ullensvang K, Lehre KP, Storm-Mathisen J, Danbolt NC (1998) The glutamate transporter EAAT4 in rat cerebellar Purkinje cells: a glutamate-gated chloride channel concentrated near the synapse in parts of the dendritic membrane facing astroglia. J Neurosci. 18:3606-19.

Diamond JS, Bergles DE, Jahr CE (1998) Glutamate release monitored with astrocyte transporter currents during LTP. Neuron 21:425-33.

Diamond JS, Jahr CE (1997) Transporters buffer synaptically released glutamate on a submillisecond time scale. J Neurosci 17: 4672-87.

Diamond JS (2001) Neuronal glutamate transporters limit activation of NMDA receptors by neurotransmitter spillover on CA1 pyramidal cells. J Neurosci. 21:8328-38.

Dowd LA, Coyle AJ, Rothstein JD, Pritchett DB, Robinson MB (1996) Comparison of Na+-dependent glutamate transport activity in synaptosomes, C6 glioma, and Xenopus oocytes expressing excitatory amino acid carrier 1 (EAAC1).Mol Pharmacol. 49:465-73.

Dowd LA and Robinson MB (1996) Rapid stimulation of EAAC1-mediated Na+-dependent L-glutamate transport activity in C6 glioma cells by phorbol ester. J Neurochem 67: 508-16.

Dumuis A, Pin JP, Oomagari K, Sebben M, Bockaert J (1990) Arachidonic acid released from striatal neurons by joint stimulation of ionotropic and metabotropic quisqualate receptors. Nature 347:182-4.

Dumuis A, Sebben M, Haynes L, Pin JP, Bockaert J (1988) NMDA receptors activate the arachidonic acid cascade system in striatal neurons. Nature 336:68-70.

Duan S, Anderson CM, Stein BA, Swanson RA (1999) Glutamate induces rapid upregulation of astrocyte glutamate transport and cell-surface expression of GLAST. J Neurosci 19: 10193-200, 1999.

Dzubay JA, Jahr CE (1999) The concentration of synaptically released glutamate outside of the climbing fiber-Purkinje cell synaptic cleft. J Neurosci 19:5265-74.

Eliasof S, Arriza JL, Leighton BH, Kavanaugh MP,. Amara SG.(1998) Excitatory amino acid transporters of the salamander retina: identification, localization, and function. J Neurosci 18: 698-712.

Eliasof S. and Jahr CE (1996) Retinal glial cell glutamate transporter is coupled to an anionic conductance. Proc Natl Acad Sci U S A 93: 4153-8.

Eliasof S, McIlvain HB, Petroski RE, Foster AC, Dunlop J (2001) Pharmacological characterization of threo-3-methylglutamic acid with excitatory amino acid transporters in native and recombinant systems. J Neurochem 77: 550-7.

Eliasof S. and Werblin F (1993) Characterization of the glutamate transporter in retinal cones of the tiger salamander. J Neurosci 13: 402-11.

Erecinska M, Wantorsky D, Wilson DF (1983) Aspartate transport in synaptosomes from rat brain. J Biol Chem 258: 9069-77.

Erecinska M, Nelson D (1987) Amino acid neurotransmitters in the CNS. Relationships between net uptake and exchange in rat brain synaptosomes. FEBS Lett 213:61-6.

Eskandari S, Kreman M, Kavanaugh MP, Wright, EM, Zampighi, GA (2000) Pentameric assembly of a neuronal glutamate transporter. Proc Natl Acad Sci U S A 97: 8641-6.

Esslinger CS, Koch HP, Kavanaugh MP, Philips DP, Chamberlin AR, Thompson CM, Bridges RJ (1998) Structural determinants of substrates and inhibitors: probing glutamate transporters with 2,4-methanopyrrolidine-2,4-dicarboxylate. Bioorg Med Chem Lett 8: 3101-6.

Fairman WA, Vandenberg RJ, Arriza JL, Kavanaugh MP, Amara SG (1995) An excitatory amino-acid transporter with properties of a ligand-gated chloride channel. Nature 375: 599-603.

Fairman WA, Sonders MS, Murdoch GH, Amara SG (1998) Arachidonic acid elicits a substrate-gated proton current associated with the glutamate transporter EAAT4. Nat Neurosci 1:105-13.

Furuta A, Martin LJ, Lin CL, Dykes-Hoberg M, Rothstein JD (1997) Cellular and synaptic localization of the neuronal glutamate transporters excitatory amino acid transporter 3 and 4. Neuroscience 81: 1031-42.

Gegelashvili G, Dehnes Y, Danbolt NC, Schousboe A (2000) The high-affinity glutamate transporters GLT1, GLAST, and EAAT4 are regulated via different signalling mechanisms. Neurochem Int. 37:163-70.

Glavinovic MI (1999) Monte carlo simulation of vesicular release, spatiotemporal distribution of glutamate in synaptic cleft and generation of postsynaptic currents. Pflugers Arch 437:462-70.

Gadsby DC, Rakowski RF, De Weer P (1993) Extracellular access to the Na,K pump: pathway similar to ion channel.Science 260:100-3.

Goldin AL, Sumikawa K, Rudy B, Iverson LE (eds) (1992) Vol. 207, pp 279-97, Academic Press, Orlando, FL.

Gonzalez MI and Ortega A (1997) Regulation of the Na+-dependent high affinity glutamate/aspartate transporter in cultured Bergmann glia by phorbol esters. J Neurosci Res 50: 585-90.

Gonzalez MI, Lopez-Colom AM, Ortega A (1999) Sodium-dependent glutamate transport in Muller glial cells: regulation by phorbol esters. Brain Res 831: 140-5.

Grewer C, Watzke N, Wiessner M, Rauen T (2000) Glutamate translocation of the neuronal glutamate transporter EAAC1 occurs within milliseconds. Proc Natl Acad Sci 97:9706-11.

Grunewald M and Kanner B (1995) Conformational changes monitored on the glutamate transporter GLT-1 indicate the existence of two neurotransmitter-bound states. J Biol Chem. 270:17017-24.

Grunewald M, Bendahan A, Kanner BI (1998) Biotinylation of single cysteine mutants of the glutamate transporter GLT-1 from rat brain reveals its unusual topology. Neuron 21: 623-32.

Grunewald M and Kanner BI (2000) The accessibility of a novel reentrant loop of the glutamate transporter GLT-1 is restricted by its substrate. J Biol Chem 275: 9684-9.

Haugeto O, Ullensvang K, Levy LM, Chaudhry FA, Honore T, Nielsen M, Lehre KP, Danbolt NC.Brain (1996) glutamate transporter proteins form homomultimers. J Biol Chem 271: 27715-22.

Häusser M and Roth A (1997) Dendritic and somatic glutamate receptor channels in rat cerebellar Purkinje cells. J Physiol (Lond) 501: 77-95.

Hilgemann DW and Lu CC (1999) GAT1 (GABA:Na+:Cl-) cotransport function. Database reconstruction with an alternating access model. J Gen Physiol. 114:459-75.

Hilgemann DW, Nicoll DA, Philipson KD.Charge movement during Na+ translocation by native and cloned cardiac Na+/Ca2+ exchanger. Nature 352:715-8.

Hilgemann DW (1994) Channel-like function of the Na,K pump probed at microsecond resolution in giant membrane patches. Science 263:1429-32.

Hille B (2001) In: Ionic channels of excitable membranes, Ed 3. Sunderland, MA: Sinauer.

Holmes WR (1995) Modeling the effect of glutamate diffusion and uptake on NMDA and non-NMDA receptor saturation.
Biophys J. 69:1734-47.

Holmgren M, Wagg J, Bezanilla F, Rakowski RF, De Weer P, Gadsby DC (2000) Three distinct and sequential steps in the release of sodium ions by the Na+/K+-ATPase. Nature 403:898-901.

Iino M, Goto K, Kakegawa W, Okado H, Sudo M, Ishiuchi S, Miwa A, Takayasu Y, Saito I, Tsuzuki K, Ozawa S (2001) Glia-synapse interaction through Ca2+-permeable AMPA receptors in Bergmann glia. Science 292:926-9.

Isaacson, JS (1999) Glutamate spillover mediates excitatory transmission in the rat olfactory bulb. Neuron 23:377-84.

Jabaudon D, Shimamoto K, Yasuda-Kamatani Y, Scanziani M, Gahwiler BH, Gerber U (1999) Inhibition of uptake unmasks rapid extracellular turnover of glutamate of nonvesicular origin. Proc Natl Acad Sci U S A 96: 8733-8.

Jackson M, Song W, Liu MY, Jin L, Dykes-Hoberg M, Lin CI, Bowers WJ, Federoff HJ, Sternweis PC, Rothstein JD (2001) Modulation of the neuronal glutamate transporter EAAT4 by two interacting proteins. Nature 410: 89-93.

Jardetzky O (1966) Simple allosteric model for membrane pumps Nature (London) 211, 969-970.

Jonas P, Major G, Sakmann, B (1993) Quantal components of unitary EPSCs at the mossy fibre synapse on CA3 pyramidal cells of rat hippocampus. J Physiol (Lond) 472: 615-63, 1993.

Kanai, Y. and Hediger, M.A (1992) Primary structure and functional characterization of a high-affinity glutamate transporter. Nature 360: 467-71.

Kanai Y, Nussberger S, Romero MF, Boron WF, Hebert SC, Hediger MA (1995) Electrogenic properties of the epithelial and neuronal high affinity glutamate transporter. J Biol Chem. 270:16561-8.

Kanai Y, Stelzner M, Nussberger S, Khawaja S, Hebert SC, Smith CP, Hediger MA (1994) The neuronal and epithelial human high affinity glutamate transporter. Insights into structure and mechanism of transport. J Biol Chem. 269:20599-606.

Kanner BI and Bendahan A (1982) Binding order of substrates to the sodium and potassium ion coupled L-glutamic acid transporter from rat brain. Biochemistry 21:6327-30.

Kanner BI and Marva E (1982) Efflux of L-glutamate by synaptic plasma membrane vesicles isolated from rat brain. Biochemistry 21: 3143-7.

Kanner BI, Kavanaugh MP, Bendahan A (2001) Molecular characterization of substrate-binding sites in the glutamate transporter family. Biochem Soc Trans 29: 707-10.

Kanner BI and Schuldiner S (1987) Mechanism of transport and storage of neurotransmitters. CRC Crit Rev Biochem. 22(1):1-38.

Kanner BI and Sharon I (1978) Active transport of L-glutamate by membrane vesicles isolated from rat brain. Biochemistry 17:3949-53.

Kataoka Y, Morii H, Watanabe Y, Ohmori HA (1997) postsynaptic excitatory amino acid transporter with chloride conductance functionally regulated by neuronal activity in cerebellar Purkinje cells. J Neurosci 17: 7017-24.

Kavanaugh MP, Bendahan A, Zerangue N, Zhang Y, Kanner BI (1997) Mutation of an amino acid residue influencing potassium coupling in the glutamate transporter GLT-1 induces obligate exchange. J Biol Chem. 272:1703-8.

Kavanaugh MP, Hurst RS, Yakel J, Varnum MD, Adelman JP, North RA (1992) Multiple subunits of a voltage-dependent potassium channel contribute to the binding site for tetraethylammonium. Neuron 8:493-7.

Kawakami H, Tanaka K, Nakayama T, Inoue K, Nakamura S (1994) Cloning and expression of a human glutamate transporter. Biochem Biophys Res Commun. 199:171-6.

Klockner U, Storck T, Conradt M, Stoffel W (1993) Electrogenic L-glutamate uptake in Xenopus laevis oocytes expressing a cloned rat brain L-glutamate/L-aspartate transporter (GLAST-1). J Biol Chem 268: 14594-6.

Klockner U, Storck T, Conradt M, Stoffel W (1994) Functional properties and substrate specificity of the cloned L- glutamate/L-aspartate transporter GLAST-1 from rat brain expressed in Xenopus oocytes. J Neurosci 14: 5759-65.

Koch HP, Kavanaugh MP, Esslinger CS, Zerangue N, Humphrey JM, Amara SG, Chamberlin AR, Bridges RJ (1999) Differentiation of substrate and nonsubstrate inhibitors of the high-affinity, sodium-dependent glutamate transporters. *Mol Pharmacol* 56: 1095-104.

Kullmann DM, Min MY, Asztely F, Rusakov DA (1999) Extracellular glutamate diffusion determines the occupancy of glutamate receptors at CA1 synapses in the hippocampus. Philos Trans R Soc Lond B Biol Sci 354:395-402.

Kullmann DM (2000) Spillover and synaptic cross talk mediated by glutamate and GABA in the mammalian brain. Prog Brain Res 125:339-51.

Larsson HP, Picaud SA, Werblin FS, Lecar H (1996) Noise analysis of the glutamate-activated current in photoreceptors. Biophys J 70: 733-42.

Läuger P (1979) A channel mechanism for electrogenic ion pumps.
Biochim Biophys Acta 552:143-61.

Läuger P (1991) In: Electrogenic ion pumps. Sunderland, MA: Sinauer.

Lehre, KP, Levy LM, Ottersen OP, Storm-Mathisen J, Danbolt NC (1995) Differential expression of two glial glutamate transporters in the rat brain: quantitative and immunocytochemical observations. J Neurosci 15: 1835-53.

Lehre KP, Danbolt NC (1998) The number of glutamate transporter subtype molecules at glutamatergic synapses: chemical and stereological quantification in young adult rat brain. J Neurosci. 18:8751-7

Leighton BH, Seal RP, Shimamoto K, Amara SG (2002) A hydrophobic domain in glutamate transporters forms an extracellular helix associated with the permeation pathway for substrates. J Biol Chem. 277:29847-55.

Levy LM, Warr O, Attwell D (1998) Stoichiometry of the glial glutamate transporter GLT-1 expressed inducibly in a Chinese hamster ovary cell line selected for low endogenous Na+-dependent glutamate uptake. J Neurosci 18:9620-8.

Lin CI, Orlov I, Ruggiero AM, Dykes-Hoberg M, Lee A, Jackson M, Rothstein JD (2001) Modulation of the neuronal glutamate transporter EAAC1 by the interacting protein GTRAP3-18. Nature 410: 84-8.

Lin CL, Tzingounis AV, Jin L, Furuta A, Kavanaugh MP, Rothstein JD (1998) Molecular cloning and expression of the rat EAAT4 glutamate transporter subtype. Mol Brain Res 63:174-9.

Linden DJ (1995) Phospholipase A2 controls the induction of short-term versus long-term depression in the cerebellar Purkinje neuron in culture. Neuron 15:1393-401.

Lolkema JS and Slotboom DJ (1998) Estimation of structural similarity of membrane proteins by hydropathy profile alignment. Mol Membr Biol.15:33-42.

Loo DD, Hirayama BA, Meinild AK, Chandy G, Zeuthen T, Wright EM.. Passive water and ion transport by cotransporters. *J Physiol* 518 (Pt 1): 195-202, 1999.

Lundy DF and McBean GJ (1995) Pre-incubation of synaptosomes with arachidonic acid potentiates inhibition of [3H]D-aspartate transport. Eur J Pharmacol. 291:273-9.

Lu CC, Hilgemann DW (1999) GAT1 (GABA:Na+:Cl-) cotransport function. Kinetic studies in giant Xenopus oocyte membrane patches. J Gen Physiol. 114:445-57.

MacAulay N, Gether U, Klaerke DA, Zeuthen T (2001) Water transport by the human Na+-coupled glutamate cotransporter expressed in Xenopus oocytes. J Physiol 530: 367-78.

MacAulay N, Gether U, Klaeke DA, Zeuthen T (2002) Passive water and urea permeability of a human Na(+)-glutamate cotransporter expressed in Xenopus oocytes.J Physiol. 542:817-28.

MacKinnon R (1991) Determination of the subunit stoichiometry of a voltage-activated potassium channel. Nature 350:232-5.

Mafra RA, Figueiredo SG, Diniz CR, Cordeiro MN, Cruz JD, De Lima ME (1999) PhTx4, a new class of toxins from Phoneutria nigriventer spider venom, inhibits the glutamate uptake in rat brain synaptosomes. Brain Res 831: 297-300.

Malandro MS and Kilberg MS (1996) Molecular biology of mammalian amino acid transporters.Annu Rev Biochem. 65:305-36..

Manfras BJ, Rudert WA, Trucco M, Boehm BO (1994) Cloning and characterization of a glutamate transporter cDNA from human brain and pancreas. Biochim Biophys Acta. 1195:185-8.

Manzoni C and Mennini T (1997) Arachidonic acid inhibits 3H-glutamate uptake with different potencies in rodent central nervous system regions expressing different transporter subtypes. Pharmacol Res. 35:149-51

Marie H and Attwell D (1999) C-terminal interactions modulate the affinity of GLAST glutamate transporters in salamander retinal glial cells. J Physiol 520: 393-7.

Marie H, Billups D, Bedford FK, Dumoulin A, Goyal RK, Longmore GD, Moss SJ, Attwell D (2002) The amino terminus of the glial glutamate transporter GLT-1 interacts with the LIM protein Ajuba. Mol Cell Neurosci 19:152-64.

Meinild A, Klaerke DA, Loo DD, Wright EM, Zeuthen T (1998). The human Na+-glucose cotransporter is a molecular water pump. J Physiol (London) 508: 15-21.

Meinild AK, Loo DD, Pajor AM, Zeuthen T, Wright EM (2000) Water transport by the renal Na(+)-dicarboxylate cotransporter. Am J Physiol Renal Physiol 278: F777-83.

Mennerick S and Zorumski CF (1994) Glial contributions to excitatory neurotransmission in cultured hippocampal cells. Nature 368: 59-62.

Mennerick S, Shen W, Xu W, Benz A, Tanaka K, Shimamoto K, Isenberg KE, Krause JE, Zorumski CF (1999) Substrate turnover by transporters curtails synaptic glutamate transients. J Neurosci 19: 9242-51.

Meves H (1994) Modulation of ion channels by arachidonic acid. Prog Neurobiol. 43:175-86.

Min MY, Rusakov DA, Kullmann DM (1998) Activation of AMPA, kainate, and metabotropic receptors at hippocampal mossy fiber synapses: role of glutamate diffusion. Neuron 21:561-70.

Mitrovic AD, Amara SG, Johnston GA, Vandenberg RJ (1998) Identification of functional domains of the human glutamate transporters EAAT1 and EAAT2. J Biol Chem 273: 14698-706.

Mort D, Marcaggi P, Grant J, Attwell D (2001) Effect of acute exposure to ammonia on glutamate transport in glial cells isolated from the salamander retina. J Neurophysiol 86: 836-44.

Nagao S, Kwak S, Kanazawa I (1997) EAAT4, a glutamate transporter with properties of a chloride channel, is predominantly localized in Purkinje cell dendrites, and forms parasagittal compartments in rat cerebellum. Neuroscience 78:929-33.

Nelson PJ, Dean GE, Aronson PS, Rudnick G (1983) Hydrogen ion cotransport by the renal brush border glutamate transporter. Biochemistry 22:5459-63.

Oliet SH, Piet R, Poulain DA (2001) Control of glutamate clearance and synaptic efficacy by glial coverage of neurons. Science 292:923-6.

Otis TS and Jahr CE (1998) Anion currents and predicted glutamate flux through a neuronal glutamate transporter. J Neurosci 18:7099-110.

Otis TS and Kavanaugh MP (1998) Glutamate transportrers and their contributions to excitatory synaptic transmission. Handb Exp Pharm 141:419-440.

Otis TS and Kavanaugh MP (2000) Isolation of current components and partial reaction cycles in the glial glutamate transporter EAAT2. J Neurosci 20:2749-57.

Otis TS, Kavanaugh MP, Jahr CE (1997) Postsynaptic glutamate transport at the climbing fiber-Purkinje cell synapse. Science 277:1515-8.

Palacin M, Estevez R, Bertran J, Zorzano A (1998) Molecular biology of mammalian plasma membrane amino acid transporters. Physiol Rev 78: 969-1054.

Panayotova-Heiermann M, Loo DD, Wright EM (1995) Kinetics of steady-state currents and charge movements associated with the rat Na+/glucose cotransporter. J Biol Chem. 270:27099-105.

Picaud SA, Larsson HP, Grant GB, Lecar H, Werblin FS (1995) Glutamate-gated chloride channel with glutamate-transporter-like properties in cone photoreceptors of the tiger salamander. J Neurophysiol 74: 1760-71.

Pines G, Danbolt NC, Bjoras M, Zhang Y, Bendahan A, Eide L, Koepsell H, Storm-Mathisen J, Seeberg E, Kanner BI (1992) Cloning and expression of a rat brain L-glutamate transporter. Nature. 360:464-7.

Pines G, Zhang Y, Kanner BI (1995) Glutamate 404 is involved in the substrate discrimination of GLT-1, a (Na+ + K+)-coupled glutamate transporter from rat brain. J Biol Chem 270: 17093-7.

Poulsen MV and Vandenberg RJ (2001) Niflumic acid modulates uncoupled substrate-gated conductances in the human glutamate transporter EAAT4. J Physiol 534: 159-67.

Ramamoorthy S and Blakely RD (1999) Phosphorylation and sequestration of serotonin transporters differentially modulated by psychostimulants. Science 285:763-6.

Rhoads DE, Ockner RK, Peterson NA (1983) Raghupathy E.Modulation of membrane transport by free fatty acids: inhibition of synaptosomal sodium-dependent amino acid uptake. Biochemistry 22:1965-70.

Rhoads DE, Peterson NA (1982) Raghupathy E.Proline transport by synaptosomal membrane vesicles isolated from rat brain: energetics and inhibition by free fatty acids. Biochemistry 21:4782-7.

Reis HJ, Prado MA, Kalapothakis E, Cordeiro MN, Diniz CR, De Marco LA, Gomez MV, Romano-Silva MA (1999) Inhibition of glutamate uptake by a polypeptide toxin (phoneutriatoxin 3-4) from the spider Phoneutria nigriventer. Biochem J 343: 413-8.

Reis HJ, Gomez MV, Kalapothakis E, Diniz CR, Cordeiro MN, Prado MA, Romano-Silva M (2000).Inhibition of glutamate uptake by Tx3-4 is dependent on the redox state of cysteine residues. Neuroreport 11: 2191-4.

Robinson MB, Hunter-Ensor M, Sinor J (1991) Pharmacologically distinct sodium-dependent L-[3H]glutamate transport processes in rat brain. Brain Res. 544:196-202.

Rossi DJ, Oshima T, Attwell D (2000) Glutamate release in severe brain ischaemia is mainly by reversed uptake. Nature 403: 316-21.

Rothstein JD, Martin L, Levey AI, Dykes-Hoberg M, Jin L, Wu D, Nash N, Kuncl RW (1994) Localization of neuronal and glial glutamate transporters. Neuron 13: 713-25.

Ryan RM and Vandenberg RJ (2002) Distinct conformational states mediate the transport and anion channel properties of the glutamate transporter, EAAT1. J Biol Chem 277:13494-500.

Rusakov DA and Kullmann DM (1998) Extrasynaptic glutamate diffusion in the hippocampus: ultrastructural constraints, uptake, and receptor activation. J Neurosci. 18:3158-70.

Sarantis M, Ballerini L, Miller B, Silver RA, Edwards M, Attwell D (1993) Glutamate uptake from the synaptic cleft does not shape the decay of the non-NMDA component of the synaptic current. Neuron 11: 541-9.

Scanziani M, Salin PA, Vogt KE, Malenka RC, Nicoll RA (1997) Use-dependent increases in glutamate concentration activate presynaptic metabotropic glutamate receptors. Nature 385, 630-4.

Schwartz EA and Tachibana M (1990) Electrophysiology of glutamate and sodium co-transport in a glial cell of the salamander retina. J Physiol 426: 43-80.

Seal RP and Amara SG (1998) A reentrant loop domain in the glutamate carrier EAAT1 participates in substrate binding and translocation. Neuron 21: 1487-98.

Seal RP, Shigeri Y, Eliasof S, Leighton BH, Amara SG (2001) Sulfhydryl modification of V449C in the glutamate transporter EAAT1 abolishes substrate transport but not the substrate-gated anion conductance. Proc Natl Acad Sci 98:15324-9.

Sepkuty JP, Cohen AS, Eccles C, Rafiq A, Behar K, Ganel R, Coulter DA, Rothstein JD. (2002) A neuronal glutamate transporter contributes to neurotransmitter GABA synthesis and epilepsy. J Neurosci. 22:6372-9.

Shigeri Y, Shimamoto K, Yasuda-Kamatani Y, Seal RP, Yumoto N, Nakajima T, Amara SG (2001) Effects of threo-beta-hydroxyaspartate derivatives on excitatory amino acid transporters (EAAT4 and EAAT5). *J Neurochem* 79: 297-302.

Shimamoto K, Lebrun B, Yasuda-Kamatani Y, Sakaitani M, Shigeri Y, Yumoto N, Nakajima T (1998) DL-threo-beta-benzyloxyaspartate, a potent blocker of excitatory amino acid transporters. Mol Pharmacol 53: 195-201.

Sims KD, Straff DJ, Robinson MB (2000) Platelet-derived growth factor rapidly increases activity and cell surface expression of the EAAC1 subtype of glutamate transporter through activation of phosphatidylinositol 3-kinase. J Biol Chem 275: 5228-37.

Slotboom DJ, Konings WN, Lolkema JS (2001) Cysteine-scanning mutagenesis reveals a highly amphipathic, pore-lining membrane-spanning helix in the glutamate transporter GltT. J Biol Chem. 276:10775-81.

Slotboom DJ, Lolkema JS, Konings WN (1996) Membrane topology of the C-terminal half of the neuronal, glial, and bacterial glutamate transporter family. J Biol Chem 271: 31317-21.

Slotboom DJ, Sobczak I, Konings WN, Lolkema JS (1999) A conserved serine-rich stretch in the glutamate transporter family forms a substrate-sensitive reentrant loop. Proc Natl Acad Sci U S A 96: 14282-7.

Sonders MS, Zhu SJ, Zahniser NR, Kavanaugh MP, Amara SG (1997) Multiple ionic conductances of the human dopamine transporter: the actions of dopamine and psychostimulants. J Neurosci. 17:960-74.

Stallcup WB, Bulloch K, Baetge EE (1979) Coupled transport of glutamate and sodium in a cerebellar nerve cell line. J Neurochem 32: 57-65.

Steele JC Jr and Nielsen TB (1978) Evaluation of cross-linked polypeptides in SDS gel electrophoresis. Anal Biochem. 84:218-24.

Stein, WD (1990) Channels, Carriers, and Pumps. San Diego: CA, Academic Press Inc.

Storck T, Schulte S, Hofmann K, Stoffel W (1992) Structure, expression, and functional analysis of a Na(+)-dependent glutamate/aspartate transporter from rat brain. Proc Natl Acad Sci U S A. 89:10955-9.

Sukharev SI, Schroeder MJ, McCaslin DR (1999) Stoichiometry of the large conductance bacterial mechanosensitive channel of E. coli. A biochemical study. J Membr Biol. 171:183-93.

Szatkowski M, Barbour B, Attwell D (1990) Non-vesicular release of glutamate from glial cells by reversed electrogenic glutamate uptake. Nature 348: 443-6.

Tachibana M and Kaneko A (1988) L-glutamate-induced depolarization in solitary photoreceptors: a process that may contribute to the interaction between photoreceptors in situ. Proc Natl Acad Sci U S A. 85:5315-9.

Takahashi M, Billups B, Rossi D, Sarantis M, Hamann M, Attwell D (1997) The role of glutamate transporters in glutamate homeostasis in the brain. J Exp Biol 200: 401-9.

Takahashi KI, Copenhagen DR (1996) Modulation of neuronal function by intracellular pH. Neurosci Res. 24:109-16.

Takahashi M, Kovalchuk Y, Attwell D (1995) Pre- and postsynaptic determinants of EPSC waveform at cerebellar climbing fiber and parallel fiber to Purkinje cell synapses. J Neurosci 15: 5693-702.

Takahashi M, Sarantis M, Attwell D (1996) Postsynaptic glutamate uptake in rat cerebellar Purkinje cells. J Physiol (Lond) 497: 523-30.

Tan J, Zelenaia O, Correale D, Rothstein JD, Robinson MB (1999) Expression of the GLT-1 subtype of Na+-dependent glutamate transporter: pharmacological characterization and lack of regulation by protein kinase. J Pharmacol Exp Ther. 289:1600-10.

Tong G, Jahr CE (1994) Block of glutamate transporters potentiates postsynaptic excitation. Neuron 13:1195-203.

Trotti D, Peng JB, Dunlop J, Hediger MA (2001) Inhibition of the glutamate transporter EAAC1 expressed in Xenopus oocytes by phorbol esters. Brain Res 914: 196-203.

Tzingounis AV, Larsson HP, Kavanaugh, MP (2002) Voltage clamp and fluorometric techniques for studying glutamate transporter function. In: Transmembrane transporters (Quick M, ed). New York:Wiley-Liss, Inc.

Tzounopoulos T, Guy HR, Durell S, Adelman JP, Maylie J (1995) min K channels form by assembly of at least 14 subunits. Proc Natl Acad Sci U S A. 92:9593-7.

Utsunomiya-Tate N, Endou H, Kanai Y (1996) Cloning and functional characterization of a system ASC-like Na+-dependent neutral amino acid transporter. J Biol Chem. 271:14883-90.

Vandenberg RJ, Arriza JL, Amara SG, Kavanaugh MP (1995) Constitutive ion fluxes and substrate binding domains of human glutamate transporters. J Biol Chem 270: 17668-71.

Vandenberg RJ, Mitrovic AD, Chebib M, Balcar VJ, Johnston GA (1997) Contrasting modes of action of methylglutamate derivatives on the excitatory amino acid transporters, EAAT1 and EAAT2. Mol Pharmacol. 51:809-15.

Vandenberg RJ, Mitrovic AD, Johnston GA (1998) Serine-O-sulphate transport by the human glutamate transporter, EAAT2. Br J Pharmacol 123: 1593-600.

Vidaver GA (1966) Inhibition of parallel flux and augmentation of counter flux shown by transport models not involving a mobile carrier. J Theor Biol. 10:301-6.

Volterra A, Trotti D, Cassutti P, Tromba C, Salvaggio A, Melcangi RC, Racagni G (1992) High sensitivity of glutamate uptake to extracellular free arachidonic acid levels in rat cortical synaptosomes and astrocytes. J Neurochem. 59:600-6.

Wadiche JI, Arriza JL, Amara SG, Kavanaugh MP. (1995a) Kinetics of a human glutamate transporter. Neuron 14:1019-27.

Wadiche JI, Amara SG, Kavanaugh MP (1995b) Ion fluxes associated with excitatory amino acid transport. Neuron 15: 721-8.

Wadiche JI and Jahr CE (2001) Multivesicular release at climbing fiber-purkinje cell synapses. Neuron 32: 301-13.

Wadiche JI, Kavanaugh MP (1998) Macroscopic and microscopic properties of a cloned glutamate transporter/chloride channel. J Neurosci 18:7650-61.

Wang KW and Goldstein SA (1995) Subunit composition of minK potassium channels. Neuron. 14:1303-9.

Watzke N, Bamberg E, Grewer C (2001) Early intermediates in the transport cycle of the neuronal excitatory amino acid carrier EAAC1. J Gen Physiol 117:547-62.

Watzke N, Grewer C (2001) The anion conductance of the glutamate transporter EAAC1 depends on the direction of glutamate transport. FEBS Lett 503:121-5.

Watzke N, Rauen T, Bamberg E, Grewer C (2000) On the mechanism of proton transport by the neuronal excitatory amino acid carrier 1. J Gen Physiol 116:609-22.

Webb DJ and Nuccitelli R (1981) Direct measurement of intracellular pH changes in Xenopus eggs at fertilization and cleavageJ. Cell Biol 91:562-567.

Williams JH, Errington ML, Lynch MA, Bliss TV (1989) Arachidonic acid induces a long-term activity-dependent enhancement of synaptic transmission in the hippocampus. Nature 341:739-42.

Yamada K, Watanabe M, Shibata T, Tanaka K, Wada K, Inoue Y (1996) EAAT4 is a post-synaptic glutamate transporter at Purkinje cell synapses. Neuroreport. 7:2013-7.

Zarbiv R, Grunewald M, Kavanaugh MP, Kanner BI (1998) Cysteine scanning of the surroundings of an alkali-ion binding site of the glutamate transporter GLT-1 reveals a conformationally sensitive residue. J Biol Chem 273: 14231-7.

Zerangue N, Arriza JL, Amara SG, Kavanaugh MP (1995) Differential modulation of human glutamate transporter subtypes by arachidonic acid. J Biol Chem. 270:6433-5.

Zerangue N and Kavanaugh MP (1996a) Interaction of L-cysteine with a human excitatory amino acid transporter. J Physiol (Lond) 493: 419-23.

Zerangue N and Kavanaugh MP (1996b) Flux coupling in a neuronal glutamate transporter. Nature 383: 634-7.

Zeuthen T, Meinild AK, Klaerke DA, Loo DD, Wright EM, Belhage B, Litman T (1997) Water transport by the Na+/glucose cotransporter under isotonic conditions.Biol Cell. 1997 Aug;89(5-6):307-12.

Zhang Y, Bendahan A, Zarbiv R, Kavanaugh MP, Kanner BI (1998) Molecular determinant of ion selectivity of a (Na+ + K+)-coupled rat brain glutamate transporter. Proc Natl Acad Sci U S A 95: 751-5.

Zhang Y and Kanner BI (1999) Two serine residues of the glutamate transporter GLT-1 are crucial for coupling the fluxes of sodium and the neurotransmitter. Proc Natl Acad Sci U S A 96: 1710-5.

APPENDIX I

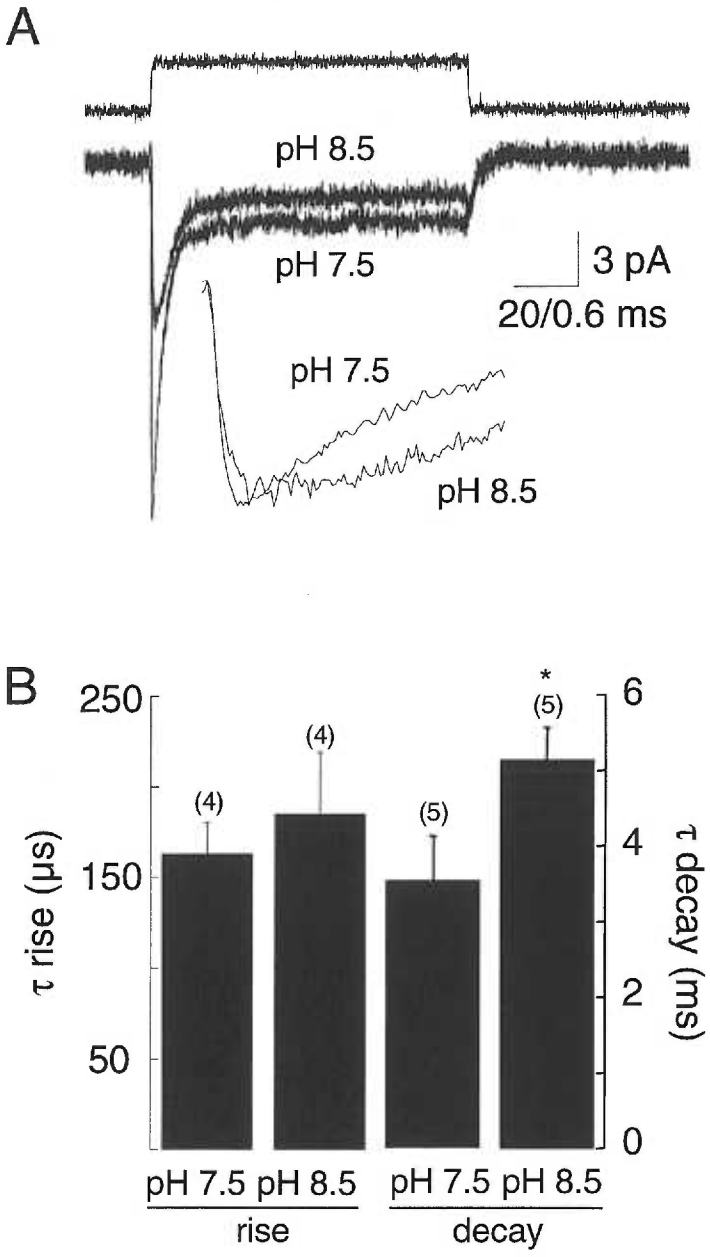
A
pH 8.5
pH 7.5
3 pA
20/0.6 ms
pH 7.5
pH 8.5
B
250
150
50
τ rise (μs)
6
4
2
0
τ decay (ms)
(4)
(4)
(5)
(5)
*
pH 7.5 pH 8.5
rise
pH 7.5 pH 8.5
decay

Figure 1. Extracellular pH determines EAAT3's anion conductance kinetics. (A) Rapid application of 10 mM L-glutamate to outside-out patches (100 ms, -70 mV) at pH_o 7.5 and 8.5. (B) Rise times were not significant different at pH 7.5 and 8.5, while the relaxation to steady state was somewhat slower at pH 8.5 (paired student t-test p=0.029).

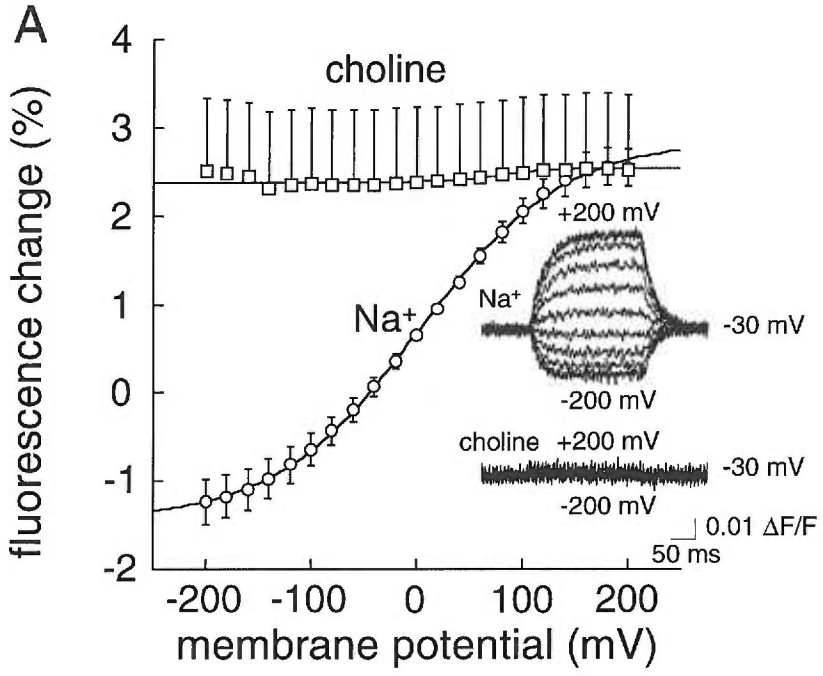
A
fluorescence change (%)
4
3
2
1
0
-1
-2
choline
+200 mV
Na+
-30 mV
-200 mV
choline +200 mV
-30 mV
-200 mV
0.01 ΔF/F
50 ms
-200 -100 0 100 200
membrane potential (mV)

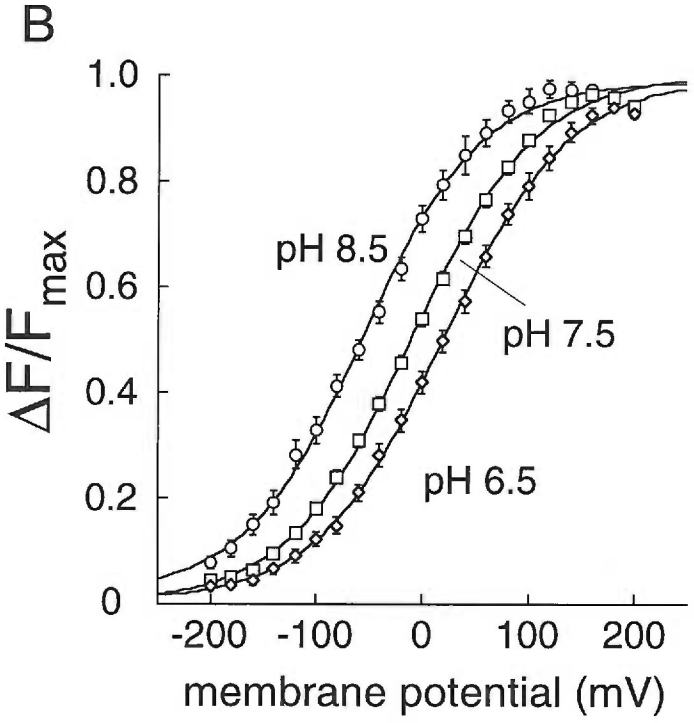
B
ΔF/Fmax
1.0
0.8
0.6
0.4
0.2
0
pH 8.5
pH 7.5
pH 6.5
-200 -100 0 100 200
membrane potential (mV)

Figure 2. Protons determine the occupancy of the Na^+-bound states. Fluorescence measurements in oocytes expressing EAAT3 A431C under two electrode voltage clamp. Oocytes have been labeled with the fluorophore Alexa 546 (Molecular probes, OR). (A) Measurement of time and membrane potential dependent fluorescence changes in the presence of 100 mM extracellular Na^+ or 100 mM choline. The responses acquired at –30 mV (100 mM Na^+) prior to the voltage perturbation or application of choline were set as 0. Inset, fluorescence records showing the voltage dependence of the fluorescence signal in 100 mM Na^+ (top traces) or 100 mM choline (bottom traces). Voltage command pulses in 20 mV increments from a holding potential of -30 mV (+200 mV to –200 mV). (B) Changing extracellular pH from shifts the midpoint of the fluorescence-V curve. The data were fitted to a Boltzmann function and normalized to their maximum response. At pH 8.5 the $V_{0.5}$ = -56.4 ± 6 mV with a slope factor = 0.42 ± 0.03 (n=11), while at pH 7.5 the $V_{0.5}$ = -12.1 ± 3 mV with a slope factor = 0.42 ± 0.009 (n=15), and finally, at pH 6.5 the $V_{0.5}$ = 19.2 ± 6 mV with a slope factor = 0.42 ± 0.01 (n=10).